AERE - PR/NP 15

INDC(UK)-9/E

INDC-296

UNCLASSIFIED

AERE - PR/NP 15

E MINIMIS MAXIMA

United Kingdom Atomic Energy Authority

RESEARCH GROUP

NUCLEAR PHYSICS DIVISION PROGRESS REPORT

For the period 1st May 1968 to 31st October 1968

Editors: C. F. COLEMAN C. A. UTTLEY

Nuclear Physics Division,

Atomic Energy Research Establishment,

Harwell, Berkshire.

1969

U.D.C.
539.1(047.1)

UNCLASSIFIED

AERE - PR/NP 15

NUCLEAR PHYSICS DIVISION

PROGRESS REPORT

For the period 1st May 1968 to 31st October 1968

Editors: C. F. COLEMAN and C. A. UTTLEY

Nuclear Physics Division,
U.K.A.E.A. Research Group,
Atomic Energy Research Establishment,
HARWELL.

May, 1969

HL.69/1743 (C17)

CONTENTS

CONTENTS (cont'd)

CONTENTS (cont'd)

CONTENTS (cont'd)

NUCLEAR PHYSICS DIVISION

Division Head: Dr. B. Rose

0.5 MV Cockroft Walton Generator, Ion-Crystal Interactions

Dr. G. Dearnaley

IBIS 3 MV pulsed Van de Graaff, 5 MV Van de Graaff

Dr. A. T. G. Ferguson

Tandem Generator

Dr. J. Freeman

Electron Linear Accelerator

Dr. E. R. Rae

Synchrocyclotron

Dr. A. E. Taylor

Charged Particle Spectrograph

Mr. D. L. Allan

Proton Physics

Dr. P. E. Cavanagh

Mössbauer Effect

Dr. T. E. Cranshaw

Miscellaneous Research

Dr. J. V. Jelley

INTRODUCTION

DR. B. ROSE

During any reporting period, it is to be expected that the analysis will appear of experimental work concluded some time earlier, and two interesting items in this report come within this category.

The first is a very detailed analysis of the neutron cross sections of lithium-6, a matter of particular importance for neutron cross section standards. The second is concerned with an extensive series of experiments carried out on the proton linear accelerator of the Rutherford Laboratory and proposes an explanation for the J-dependence observed in the angular distribution of the (p,d) reaction on even tin isotopes.

Some new results from the VEC show the production of a large number of new isomeric states between holmium and lead, and an interesting suggestion is made for yet another manifestation of the double-humped Strutinsky potential in the prediction of many shape-isomers in the barium region.

It is interesting to observe several examples in this report of the continuous development of the techniques of neutron measurement, exemplified here by one developed for the measurement of Pu-α, another being designed to have a flat response for use in time-of-flight neutron spectroscopy, and also by the recalibration by a new method of an old detector (the 'long counter' on IBIS), on the accuracy of whose calibration a number of important 'reactor data' quantities depend. This is unspectacular work, but is of the highest importance and calls for physical insight at the highest level if accurate results are to be obtained.

B. Rose

19th March, 1969.

EDITORIAL NOTE

Since the results obtained from the various machines are not easily classified according to the energy of the charged beams, individual research items are labelled with a single letter indicating on which machine the experiments were performed. These labels are as follows:

Cockcroft Walton Generator (G. Dearnaley)	A
3 MV pulsed Van de Graaff Generator IBIS (A. T. G. Ferguson)	B
5 MV Van de Graaff Generator (A. T. G. Ferguson)	C
13 MV Tandem Generator (J. M. Freeman)	D
45 MeV Electron Linac (E. R. Rae)	E
50 MeV Proton Linac : S.R.C.	F
Variable Energy Cyclotron : Chemistry Division	G
Synchrocyclotron (A. E. Taylor)	H
Nimrod Proton Synchrotron : S.R.C.	I

The running analyses for the various machines operated by the division are presented as far as possible in a uniform format, but some differences exist in the way in which the scheduling is arranged, and machines such as the Electron Linac can accommodate several experiments simultaneously.

GENERAL REACTOR TECHNOLOGIES AND STUDIES

NUCLEAR DATA FOR FAST REACTORS

3. Elastic and inelastic scattering of neutrons by Pu^{239} (D. A. Boyce, P. E. Cavanagh, C. F. Coleman, G. A. Gard, A. G. Hardacre, J. C. Kerr and J. F. Turner)

An error has been found in the fitting of the observed fission neutron spectra with an $E^{1/2}e^{-E/\theta}$ distribution, so that the value of the "temperature" θ quoted earlier(1) is incorrect. Correct fitting leads to a value 1.47 ± 0.10 MeV, in better agreement with Bonner's(2) result.

Design of a neutron detector with a flat energy response for use in time of flight experiments (M. S. Coates and W. Hart (Risley))

Using the GEM 4(3) code on the Risley IBM 7090 computer further Monte Carlo calculations have been made to study the neutron sensitivity of the homogeneous ^{10}B-Vaseline detector reported earlier(4). The program tracks monoenergetic neutrons incident on the inner end of a re-entrant hole. When a neutron is absorbed its energy, spatial co-ordinates and time to absorption are recorded. A second part of the program tracks the 480 keV γ-rays produced in the $^{10}B(n,\alpha)^7Li^*,\gamma Li^7$ reaction and gives the position and energy of the γ-ray when it emerges from the surface of the sphere. In practice only γ-rays in a chosen energy range emerging from a chosen region of the sphere will be detected.

The calculations allow one to assess whether it is feasible to make a detector with an efficiency insensitive to the accuracy of the input nuclear data over the energy region of interest (~100 eV - several MeV), which responds rapidly enough to be used in time of flight experiments. So far more detailed calculations have been made only for spheres containing 1 kg of ^{10}B, with a re-entrant hole diameter of 2.5 cm and the inner end at a depth of ¼ sphere diameter (this depth was found to minimise the leakage of high energy neutrons for a given boron content). In particular we have studied a sphere of radius 12 cm, and have already shown that in this detector at least 95% of incident neutrons with $E \lesssim 1$ MeV are absorbed within a time ~0.7μs. The distribution of the number of γ-rays emerging from the sphere surface at a given incident neutron energy is symmetrical about the direction of the incident beam, but is not expected to be uniform over the surface. This is because high energy incident neutrons tend to be absorbed in the downstream, and lower energy neutrons in the upstream half of the sphere. Distributions have been obtained for the number of γ-rays with residual energies from 480-400 keV emerging from five equal segments of the sphere surface (indicated in Fig. 1a (see page 2)) as a function of incident neutron energy. The distributions are given in Fig. 1b (see page 2). The distributions are relatively flat for the three central segments but show large variations for the two capping segments. It is interesting to note that the distributions summed over all five segments vary by only 3% over the neutron energy range 100 eV - 1 MeV. A practical detector would accept γ-rays from the central region. Fig. 2 (see page 2) shows the distribution for a segment comprising half each of segments 2 and 3 in Fig. 1a. The variation is 3% in the neutron energy range 100 eV - 700 keV. To test the sensitivity of the results to the input nuclear data calculations were made with the $^{10}B(n,\alpha)$ cross section and the hydrogen scattering cross section displaced systematically by approximately two standard deviations from the best quoted values. This involved changes in the $^{10}B(n,\alpha)$ cross section of ~1% at 20 keV, 4% at 100 keV and 57% at 1 MeV and a change of ~3% in the hydrogen scattering cross section. The distribution of Fig. 2 changed relatively by 1-2%.

---

(1) Nuclear Physics Division Progress Report PR/NP 14 p. 3.

(2) Bonner T. W., Nucl. Phys. 23, 116 (1961).

(3) Hemmings P. J. UKAEA Report AHSB(S)R146 (1968).

(4) Nuclear Physics Progress Report AERE PR/NP14 (1968) p. 8.

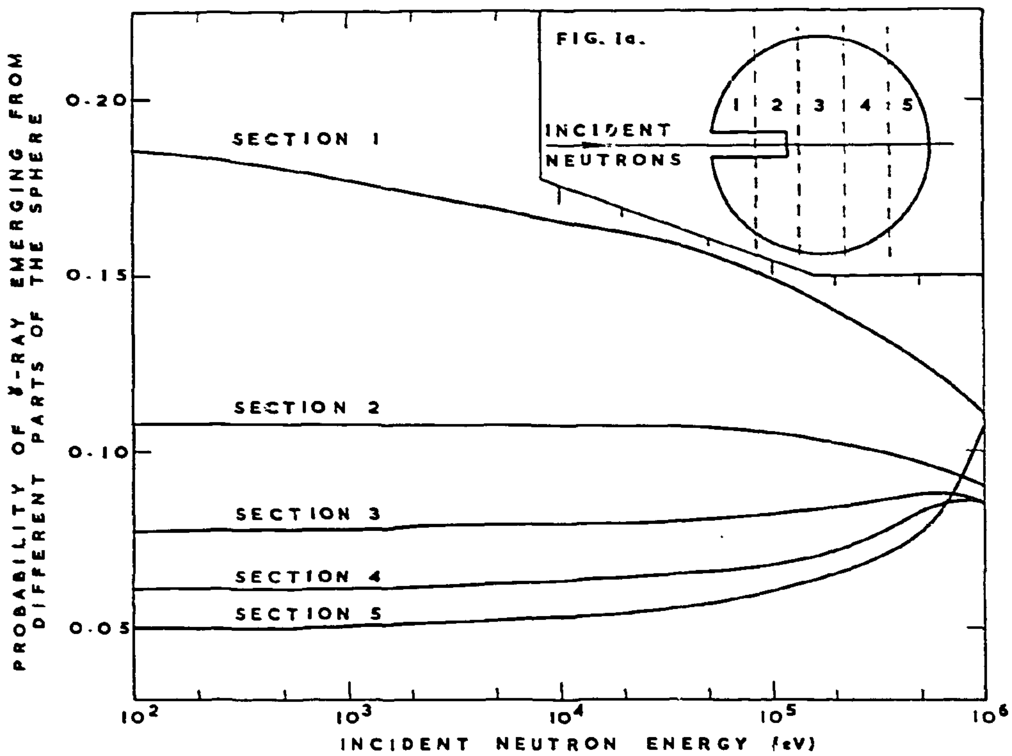

Fig. 1. (a) Five equal areas on sphere surface.

(b) Probability of emergence from specified areas of sphere surface of gamma rays with energies in the range 400 → 480 keV as a function of the energy of the incident neutrons.

It would be desirable to extend the range of flat response to higher incident neutron energies. It appears that significant improvements can only be achieved by increasing the detector size, since calculations show that the maximum energy at which at least 95% of incident neutrons are absorbed is insensitive to ^{10}B concentration. On the other hand the ^{10}B concentration strongly affects the mean delay in the counter response. To a good approximation the fraction of neutrons captured after a given time t is given by $1 - e^{-50.5\rho t}$ where ρ is the effective boron density in $gm.cm^{-3}$ and t is in μs. For a 12 cm radius sphere containing 1 kg of ^{10}B only 1% of the incident neutrons are detected more than 0.66 μs after entry. This response is just fast enough to allow good time of flight measurements on the 300 m flight path of the neutron booster. The criterion is that the timing resolution of the detector should be sufficient to allow an accurate background determination using the black resonance technique. We intended to make a detector 12 cm radius containing 1 kg ^{10}B. Since a faster counter would be advantageous further calculations will be made to determine the γ-ray response with higher ^{10}B concentrations.

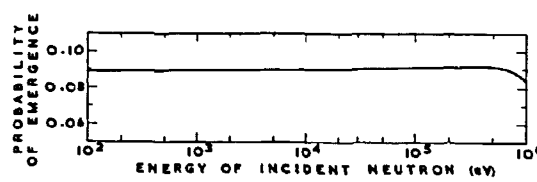

Fig. 2. Probability of emergence from segments 2-3 as a function of energy of incident neutrons.

3. Measurement of the absolute sensitivity of neutron detectors (J. M. Adams, A. T. G. Ferguson and C. D. McKenzie*)

The measurements described previously[5] of the absolute sensitivity of a Harwell long counter[6] at incident neutron energies between 50 keV and 1.3 MeV have now been completed. The data are still being analysed.

To reduce the uncertainties in the measurements several technical improvements were introduced. The initial measurements of the neutron angular distributions from the reactions $^{51}V(p,n)^{51}Cr$ (Q = -1.534 MeV) and $^{57}Fe(p,n)^{57}Co$ (Q = -1.619 MeV) exhibited pronounced 'dips' around 90° which arose because the target was inclined at 90° to the incident proton beam. This effect was eliminated by using targets inclined at 45° and 135° to the beam as shown in Fig. 3. The neutron angular distributions in the two

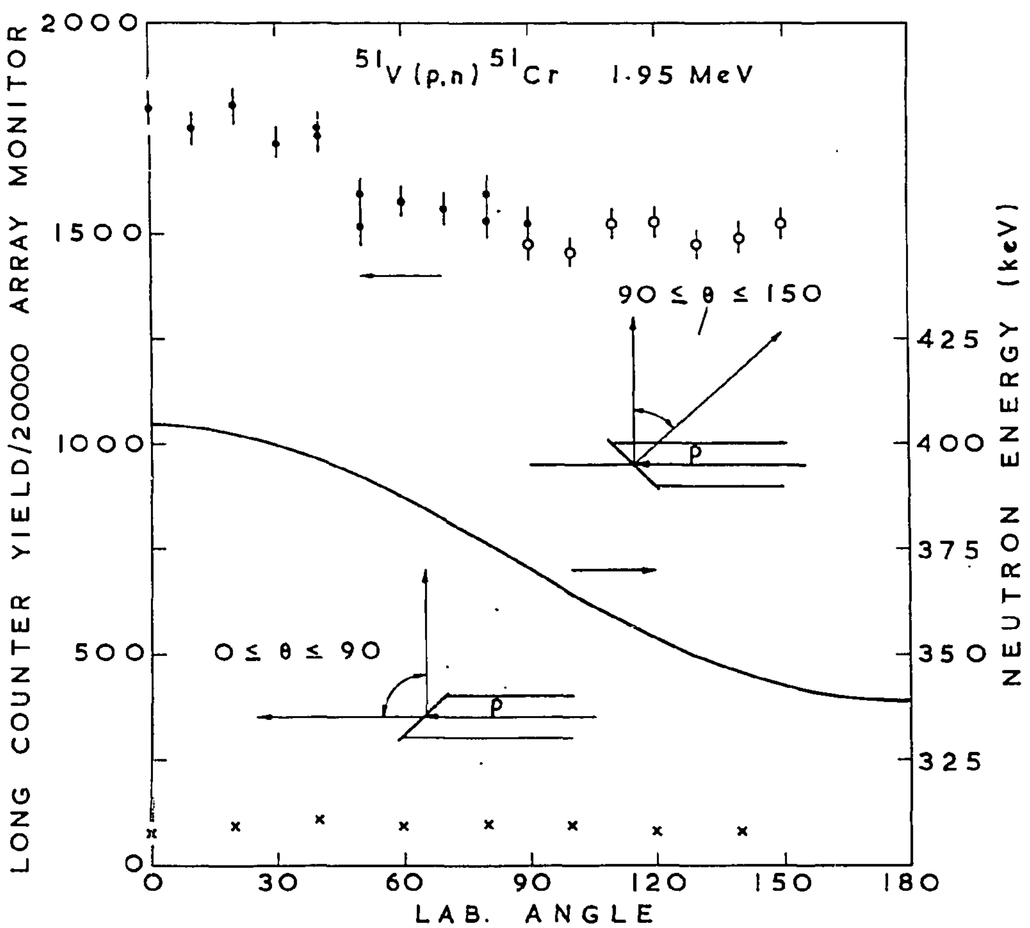

Fig. 3. Target orientation, angular dependence of neutron energy and angular dependence of long counter counts for ^{51}V target.

* On leave from the University of Melbourne, Australia. Since returned there.

(5) Adams J. M., Ferguson A. T. G. and McKenzie C. D. AERE PR/NP14, (1968).

(6) Allen W. D., AERE NP/R 1667.

hemispheres from the reaction $^{51}V(p,n)^{51}Cr$ can be obtained from the counting rate curve which along with the angular variation of the neutron energy is also shown in Fig. 3. The second long counter, which had previously been used to monitor the angular distribution measurements and introduced a large statistical counting error, was replaced by a 'super' long counter consisting of any array of seventeen 1 in. diam by 16 in. long BF_3 proportional counters. The background in the long counter, which had been a serious problem at lower neutron energies where the reaction yields are small(7), was greatly reduced by operating GLEEP at very low power.

We have also determined as a function of neutron energy the depth R_0 inside the long counter at which effective thermalisation occurs. This redetermination was carried out with monoenergetic neutrons from the $^7Li(p,n)^7Be$ and $T(p,n)^3He$ reactions, measuring the yield as a function of distance from the target. Preliminary results indicate that the values of R_0 are significantly greater than indicated by previous determinations made with neutron sources(6). This is an important result in specifying the absolute efficiency of a long counter because it is not always either desirable or practicable to use the counter in exactly the same geometry as that employed for the calibration.

We pointed out before(5) that one of the main sources of error in the measurements arose from uncertainties in strengths of the ^{51}Cr and ^{57}Co sources used to determine the target activities. To reduce this error several ^{51}Cr sources calibrated to $<0.5\%$(8), were obtained from NPL Teddington. The counting of the activated ^{51}V targets and of earlier ^{51}Cr sources with respect to these standard sources has now been completed and the data are being analysed. The decay of the ^{51}Cr sources obtained from NPL is now being measured, since previous determinations of the ^{51}Cr half life are not completely consistent(9).

E. Fast neutron spectra in reactor materials (A. J. H. Goddard and J. G. Williams (Imperial College) and H. Lichtblau (Birmingham University))

Theoretical and experimental studies of fast neutron spectra in spherical shells are continuing, following the work of Coates et al(10). Here we report work concerned with natural uranium. Survey calculations have been carried out using the neutron transport theory code DTFIC, which is based on the Carlson S_n method(11). We have studied: (1) The sensitivity of the spectra to changes in ^{238}U inelastic scattering cross-section. For a typical system at 2 MeV a 40% change in the spectrum results from a 20% change in the whole inelastic matrix; (2) the importance of a knowledge of the distribution of neutron sources within the target, using several possible source distribution models. We find that the leakage spectra from uranium shells at angles other than 0° (the radial direction) are not changed by significant amounts as a result of plausible changes in the source model; (3) the effect of room return from the concrete walls of the target cell. This is likely to be significant only at energies below 50 keV (see Table I (page 5)).

In our experimental studies we used the $^{58}Ni(n,p)^{58}Co$ reaction to monitor the fast neutron output. Comparisons of measurements using this method with DTFIC calculations have shown that correct electron beam alignment is essential to obtain the source geometry assumed in the calculations. A beam sensing device developed by B. P. Clear of Nuclear Physics Division and described elsewhere in this report(12), has been installed to monitor the electron beam alignment during experimental runs.

We have carried out experiments to measure room return, using a uranium target displaced from its usual position so that most of the neutrons which reached the detector did so after scattering in the cell

---

(7) Johnson C. H., Galonsky A. and Inskeep C. N., ORNL-2910, p. 25.

(8) Campion P. J., Int. J. Appl. Rad. Isotops 4, 232 (1959).

(9) Lederer C. M., Hollander J. M. and Perlman I., Table of Isotopes (6th ed.) (Wiley, 1967).

(10) Coates M. S., Gayther D. B. and Goode P. D., AERE - R 5364 (1968).

(11) Carlson B. G., Los Alamos - LA 1891 (1955).

(12) Clear B. P. AERE PR/NP 15 p. 54.

wall. On the basis of this measurement the effect that the cell walls would have on a target spectrum has been calculated and is shown in Table 1 in the column headed 'Experiment'. Results based entirely on S_n calculations are shown for comparison in the column headed 'Theory' and a similar calculation for a typical shell spectrum is quoted in the final column. The larger percentages in the latter case reflect not an increase in the number of room return neutrons but a decrease in the number of neutrons in the target spectrum proper. For this spectrum experiment and theory disagree by a factor of two. This is outside statistical errors, and probably reflects an over-simplification in the calculations. The effect of room return is shown to be small overmost of the energy range of interest. It is hoped that further measurements and calculations will establish reliable corrections where they are needed.

TABLE I

Percentage of spectra contributed by room return

Energy	Target spectrum		11 cm radius shell spectrum
	Experiment	Theory	Theory only
85 keV	0.5%	0.2%	1.3%
50 keV	0.9%	0.4%	1.8%
32 keV	1.2%	0.6%	3.3%
19 keV			10.0%
10 keV			25.0%

II. $\bar{\nu}$ for ^{238}Pu (D. W. Colvin)

A detailed evaluation has been made of $\bar{\nu}$ (the average number of neutrons/fission) for ^{239}Pu from thermal energies to 15 MeV. Preliminary fits to the existing data indicate that fast reactor requests for this parameter are already met at thermal energies and above 1-2 MeV if the comparison standard, ^{252}Cf, is assumed without error. However, in view of the theoretical and experimental evidence for structure below 1 MeV, consideration has been given to the design of an experiment to measure $\bar{\nu}$ as a continuous function of energy in the range from a few keV to 10 MeV using the time-of-flight facilities on the synchrocyclotron. This will avoid certain criticisms normally levelled at "spot-point" measurements carried out on electro-static generators.

H. Capture cross-section for ^{238}U (D. W. Colvin and P. H. Bowen)

First steps have been taken to set up the A.W.R.E. 80 cm liquid scintillator on the 45 MeV electron linac for feasibility tests. The counter will be used to entend measurements of the capture cross-section of ^{238}U to higher energies either on the synchrocyclotron or the linac or both.

E. The direct measurepments of alpha for ^{239}Pu over the energy range 10 eV to 30 keV (M. G. Schomberg, M. G. Sowerby and D. A. Boyce)

The work previously reported(13,14,15) has been continued and data have been obtained on a third ^{239}Pu sample of thickness 0.0044 atoms/barn, a ^{235}U sample of thickness 0.00109 atoms/barn and two

(13) Schomberg M. G., Sowerby M. G. and Evans F. W. Nuclear Physics Division Progress Report AERE - PR/NP 13 (1968).

(14) Schomberg M. G., Sowerby M. G. and Evans F. W. Fast Reactor Physics IAEA Vienna, I 289 (1968).

(15) Schomberg M. G., Sowerby M. G. and Evans F. W. Nuclear Physics Division Progress Report AERE - PR/NP 14 (1968).

lead samples. The data on the ^{235}U and lead samples are for checking that the system is operating correctly. The data from the third ^{239}Pu sample and ^{235}U sample are at present being analysed. The experiments with the lead samples show that both the fast neutron detectors and the capture gamma ray detectors are insensitive to scattered neutrons.

In the last progress report(15) it was stated that the observed efficiency of the capture gamma ray detector for fission events was higher than expected. This is thought to be mainly due to coincidences produced by two gamma rays and/or neutrons being detected in the two halves of detector. The effect is more pronounced for fission events because of the high gamma ray multiplicity and of the contribution from fission neutrons. To overcome it some changes have been made to the detector system. Two new detectors have been constructed with the thickness of the scintillator layers increased to improve the linearity of the response at lower gamma ray energies. These two detectors are arranged as shown in Fig. 4 and coincidences are taken between the following pairs of sections: AB, CD, AC and BD. The

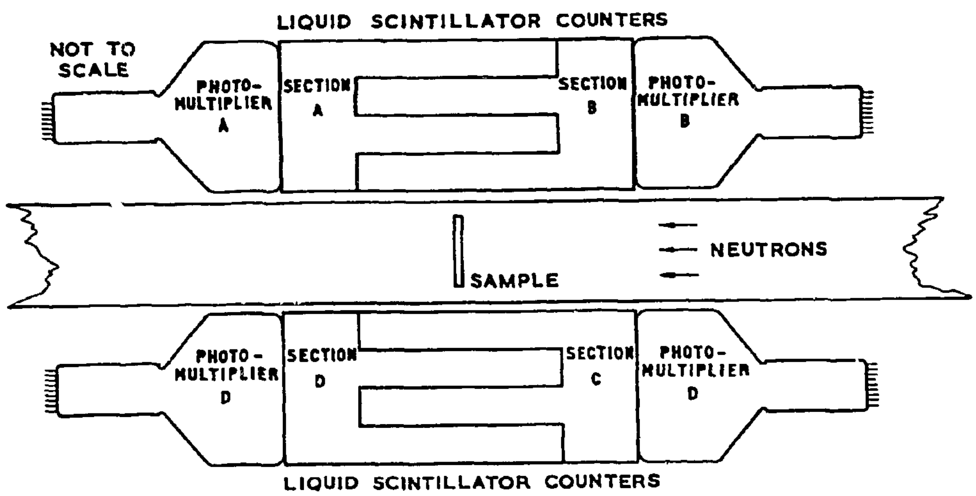

Fig. 4. Sketch showing layout of detector sections for ^{239}Pu alpha measurements.

coincidences AC and BD give a measure of the contribution from coincidences due to multiple events included in the number of AB and CD coincidences observed in each time-of-flight channel, so that this background can be subtraded off. Finally anti-coincidence techniques are used to subtract from the four coincidence outputs all events identified by the fast neutron detectors as fission events.

The re-designed detector system is now installed and is undergoing confirmatory checks to ensure that it has the desired characteristics. We now plan to make a further series of measurements of capture and fission yields from samples of ^{239}Pu with a range of different thicknesses.

Because alpha, or more specifically $\langle\sigma_{nc}\rangle/\langle\sigma_{nf}\rangle$, is one of the key quantities necessary for the efficient design of fast breeder reactors, the policy adopted with this experiment has been to publish provisional results as they become available and to reduce the uncertainty of these results as more data are obtained and the methods of analysis are improved. At the time of writing, October 1968, the provisional results of the present experiment together with other measurements and evaluations are shown in Fig. 5 (see page 7). In particular comparison can be made with the preliminary data of Gwin et al.(16) obtained at R.P.I. They discriminated between capture and fission events by observing the gamma rays produced in both types of reaction with a large liquid scintillator and using the fact that about 15% of fission events result in a pulse amplitude greater than the pulse amplitude produced by ~99% of the capture gamma ray cascades. Fairly large uncertainties are associated with both sets of data, but one can say that the results of the two experiments are in reasonable agreement. The evaluation from the

(16) Gwin R., Weston L. W., De Saussure G., Ingle R. W., Todd J. H., Gillespie F. E., Hockenbury R. W. and Block R. C. (1968) Private communication.

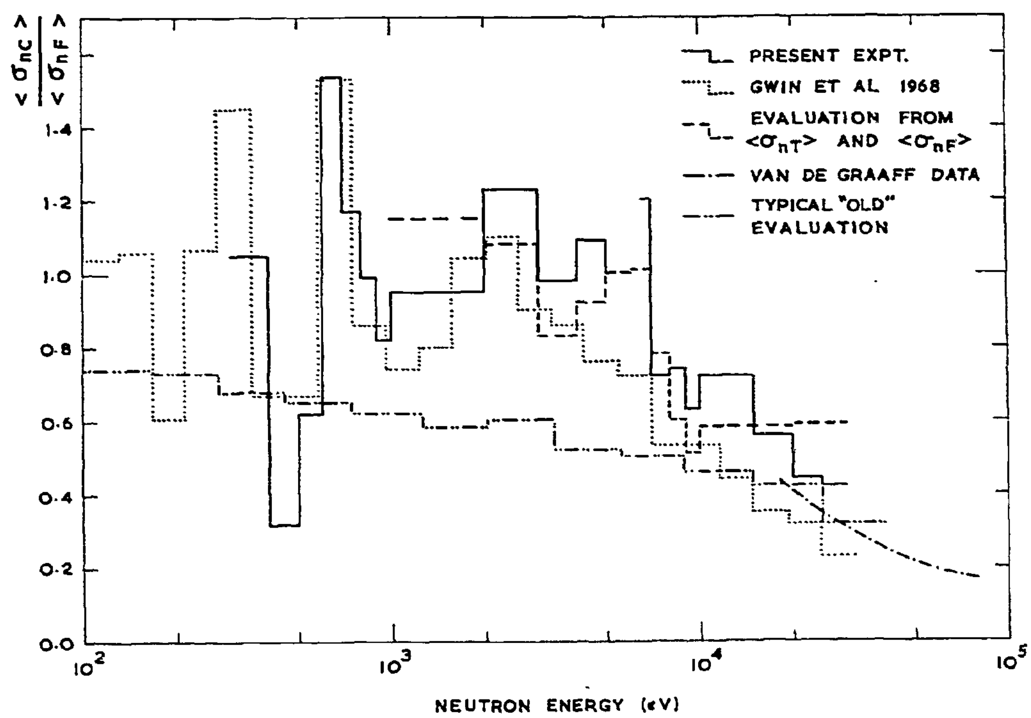

Fig. 5. Measured values of $\langle\sigma_{nc}\rangle/\langle\sigma_{nf}\rangle$ from various sources.

fission and total cross sections is very similar to that used in the last progress report[15] and is included to demonstrate that the results of the two direct measurements of alpha also agree with an indirect evaluation.

E. Evaluation of the ^{239}Pu fission cross section in the energy range 1 keV to 100 keV (G. D. James and B. H. Patrick)

Some of the input data used in this evaluation[17] depend on the $^{10}B(n,\alpha)$ cross section. These data have been revised to allow for the fact that this cross section is not strictly proportional to $1/\sqrt{E}$ but is more accurately represented below 30 keV by the equation

$$\sigma_{n,\alpha} = \frac{c}{\sqrt{E}} + \alpha \qquad \ldots (1)$$

The constants c = 610.3 ± and α = -0.28 ± 0.12b have been deduced from the total cross section data of Diment[18] and the scattering data of Asami and Moxon[19]. A least squares analysis designed to minimise the sum of the squares of the deviations of the input data shown in Table II has been employed to deduce the recommended ^{239}Pu fission cross section which is given in column 12 of Table II. This work will be described in a forthcoming memorandum[20].

(17) James G. D. and Patrick B. H. AERE - PR/NP 14 p. 17.

(18) Diment K. M. AERE - R 5224 (1967).

(19) Asami A. and Moxon M. C., this report. p. 14.

(20) James G. D. and Patrick B. H. AERE - M 2065.

TABLE II

^{239}Pu and ^{235}U fission cross sections and ratios

E (keV)	Allen and Ferguson R	Gilboy and Knoll R	Bollinger et al. $\sigma_f(239)$	James $\sigma_f(239)$	Shunk et al. $\sigma_f(239)$	Patrick et al. $\sigma_f(239)$	White et al. $\sigma_f(239)$	Michaudon $\sigma_f(235)$	de Saussure et al. $\sigma_f(235)$	Hart evaluated $\sigma_f(235)$	Deduced Cross Sections $\sigma_f(239)$	$\sigma_f(235)$
95	0.930	0.808					1.47			1.66	1.46 ± 0.06	1.67
85	0.910	0.807					1.47			1.70	1.47 ± 0.05	1.70
75	0.885	0.793					1.46			1.76	1.46 ± 0.05	1.75
65	0.867	0.771					1.46			1.82	1.47 ± 0.05	1.81
55	0.848	0.736					1.46			1.91	1.47 ± 0.06	1.90
45	0.825	0.698					1.45			2.02	1.48 ± 0.08	2.00
35	0.800	0.668								2.16	1.58 ± 0.14	2.16
25		0.639		1.62		1.53				2.36	1.57 ± 0.08	2.37
15		0.598		1.76		1.67				2.82	1.71 ± 0.04	2.82
9.5		0.554	2.28	1.85	2.14	1.99		3.27	3.04		2.06 ± 0.10	3.16
8.5		0.572	2.02	2.25	2.46	2.32		3.36	2.90		2.25 ± 0.12	3.14
7.5		0.600	1.86	2.27	2.24	2.17		3.41	3.69		2.14 ± 0.07	3.55
6.5		0.557	2.64	1.97	2.20	1.96		3.65	3.59		2.19 ± 0.13	3.62
5.5		0.548	2.74	2.41	2.71	2.17		4.13	3.77		2.50 ± 0.13	3.97
4.5			2.62	2.54	2.31	2.31		4.36	4.50		2.45 ± 0.09	4.43
3.5			3.45	2.86	2.74	2.73		4.75	5.02		2.95 ± 0.17	4.89
2.5			3.35	3.46	2.64	2.83		5.63	5.53		3.07 ± 0.20	5.58
1.5			3.91	4.40	3.43	3.64		7.42	7.42		3.85 ± 0.21	7.42

R = $\sigma_f(239)/\sigma_f(235)$

Cross sections are in barns

Results given in the last two columns are a least squares fit to the data shown in the rest of the Table.

E. Fluctuation analysis of the fission cross section of ^{239}Pu (B. H. Patrick and G. D. James)

The results of the fluctuation analysis of the fission cross section of ^{239}Pu first reported in the last progress report[21] have studied further and are now thought to be fairly well understood. The main results of the analysis are displayed in Fig. 6. In this figure every value of the serial correlation coefficient $r_k(W)$ which lies above the 1% significance level is plotted by a cross in the k-W plane. It can be seen that the highly significant values lie on parabolas corresponding to kW = 9 eV, 460 eV and 830 eV. Now the average spacing of the 0^+ levels in ^{240}Pu is 9.6 eV[22] and hence the correlation corresponding to kW = 9 eV is probably due to these levels. It is therefore reasonable to assume that the correlation corresponding to kW = 460 eV is due to levels with average spacing of 460 eV. Such levels are immediately explained by the theory of Strutinsky[23] who showed that when shell effects are taken into account, the deformed nucleus may have a second minimum in its potential energy. The 1^+ channel in the fission of ^{239}Pu + n lies ~200 keV below the neutron separation energy and hence we suggest that the levels built on the second minimum of the 1^+ channel, designated Class II levels by Lynn[24], have an average spacing of 460 ± 80 eV in ^{240}Pu. The error in the spacing arises from the limited number of levels in the region studied and assuming a Wigner distribution for the spacing. The correlation corresponding to kW = 830 eV is probably due to the Class II levels taken in pairs.

A paper describing the results of the correlation analysis in more detail has been accepted for publication in Physics Letters.

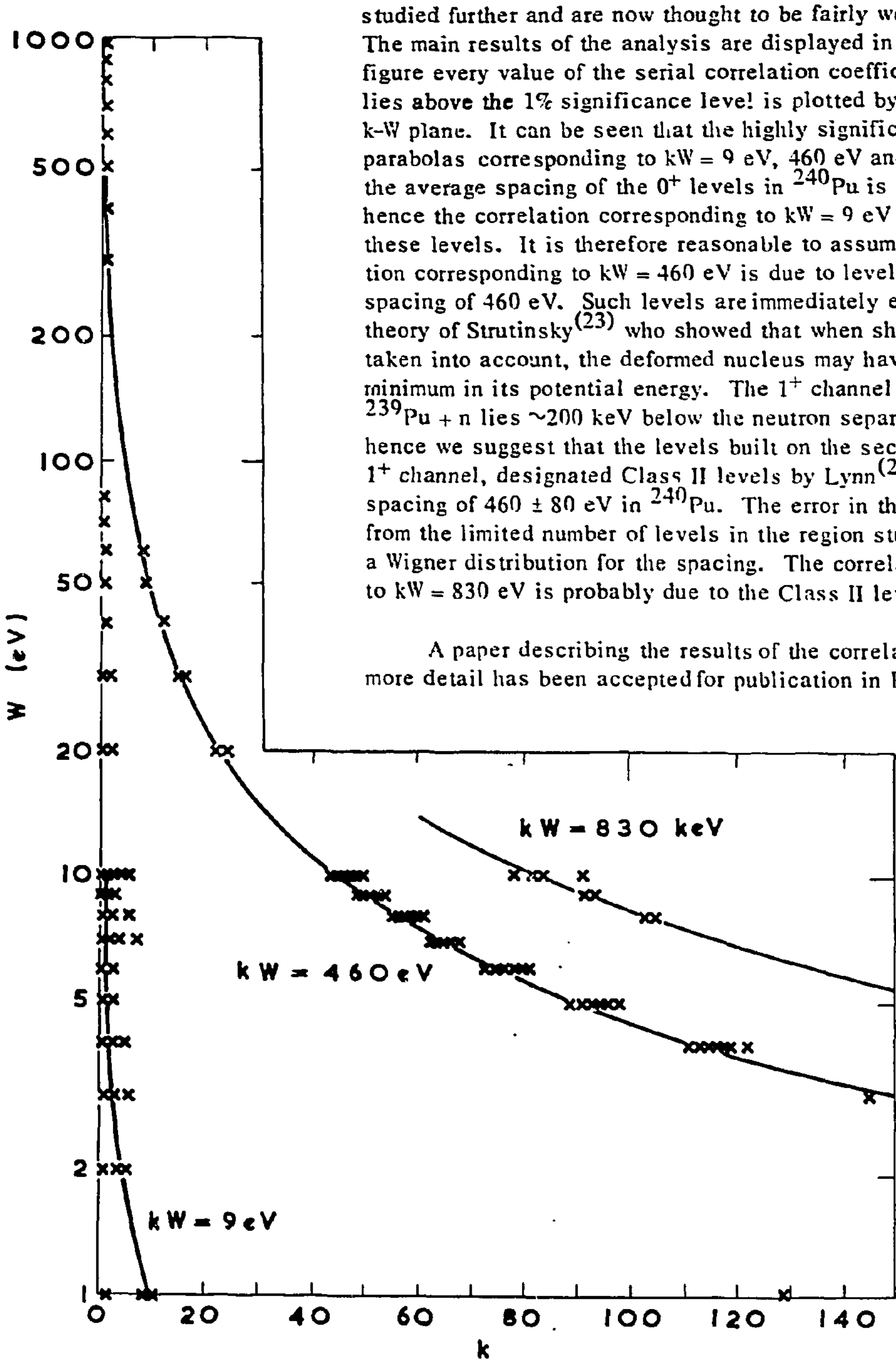

Fig. 6. Plot of k against kW for those values of $r_k(W)$ lying above the 1% significance level.

E. Search for $^{240}Pu(n,\alpha)$ reaction (N. J. Pattenden and J. E. Jolly)

Accurate measurements of neutron transmission, capture and scattering yields for ^{240}Pu performed previously on the linac gave values of resonance parameters which indicated that the three types of results were mutually inconsistent(25). This inconsistency could be resolved if another reaction were providing an anomalously large yield. The (n,α) reaction is energetically possible, with 10.4 MeV available. An experiment was therefore carried out to see if long-range α particles could be detected at neutron resonance energies. A platinum foil coated over an area of about 3 cm^2 with 1.78 mg of ^{240}Pu was mounted about 2 cm from a surface barrier semiconductor, with 5.4 mg/cm^2 foil of Al between them (corresponding to the range of a 4.7 MeV α particle). The energy of the natural α particles from ^{240}Pu is 5.16 MeV. The discriminator threshold for the detector was set at 1.5 MeV, ensuring that natural α particles were not counted, but only those with energies greater than 6.2 MeV. The system was mounted in an evacuated chamber, and placed in a neutron beam from the linac booster at 10 m from the target.

Despite precautions there was a considerable background, some of it presumably partly due to pile-up in the detecting electronics. No effects were observed at neutron times of flight corresponding to resonances. Subsequently, runs were performed with a ^{235}U target and without the Al, the electronics bring set to count fission fragments only. The areas of the peaks in the spectrum of fission fragment yield as a function of energy were combined with the known ^{235}U resonance parameters, to fix an approximate scale to the upper limits which could be given to the α widths (Γ_α) for the ^{240}Pu resonances below 100 eV neutron energy. For the 1.06 eV resonance, the limit is $<4 \times 10^{-6}$ eV, for other resonances below 91 eV Γ_α is $<5 \times 10^{-4}$ eV and for the 92.6 eV resonance Γ_α is $<2 \times 10^{-3}$ eV.

Thus the inconsistencies in the previous measurements cannot be explained by the existence of an (n,α) reaction.

E. Total cross section measurement of ^{234}U (G. D. James, G. G. Slaughter (ORNL) and D. A. J. Endacott).

The total cross section of ^{234}U has been measured with the small sample time-of-flight spectrometer of the Harwell neutron project. The path length was 15 m, the timing channel width ¼ μs and the electron burst width ¼μs. Transmission measurements were made with a 767 mg sample of 99.37% ^{234}U at sample thicknesses of 0.00258, 0.00619 and 0.01674 atoms per barn. These data are being analysed by the area method to deduce the resonance neutron widths. It is hoped thereby to extend the analysis of those resonances which James and Rae(26) found to have fission components.

E. Fission components in ^{242}Pu resonances (G. D. James and D. A. J. Endacott)

At least three nuclei, ^{240}Pu(27,28), ^{237}Np(29) and ^{234}U(30) are now known to have groups of

(21) A.E.R.E. report PR/NP 14, p. 18, (1968).

(22) Derrien H., Blons J., Eggermann C., Michaudon A., Paya D. and Ribon P. Proc. IAEA Conf. on Nuclear Data for Reactors, Paris (1966) Vol. II, p. 195.

(23) Strutinsky W. M. Nucl. Phys. A95, 420 (1967).

(24) Lynn J. E. Conf. on Low and Medium Energy Nuclear Physics (A.E.R.E., 1968), Report R 5744, p. 3 and "The Theory of Neutron Resonance Reactions" (Clarendon Press, Oxford, 1968) p. 463.

(25) Asghar M., Moxon M. C. and Pattenden N. J. AERE Report R - 5945 (1968) to be published.

(26) James G. D. and Rae E. R. Nucl. Phys. A118 313 (1968).

(27) Weigmann H. and Schmid H. J. Nucl. Energy 22, 317 (1968).

(28) Migneco E. and Theobald J. P. Nucl. Phys. A112, 603 (1968).

(29) Paya D., Derrien H., Fubini A., Michaudon A. and Ribon P. Nuclear Data for Reactors, Vol. II (IAEA Vienna, 1967) p. 128.

(30) James G. D. and Rae E. R., Nucl. Phys. A118, 313 (1968).

resonances in their sub-threshold fission cross sections which according to Weigmann[31] and Lynn[32] can be explained in terms of the second minimum in the fission potential barrier predicted by Strutinsky[33]. A measurement over the energy range 16 eV to 35 keV of the fission cross section for ^{242}Pu shows that this nuclide also has fission components in some of its sub-fission-threshold resonances, as illustrated in Fig. 7. The separation between the two groups near 800 eV and near 30 keV is taken to be the spacing between the levels in the second potential minimum designated by Lynn[32] as Class II states. Thus $D_{II} = 29 \pm 15$ keV corresponding to an energy difference of $3.2^{+0.6}_{-0.2}$ MeV between the first level in the second minimum and the ground state in ^{242}Pu. It has been possible to correlate the two resonances at 767 eV and 799 eV with dips in the transmission data obtained by Pattenden[34] and to deduce for these resonances the resonance parameters given in Table III.

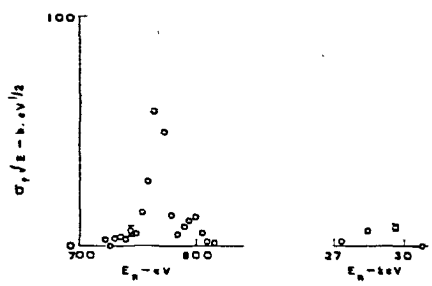

Fig. 7. ^{242}Pu *fission resonances below 35 keV.*

Lynn[32] has shown that under conditions of very weak coupling when the situation can be treated by perturbation theory, the observed fission widths are spread over only a few levels, and from Table III, this state of affairs appears to exist in ^{240}Pu. He shows that a level which contains a large fraction of the Class II strength, as deduced from its fission width should contain a correspondingly small fraction of the Class I strength, as deduced from its neutron width. For the two levels near 800 eV in Table III, it will be seen that at one standard deviation from the mean the proportion of Class II strength in the level at 767 eV is 84.2% from the ratio of neutron widths and 85% from the ratio of fission widths which shows that the equations of perturbation theory can be satisfied.

TABLE III

Parameters of ^{235}Pu resonances which show fission components

E_r (eV)	E_T (eV)	$\sigma_0\Gamma_f$ (b.eV)	Γ_n[a] (meV)	Γ_f[a] (meV)	Γ_γ (meV) (assumed)
767	764	47.2 ± 6.0	$89^{+49}_{-33}{}^{+24}_{-16}$	$22^{-4}_{+16} \pm 3$	27
799	800	7.8 ± 1.4	$465^{+105}_{-100} \pm 50$	2.5 ± 0 ± 0.44	27
29.6 keV		108 ± 27			

[a] The first errors quoted in these columns are systematic and therefore correlated, the second errors are statistical.

---

(31) Weigmann H. Zeits. fur Phys. 114, 7 (1968).

(32) Lynn J. E. The Theory of Neutron Resonance Reactions (Clarendon Press, Oxford, 1968) p. 463 and AERE Report R - 5891.

(33) Strutinsky V. M. Nucl. Phys. A95, 420 (1967).

(34) Pattenden N. J. Nuclear Structure with Neutrons, EANDC-50S, Vol. I, 93 (1965).

E. The total cross-section of ^{6}Li (K. M. Diment and C. A. Uttley)

In the last progress report[35] we described the results of analysing the total cross-section of ^{6}Li from 70 eV to 5 keV by fitting a curve of the form $c/\sqrt{E} + b$ to the data, and presented a preliminary analysis of the p-wave resonance at 250 keV in which it is assumed that the resonance is superimposed on an s-wave background total cross-section which is the sum of the $c/\sqrt{E}$ absorption cross-section and a potential scattering cross-section for which the value at low energies is equal to b.

The parameters of the p-wave resonance, which are determined by fitting a single level Breit-Wigner formula to the resonance, are the reduced neutron width γ_n^2, the reduced alpha width γ_α^2 and the energy eigenvalue E_λ'. These parameters depend in principle on the choice of interaction radii R_n, R_α for the entrance and exit channels respectively, but the almost constant values of χ^2 obtained show that the fits are insensitive to variations in R_n from 2.5 to 3.9 fm and in R_α from 3 to 4 fm, within which limits the channel radii are expected to lie. In fact for $R_n < 2.5$ fm the reduced neutron width γ_n^2 becomes greater than the sum rule limit $3\hbar^2/4\mu R_n^2$, where μ is the reduced neutron mass. Furthermore it is found that the p-wave absorption and scattering cross-section at energies below the resonance are also insensitive to the choice of interaction radii. Thus the presence of a minimum in the total cross-section at about 75 keV should allow the validity of the above mentioned extrapolation of the s-wave interaction to higher energies to be tested by comparing the calculated s-wave and the p-wave resonance total cross-sections with the measured data near 75 keV. This comparison is shown in Fig. 8, where the dotted curve is seen to lie systematically higher than the experimental points.

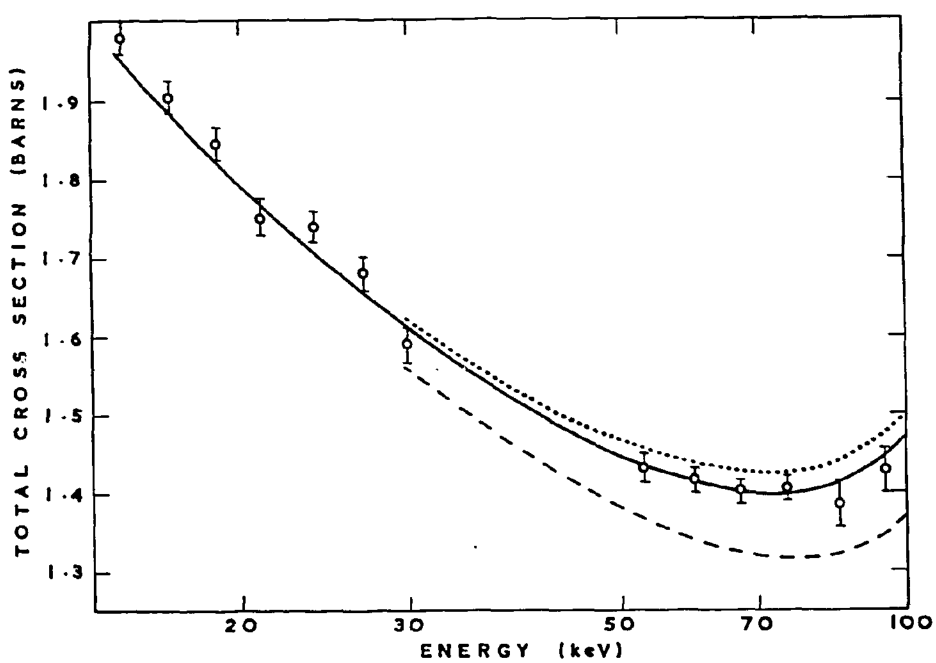

Fig. 8. Comparison of calculated and experimental cross sections for ^{6}Li near the 70 keV minimum.

(35) Diment K. M. and Uttley C. A. Nuclear Physics Division Report AERE PR/NP14 (1968).

A similar comparison can be made with the measured total cross-section near the minimum at 1 MeV and also between the calculated s- and p-wave scattering cross-section and the experimental elastic scattering data obtained by Lane et al.(36) and by Knitter and Coppola(37) at 1 MeV. In these calculations, shown as dashed curves in Fig. 9, the minimum p-wave resonance contribution was used, corresponding to an entrance channel radius of 2.5 fm. At this energy the calculated total and scattering cross-sections are both too large, indicating that the s-wave scattering at least must decrease with increasing energy faster than potential scattering.

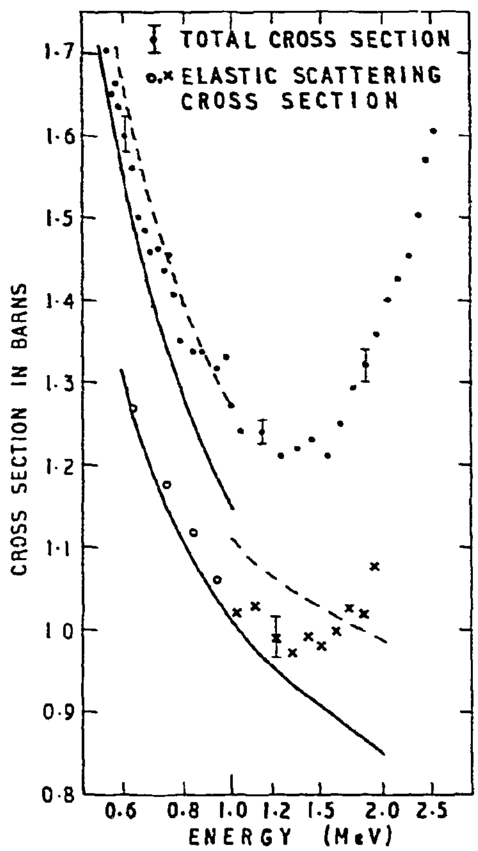

Fig. 9. Comparison of calculated total and scattering cross-sections with experimental results near 1 MeV.

The fact that the s-wave scattering cross-section varies somewhat more rapidly with energy than would be expected if the s-wave interaction were due to very distant s-states can be explained by considering the scattering lengths. The scattering lengths a_+ and a_- for the $^3\!/_2+$ and $\frac{1}{2}+$ s-wave spin sequences respectively are complex, because the absorption width in each channel is appreciable. If it is assumed that for each spin sequence only one resonance contributes significantly at low energies then the parameters which define the imaginary parts of the scattering lengths are those which determine the fraction of the low energy, e.g. thermal, absorption cross-section due to each spin state. It has been found(38) that 75% of the s-wave absorption cross-section is due to the $\frac{1}{2}+$ spin sequence. The real parts of the scattering lengths a_+, a_- can now be determined by combining the real part of the coherent scattering length (+1.8 fm) measured by Peterson et al.(39) with the measured constant b = 0.7 barns(35), which is close to the zero energy (free atom) scattering cross-section. Of the two possible pairs of real scattering lengths derived from this analysis, one is incompatible with the observations of Lane et al.(40) on the scattering of polarized neutrons by ^{6}Li, which show that most of the s-wave scattering cross-section takes place with channel spin $\frac{1}{2}$. The alternative pair makes the real parts of a_+, a_- +0.2261 fm and +4.174 fm respectively, and the large value of the latter for such a light nucleus suggests that a bound $\frac{1}{2}+$ state is present in ^{7}Li. The only possible location of this state is the broad level at 6.56 MeV which does not have a definitely assigned spin and parity(41). Specifying the position of this $\frac{1}{2}+$ state allows one to derive both the reduced neutron width and the alpha width from the real and imaginary parts of a_- for a given choice of entrance channel radius R_n. A similar calculation can be made for the $^3\!/_2+$ state, which is much less important than the $\frac{1}{2}+$ state since it contributes only 25% of the absorption cross-section and a negligible fraction of the scattering cross-section. Since the real part of a_+ is small this state must be at positive energies, and it has been assumed to be the first unassigned level at 2.447 MeV (C.M.)

(36) Lane R. O., Langsdorf A., Monahan J. E. and Elwyn A. J. Ann. Phys. 12, 135 (1961).

(37) Knitter H. H. and Coppola M. EANDC(E)100 AL (1967).

(38) Mahaux C. and Robaye G. Nucl. Phys. 74, 161 (1965).

(39) Peterson S. W. and Smith H. G. J. Phys. Soc. Japan 17, Supplement B-11, 335 (1962).

(40) Lane R. O., Elwyn A. J. and Langsdorf A. Phys. Rev. 136, B 1710 (1964).

(41) Lauritsen T. and Ajzenberg-Selove F. Nucl. Phys. 78, 1 (1966).

The s-wave total and partial cross-section can now be calculated for different values of R_n. The value $R_n = 2.5$ fm gives a very poor fit to the total cross-section, even below 100 keV, as the dashed curve in Fig. 8 shows, because the scattering cross-section decreases too rapidly with increasing energy. An effective radius of 3.9 fm, however, produces parameters $\gamma_n^2 = 0.214$ MeV and $\Gamma_\alpha = 2.58$ MeV for the bound state, which gives a good fit, as shown by the solid curve in Fig. 8. In this case the resonance scattering is much less and potential scattering dominates. Extending the comparison to the measured data near 1 MeV we see from the solid curve in Fig. 9 that the calculated scattering cross-section joins smoothly with the measured one while the calculated total cross-section falls increasingly below the measured total cross-section as the energy rises towards 1 MeV. This is to be expected, since the states forming the maximum near 4 MeV will contribute an absorption cross-section below 1 MeV which decreases linearly with penetrability, while the resonance scattering will fall even more rapidly than the square of the penetrability because of the negative contribution from resonance - potential interference.

The s-wave absorption cross-section derived from this analysis can be expressed as (E in eV)

$$\sigma_{n,\alpha} = 149.56/\sqrt{E} + \Delta(E)$$

where $\Delta(E)$ is constant at -0.024 barns up to a few keV and decreases to -0.048 barns at 1 MeV. However the absorption cross-section still remains somewhat sensitive to the initial assumptions involved, particularly the assumed position of the $\frac{3}{2}^+$ state. We suggest therefore that the ^{6}Li(n,α)T cross-section up to the threshold for the ^{6}Li(n,dn)α reaction at 1.7 MeV can be obtained by subtracting the scattering cross-section from the measured total cross-section.

E. Neutron scattering measurements on ^{10}B and ^{6}Li. (A. Asami (J.A.E.R.I. Japan) and M. C. Moxon)

The neutron scattering measurements on ^{10}B have been completed and the data have been analysed. The observed values of the scattering cross section in the energy range 0.9 to 130 keV are given in Table IV. The measurements of the scattering cross-section of ^{6}Li have been completed and are now being analysed.

GENERAL NUCLEAR DATA FOR REACTORS

Shape quantum numbers in sub-threshold fission (J. E. Lynn)

It has long been believed that the fission mode of motion of an excited nucleus is one that is strongly damped; i.e. the elementary fission mode, a prolate shape vibration leading to division of the nucleus, is dissolved among the compound nucleus states over a very broad energy interval. Now, however, there is evidence that the strong damping mechanism breaks down, at least for sub-threshold fission, and that this breakdown is associated with the existence of metastable shapes of the nucleus.

There are four main groups of evidence. The first starts from the discovery of spontaneous-fissioning isomers by Flerov and Polikanov in 1964. Since the original discovery, a number of these highly interesting isomeric states have been discovered, and their properties investigated, mainly by Flerov and Polikanov's group in Russia(42) and by Bjørnholm and his colleagues(43) in Copenhagen. Their half-lives are in the nanosecond to millisecond range and the principal mode of decay appears to be spontaneous fission. The energies of these states have been found in a few cases to be about 3 MeV above the ground state of the respective isotope, thus showing that their peculiar property is not the decay by spontaneous fission, but the extraordinary inhibition of gamma-decay to lower states. Analysis of the shapes of the yield curves for formation of the isomers shows that their spins are not particularly high (≈ 7).

(42) Flerov G. N., Polikanov S. M. et al., Nucl. Phys. A97, 444 (1967).

(43) Borggren J., Gangrsky Y. P., Slettin G. and Bjørnholm S. Phys. Letters 25B, 402 (1967).

TABLE IV

Total scattering cross section for ^{10}B (averaging intervals indicated).

Energy (keV)	Energy Interval (keV)	Scattering Cross Section (barns)	Total Uncertainty
0.1271E 03	0.2182E 02	0.2974E 01	0.3316E 01
0.1065E 03	0.1677E 02	0.2892E 01	0.4656E 01
0.7803E 02	0.1052E 02	0.2621E 01	0.4666E 01
0.6788E 02	0.8550E 01	0.2561E 01	0.4457E 01
0.5960E 02	0.7030E 01	0.2565E 01	0.4846E 01
0.5274E 02	0.5860E 01	0.2502E 01	0.5211E 01
0.4701E 02	0.4930E 01	0.2499E 01	0.5354E 01
0.4216E 02	0.4190E 01	0.2510E 01	0.6722E 01
0.2752E 02	0.4430E 01	0.2320E 01	0.4988E 01
0.2335E 02	0.3460E 01	0.2298E 01	0.5075E 01
0.2006E 02	0.2760E 01	0.2246E 01	0.5062E 01
0.1743E 02	0.2230E 01	0.2237E 01	0.5188E 01
0.1528E 02	0.1830E 01	0.2252E 01	0.5332E 01
0.1350E 02	0.1520E 01	0.2210E 01	0.5457E 01
0.1202E 02	0.1280E 01	0.2248E 01	0.5590E 01
0.1025E 02	0.2012E 01	0.2230E 01	0.5526E 01
0.8400E 01	0.1493E 01	0.2237E 01	0.5789E 01
0.7010E 01	0.1139E 01	0.2259E 01	0.6026E 01
0.5940E 01	0.8880E 00	0.2264E 01	0.6687E 01
0.5100E 01	0.7060E 00	0.2203E 01	0.6343E 01
0.4420E 01	0.5710E 00	0.2236E 01	0.6817E 01
0.3870E 01	0.4680E 00	0.2191E 01	0.7858E 01
0.1935E 01	0.3300E 00	0.2203E 01	0.7778E 01
0.1625E 01	0.2540E 00	0.2163E 01	0.7515E 01
0.1385E 01	0.2000E 00	0.2153E 01	0.7598E 01
0.1195E 01	0.1600E 00	0.2170E 01	0.7833E 01
0.1040E 01	0.1310E 00	0.2169E 01	0.8103E 01
0.9150E 00	0.1070E 00	0.2155E 01	0.8238E 01
0.7000E 00	0.2840E 00	0.2108E 01	0.8223E 01
0.4700E 00	0.1570E 00	0.2063E 01	0.8881E 01

The second line of research, due to Strutinsky[44], is a purely theoretical investigation into the deformation energy of nuclei. In an effort to explain the equilibrium deformations of non-magic nuclei as well as the heights and saddle-point deformations of fission barriers, Strutinsky adopted a combination of liquid-drop model, which provides the major component of the nuclear mass, and a Nilsson deformed shell-model; the latter provides a correction term to the liquid-drop energy. Minima in the shell-correction term occur where there are gaps in the single-particle level structure near the Fermi energy of the system. For spherical nuclei these minima are most pronounced at the magic numbers, but the important property of the Nilsson diagram which Strutinsky emphasises is that other gaps occur at non-zero deformations, and that for a given nucleon number such gaps recur with increasing deformation. Thus according to the calculations several minima can occur in the potential energy of deformation of a nucleus, and in particular a secondary minimum of this kind is expected to be strongly pronounced in the trans-uranic nuclei. This secondary minimum provides a possible explanation of the spontaneous fissioning isomers; such an isomer would be the lowest vibrational state of the secondary minimum. For such an isomer tunnelling towards decay by spontaneous fission would be less inhibited than usual, while gamma decay would be strongly reduced because of the small amplitude of the wave function in the normal minimum.

The Strutinsky theory also provides a possible explanation of the third phenomenon. This is the coarse structure found in neutron-induced sub-threshold fission cross-sections. Typical of these data (averaged over many resonances) are the peak at 750 keV in the cross-section of ^{230}Th, which rises[45] to 50 mb and falls to 10 mb in less than 100 keV, the peaks at 1.6 and 1.7 MeV in the cross-section of ^{232}Th, and the 15 keV wide peak[46] at 12 keV in the cross-section of ^{241}Am. Such structure cannot be explained quantitatively in terms of competition from inelastic scattering. It appears to be gross structure in the fission mode, of a kind that can be explained phenomenologically by a complex potential model having a very small damping component (of the order of tens of keV). Damping widths are believed to be strong functions of the intrinsic excitation energy available to a compound nucleus, so the small width might be explained as being due to the occurrence of the sub-threshold fission mode as a vibration in a shallow, secondary minimum.

The fourth phenomenon lends still more support to the idea of a secondary minimum in the deformation energy. This phenomenon was discovered originally in the compound nucleus ^{238}Np at Saclay[47], in ^{241}Pu at Geel[48] and a little later in ^{235}U, ^{240}Pu and ^{243}Pu at Harwell[49], when observations revealed that in the slow neutron cross-sections of these fissionable, but sub-fissile, nuclei narrow bands of resonances with large fission widths occurred among the normal resonances with very weak fission. These 'fissile bands' are spaced at intervals of the order of 50 to 1000 times that of the fine structure resonances. This kind of resonance structure indicates the influence of a new, nearly good, quantum number, in addition to the usual ones of total angular momentum and parity. The properties of the observed structure strongly suggest that this new quantum number is a shape quantum number associated with the Strutinsky deformation potential[50,51]. The second minimum in the potential energy curve provides a second class of states, of complicated 'compound nucleus' type, that are associated

---

(44) Strutinsky V. M. Nucl. Phys. A95, 420 (1967).

(45) Evans J. E. and Jones G. A. - private communication (1965).

(46) Seeger P. A., Hemmendinger A. and Diven B. C. Nucl. Phys. A96, 605 (1967).

(47) Fubini A., Blons J., Michaudon A. and Paya D. Phys. Rev. Letters 20, 1373 (1968).

(48) Migneco E. and Theobald J. P. Nucl. Phys. A112, 603 (1968).

(49) James G. D. and Rae E. R. Nucl. Phys. A118, 313 (1968).
Patrick B. H. and James G. D. Phys. Letters (in press)
James G. D. Nucl. Phys. (to be published) and Harwell Report AERE - R 5924.

(50) Lynn J. E. "Theory of Neutron Resonance Reactions", (Clarendon Press, Oxford 1968) p. 461.
Harwell Report AERE - R 5891 (1968).
Structure effects in nuclear fission, invited paper at Dubna International Symposium on Nuclear Structure, July 1968.

(51) Weigmann H. Zeits fur Phys. 114, 7 (1968).

with prolate shape vibrations having most of their amplitude in this minimum. The lowest, or 'ground', state of this class of states is the spontaneously fissioning isomer. For a given total energy of the compound nucleus, these states are much less dense than compound states of the other class (associated with vibrations in the deeper minimum), because the effective excitation energy for intrinsic nucleonic motion is less. At the same time they have a much greater probability of fissioning (having only one barrier, the saddle-point barrier, to tunnel through) and negligible chance of elastic neutron emission. The high intermediate maximum between the two wells causes the coupling between the two classes of states to be weak, thus accounting for the observed phenomenon that the fission width of each class II state spread into a few only of its class I neighbours.

The detailed quantitative structure in the cross-section depends on a number of factors. The spacing of the fissile bands (the class II level spacing) relative to the normal resonance spacing (the class I level spacing) is governed principally by the potential energy difference between the two minima. The application of a statistical level density law to the cross sections so far measured suggests that this difference ranges from about 1.9 MeV (in ^{241}Pu) to about 3.3 MeV (in ^{243}Pu). The widths of the fissile bands are expected to depend in a rather complex manner on the height of the intermediate maximum (which determines a 'damping' or 'spreading' width of the class II states into the denser class I states) and on the height of the saddle-point barrier which governs the 'natural' decay of the class II states by fission. These relations are complicated even more by the possible existence of gross structure in the class II fission and by statistical fluctuations of the individual coupling matrix elements and the class II fission widths; such statistical fluctuations are of the kind very familiar in normal resonance cross sections.

Some of these effects have already been studied semi-quantitatively[50] and we are now beginning more detailed theoretical studies. In particular, we are attempting numerical calculations of complicated intermediate coupling situations so that experimental data can be analysed more fully, and we are also making a quantitative study of the dependence of coupling widths on the height and 'thickness' of the intermediate barrier.

E. Capture γ-ray spectra following resonance neutron capture (P. Axmann (Vienna), M. C. Moxon and P. Riehs (Vienna))

In many laboratories germanium crystal diodes have been used in conjunction with time of flight techniques to examine γ-ray spectra following resonance neutron capture. However, because the efficiency of these detectors is low, high neutron fluxes are required in these measurements and only a few low energy resonances can be resolved well enough to allow the γ-ray spectra to be examined. Although large sodium iodide crystals have a much poorer γ-ray energy resolution than germanium detectors, their overall efficiency for detecting high energy γ-rays is at least an order of magnitude greater, so that they can be used with longer flight paths and hence, better neutron energy resolution. Thus they allow more resonances to be examined, and so indicate elements and neutron energy regions where germanium crystals can be usefully employed to study the spectra in finer detail.

We have used an 8 inch diameter 6 inch thick NaI crystal at the end of a 45 m flight path to examine γ spectra following neutron capture. The overall timing resolution ranged from ~23 nsec/m for $E_n < 50$ eV to ~5 nsec/m for $E_n \leqslant 1$ keV. The data were recorded in 16 bit binary form on 1 inch magnetic tape, 10 bits for the time of flight data and 6 bits for the gamma ray energy information.

The γ-ray spectrum for each individual resonance was obtained by summing each gamma ray energy channel over the time of flight channels spanning the resonance. The background for each summed gamma ray channel was calculated from the gamma spectra for time of flight channels on either side of the resonance. The resulting γ-ray spectra were then normalised to unit area, so that the gamma ray spectra of several resonances could be easily compared.

The high energy γ-ray spectra emitted following neutron capture by ^{198}Hg showed marked fluctuations over the first five resonances, and suggested that the γ spectrum for the 23 eV resonance was more typical of the isotope than the spectrum for the 98 eV resonance. The nature of these spectra suggested that this isotope should be studied with a germanium spectrometer[52]. Data for the other isotopes of Hg, for ^{197}Au and for ^{181}Ta have also been accumulated and are at present being analysed. In the case of ^{197}Au, where 55 resonances could be easily examined, the observed fluctuations in the spectra can probably be explained in terms of Porter-Thomas distributions for the partial radiation width.

E. Gamma-ray spectra from resonance neutron capture (B. W. Thomas, J. Murray, E. R. Rae and C. A. Uttley)

Much of the work carried out during the last six months has been a measurement of the resonance capture gamma-ray spectra of mercury, particularly for the reaction ^{198}Hg(n,γ)^{199}Hg[53].

Experimental data from a target of natural mercuric oxide were collected on the 10 metre flight path of the Harwell linear accelerator, using a 25 cm^3 co-axial Ge(Li) detector for the gamma rays. The raw data were handled by an on-line system based on the PDP-4 computer, which permits the storage of capture data for continuous ranges of neutron and gamma-ray energy, by associating with each capture event both time-of-flight and pulse height co-ordinates.

Analysis of the data into resonance gamma-ray spectra was carried out by selecting those events falling in the appropriate intervals in the time-of-flight spectrum. In this way gamma-ray spectra were obtained for known resonances in ^{198}Hg and ^{201}Hg, the background spectra being deduced from analysis of data between resonances.

Figure 10 shows a time-of-flight spectrum for mercury obtained by summation over pulse heights $\geq$800 keV, while Figure 11 shows high energy (4-7 MeV) gamma-ray spectra for five resonances in ^{198}Hg.

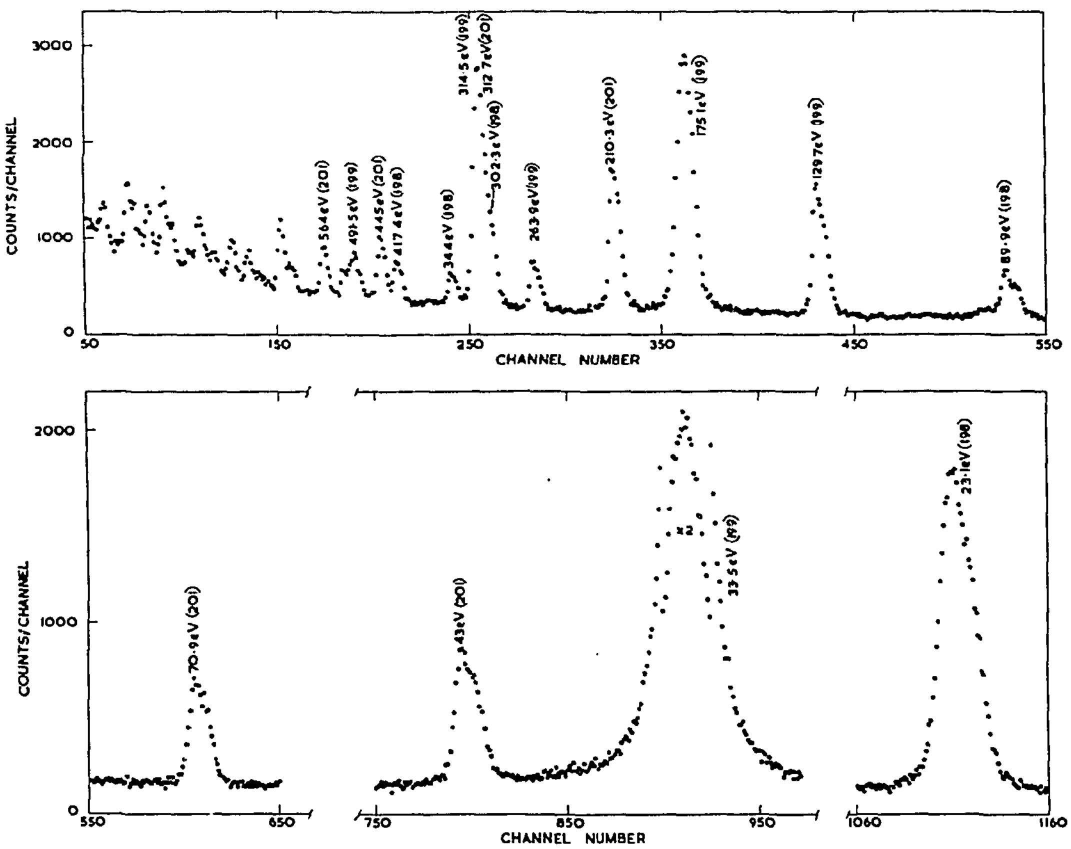

Fig. 10. Time of flight spectrum of mercury for E_γ > 800 keV.

(52) Thomas B. W., Murray J., Rae E. R. and Uttley C. A. This report p. 18.

(53) Thomas B. W., Uttley C. A. and Rae E. R. Nuclear Physics Division Progress Report AERE - PR/NP 14 p. 23, (1968).

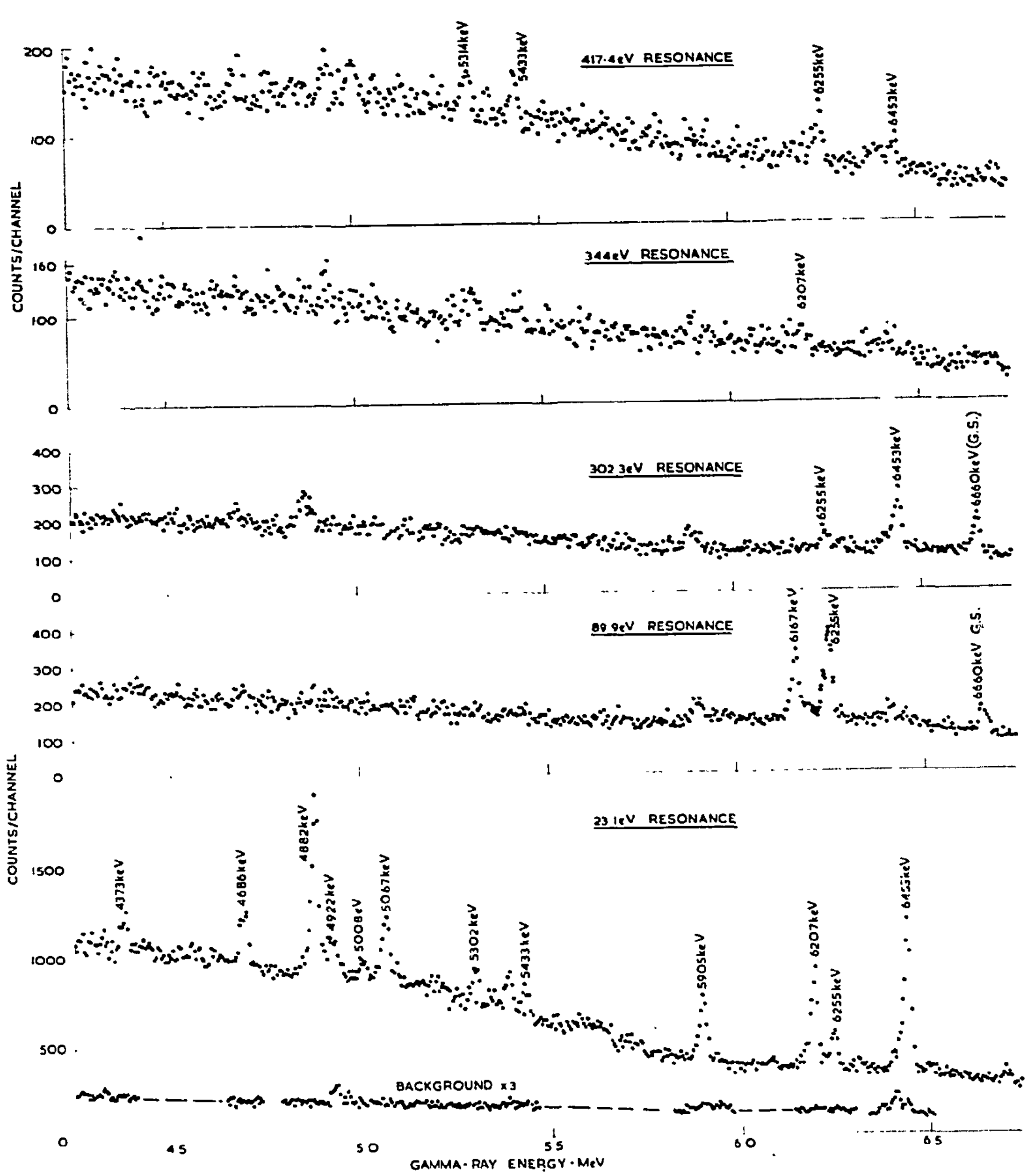

Fig. 11. Gamma rays in range 4 → 7 MeV from five slow neutron capture resonances of ^{198}Hg.

Table V (see page 20) lists estimates of the relative intensities of the gamma-rays observed. Several gamma-rays with energies below 2 MeV were distinguishable only at the relatively strong 23 eV resonance. An outstanding feature of the ^{198}Hg data is the sharp contrast in the 23 eV and 90 eV resonance spectra between 4.5 and 5.5 MeV.

An energy calibration was obtained by comparing the caputre spectrum of the 34 eV resonance in ^{199}Hg with published data on thermal neutron capture[54] and the resonance spectra were normalised using the integrated pulse height spectrum between 1.5 and 2.3 MeV.

(54) Schult O. W. B. et al. Phys. Rev. 164, 1548 (1967).

TABLE V

Relative intensities of gamma ray transitions in ^{199}Hg following its formation in various slow neutron capture resonances.

E_γ keV	Relative intensities of Gamma-rays(b)				
	23.1 eV res.	89.9 eV res.	301 eV res.	344 eV res.	417 eV res.
(a) 755	7.9 (0.8)				
876	1.7 (0.8)				
896	1.3 (0.8)				
1012	6.6 (0.9)				
1055	3.8 (0.9)				
1138	4.3 (1.0)				
1321	3.8 (1.1)				
1381	8.5 (1.0)				
1532	4.8 (1.2)				
1568	8.6 (1.2)				
1775	6.8 (1.0)				
4373	3.5 (0.5)	-0.6 (1.8)	2.8 (1.7)	2.9 (4.3)	-1.6 (3.0)
4686	6.7 (0.6)	2.9 (1.1)	4.2 (1.6)	4.1 (3.8)	5.6 (2.8)
4882	23.0 (0.8)	3.2 (1.6)	7.4 (1.5)	-1.3 (3.9)	1.3 (3.3)
4922	5.3 (0.6)	1.7 (1.7)	-0.1 (1.6)	3.2 (3.4)	0.8 (2.5)
5008	3.5 (0.4)	-0.7 (1.7)	-0.2 (1.8)	2.9 (3.6)	14.7 (3.5)
5067	7.4 (0.6)	0.1 (1.8)	0.9 (1.6)	0.2 (3.8)	3.8 (2.7)
5302	3.9 (0.5)	-1.3 (1.6)	-0.1 (1.0)	5.5 (2.8)	-
5314	-	0.7 (1.4)	0.6 (1.2)	10.4 (3.1)	13.6 (3.4)
5433	3.2 (0.5)	1.3 (1.3)	2.4 (1.5)	4.5 (3.1)	12.5 (3.1)
5517	0.2 (0.4)	-0.5 (2.0)	-1.0 (1.3)	2.7 (2.8)	0.2 (4.0)
5905	7.2 (0.4)	8.1 (1.2)	4.2 (1.2)	7.2 (2.9)	-0.3 (2.5)
6167	0.2 (0.3)	33.2 (2.3)	0.2 (1.6)	1.1 (2.8)	0.8 (2.4)
6207	9.7 (0.4)	6.8 (1.7)	1.3 (1.2)	10.1 (3.1)	1.5 (2.0)
6255	4.3 (0.4)	39.8 (2.0)	8.0 (1.3)	-0.7 (2.8)	14.1 (2.2)
6453	17.2 (0.5)	1.6 (1.6)	25.5 (1.8)	0.8 (2.5)	8.4 (2.1)
6660	0.1 (0.2)	11.9 (1.5)	14.7 (1.5)	2.0 (2.2)	-0.9 (1.5)

(a) Energies are in most cases accurate to ± 3 keV.

(b) Numbers in parentheses denote statistical errors. Systematic errors due to uncertainties in the efficiency curve and the normalisation may add a further 15%.

The resolution of the mercury gamma ray spectra is poorer than expected and the lines show low energy tails characteristic of radiation damage, which would arise in this experiment because of the fast neutrons scattered into the detector from the target. The resolution was recovered by annealing at 0°C.

A second flight path at 20 metres has now been established to obtain resonance capture gamma-ray spectra with better time of flight resolution.

E. Angular distributions of fragments from ^{235}U neutron-induced fission in resonances (N. J. Pattenden, J. E. Jolly, H. Postma and K. Ravensberg (F.O.M. Netherlands) and J. C. Waldron (Chemistry))

A new experiment is being prepared to study the angular distribution of fragments omitted from ^{235}U nuclei undergoing fission induced by slow neutrons. The resonances found in slow neutron cross sections correspond to compound nucleus levels with total angular momentum $J = |I \pm \frac{1}{2}|$ (I is the target spin) and with the parity of the target nucleus. The total angular momentum and parity are almost certainly the only remaining good quantum numbers for the levels of a highly excited nucleus (the excitation energy is about 6 MeV for fissile targets). In the process of fissioning, the compound nuclei formed from the commoner fissile targets pass over the saddle point in the deformation energy surface with an "internal" excitation of about 1 MeV; at this low excitation value the number of transition states at the saddle point is very small, their wave functions are "collective" in character, and they have the projection K of the angular momentum on the cylindrical symmetry axis of the nucleus as an additional good quantum number. Furthermore, all the evidence points to the fact that K remains a good quantum number as the nucleus deforms from its saddle point shape to its scission point. If, now, the spin axes of the target nuclei are aligned, say, perpendicular to the incident neutron beam, the total angular momentum of the compound nuclei will be aligned mainly in this direction too. Consequently, when fission proceeds through a particular transition state, the value of K of the transition state determines the probable direction of the nuclear symmetry axis with respect to the beam, and this is the direction for emission of fission fragments. Thus, by measuring the angular distribution of fission products it is possible to find the probability that the fissioning nucleus passes through transition states of different K. If this information is known for a large number of compound nucleus levels it becomes possible to answer the following questions of nuclear theory in general and fission theory in particular:-

(1) The mean rate of fission through a transition state that is known to be low-lying (e.g. one with $K = 0$) with show whether the transition state is strongly coupled to the compound nucleus wave function (as intuitively expected) or is more weakly coupled (the case for neutron and proton single particle states).

(2) It may be possible to determine the positions of some of the higher transition states. This will provide evidence of the behaviour of nuclear collective states as a function of deformation.

It may also be possible to see if other phenomena (e.g. mass yields or ternary fission) are associated with particular transition states.

To produce anisotropic angular distributions the ^{235}U nuclei in the sample must be partially aligned. Dabbs [55] achieved alignment by cooling a crystal of rubidium uranyl nitrate, $RbUO_2(NO_3)_3$, to about $0.5^{\circ}K$ in a ^3He cryostat. The nuclear electric quadrupole moment interacts with the crystal field to give alignment of the major nuclear axis in a plane perpendicular to the c-axis of the crystal. The degree of alignment is approximately inversely proportional to the absolute temperature. We will depart from Dabbs' technique in certain details, which should produce significantly lower sample temperatures and thus increase the experimental anisotropies. In particular we will use a ^3He-^4He dilution refrigerator [56,57] in the cryostat, instead of an ^3He evaporation refrigerator.

The experiment is an example of co-operation between laboratories in different countries viz. the Stichting voor Fundamenteel Onderzoek der Materie (Organization for Fundamental Research on Matter, abbreviated to F.O.M.) Netherlands, and A.E.R.E. A preliminary experiment was performed at the Dutch high flux reactor at Petten, using the F.O.M. facilities of a neutron beam, crystal monochromator and nuclear orientation cryostat, to show that our method would produce anisotropy effects of the right order. The cryostat was designed and made by the F.O.M. Group, and then brought to the Harwell electron linac,

(55) Dabbs J. W. T., Walter F. J. and Parker G. W. Proc. Physics and Chemistry of Fission Conference, 1, 39 (1965).

(56) London H.; Clarke G. R. and Mendoza E. Phys. Rev. 128, 1992 (1962).

(57) Wheatley J. C., Vilches D. E. and Abel W. R. Physics 4, 1 (1968).

and reassembled on a 10 m flight path in a specially designed blockhouse. Tests have shown that the refrigerator can attain temperatures of less than about $0.06^{o}K$. The next step, which is to mount a sample and fission fragment detectors in the cryostat and to make the first run on the linac, will take place shortly.

The technique of growing crystals with a coating of enriched ^{235}U has been learned by the Preparative Group, Chemistry Division, who are now producing samples for the linac experiment.

FUNDAMENTAL AND BASIC RESEARCH

NUCLEAR STRUCTURE AND DYNAMICS

Experiments relating to pure Fermi beta decays and to theories of weak interactions (J. M. Freeman, D. C. Robinson, G. L. Wick, T. T. Thwaites, G. Murray (Manchester) and W. E. Burcham (Birmingham))

As we pointed out in the last progress report, the most valuable precise determinations of ft values for superallowed Fermi decays at present would be those for which Z is small, since the theoretical interpretation in terms of the strangeness-conserving vector coupling constant is then more reliable. We are therefore continuing to concentrate on the decay rates of low Z isotopes, particularly ^{10}C, but are also investigating ^{35}A, since here the Fermi decay mode happens to be dominant, and a direct comparison is possible with ft values for even mass isotopes.

I The Decay $^{35}A(\beta^{+})^{35}Cl$

Eleven determinations of the $^{35}Cl(p,n)^{35}A$ reaction threshold have been made by the method which we used previously to measure even Z thresholds. The preliminary result is 6939.5 ± 0.8 (± 1.3) keV. Here the first error is purely statistical, while the second includes possible systematic errors.

To determine the strength of the two weak branches in the ^{35}A decay a continuous flow target system has been build in which carbon tetrachloride vapour is irradiated with protons. A refrigerator and liquid nitrogen trap subsequently condense out the CCl_4 vapour and active contaminants, while the radioactive ^{35}A passes on through a shielded decay chamber. Gamma-rays following the decay of ^{35}A within the chamber can be detected with a Ge(Li) detector, and their intensities compared with that of the annihilation radiation, which is a measure of the total decay rate. The system is at the testing stage.

II The $^{10}C(\beta^{+})^{10}B^{**}$ decay

Following up our comments in the preceeding Progress Report(58) the branching ratio for the ^{10}C Fermi decay has been carefully remeasured.

With a pneumatic target system we have obtained a large amount of data, to analyze which a computer programme is at present being developed. The problem is to determine to better than 1% accuracy a branching ratio which itself is only ~1%. The programme seeks to fit the gamma ray photopeak by superposing two gaussian distributions and an arc tangent function. When properly normalized, the parameters describing the subsidiary gaussian and the arctangent function are smooth functions of the gamma ray energy. In this way the peak shape can be accurately described in terms of the three parameters of the main gaussian. So far this approach seems very promising.

---

(58) Nuclear Physics Division Progress Report AERE PR/NP 14, (1968).

III The decay $^{26}Al^m(\beta^+)^{26}Mg$

The data for determining the threshold of the reaction $^{26}Mg(p,n)^{26}Al^m$ have been carefully analysed, paying particular attention to the shape of the excitation curve, which exhibits a resonance-like behaviour just above the threshold. Calculations show that the use of the non-resonant $E^{3/2}$ formula introduces an error of not more than ±0.8 keV into the estimated value for the threshold. Our final result is E_{th} = 5208.2 ± 2.0 keV and the corresponding beta end-point for the $^{26}Al^m$ decay is 3208.8 ± 1.9 keV.

The decay data obtained from a series of measurements on $^{26}Al^m$ have been re-analysed, avoiding certain systematic errors[59] by fitting an exponential curve to the experimental decay data with weighting factors in the least squares calculation proportional to the inverse of the computed counts per channel. The final result obtained, $t_{1/2}$ = 6.346 ± 0.005 sec., is approximately 0.5% lower than the value published previously, which was derived by the normal method of analysis.

The ft value calculated from the above results, using presently accepted values of the Fermi functions[60], is 3026 ± 7 sec. Applying the radiative correction calculated by Källén[61] the ft value becomes 3081 ± 7 sec. This result emphasises the anomalous nature of the ^{26}Al ft value, which was recently discussed in the context of the Cabibbo theory of weak interactions by Brene et al[62].

IV The threshold for the reaction $^{25}Mg(p,n)^{25}Al$

This measurement arose as a by-product of the study of the $^{26}Mg(p,n)^{26}Al^m$ reaction, during a comparison of the decay characteristics of the positrons following (p,n) reactions in similarly prepared ^{26}Mg and ^{25}Mg targets. The difference between the the thresholds for the two reactions was found to be 54.7 ± 5.3 keV giving the result 5264 ± 6 keV for the $^{25}Mg(p,n)^{25}Al$ threshold. This value is not inconsistent with the measurement of Kington et al. (5289 ± 25 keV)[63], but the corresponding Q-value (-5058 ± 6 keV) is appreciably greater in absolute magnitude than that given in the 1964 mass tables (-5042 ± 6 keV)[64].

The $^{31}P(n,n'\gamma)^{31}P$ reaction (B. H. Armitage, A. T. G. Ferguson, G. C. Neilson* and W. D. N. Pritchard+)

We have investigated the gamma-rays emitted following inelastic neutron scattering from phosphorus, using equipment described in a preceding Progress Report[65]. The scattering sample consisted of red phosphorous powder contained in a thin walled polystyrene can, and formed a hollow right circular cylinder 5 cm in length, with inner and outer diameters of 1.3 and 5.2 cm respectively.

Gamma-ray spectra were taken using 5.3 MeV and 4.3 MeV neutrons, with the detector at 90° to the beam, and backgrounds were obtained from corresponding "sample out" measurements. The spectra obtained from the empty polystyrene can did not differ significantly from those obtained in the corresponding sample-out measurements.

The gamma-ray spectra produced in the $^{31}P(n,n'\gamma)^{31}P$ reaction are consistent with the level scheme shown in Fig. 12 (see page 24). All the transitions shown correspond to gamma-rays observed in our

(59) Nuclear Physics Division Progress Report AERE - PR/NP 12 (1967).

(60) Blin-Stoyle R. J. and Nair S. C. K. Nucl. Phys. A105, 640 (1967).

(61) Källén G. Nucl. Phys. 31, 225 (1967).

(62) Brene N., Roos M. and Sirlin A. Nucl. Phys. 36, 255 (1968).

(63) Kington J. D., Bair J. K., Cohn H. D., and Willard H. B. Phys. Rev. 99, 1393 (1955).

(64) Mattauch J. H. E., Thiele W., and Wapstra A. H. Nucl. Phys. 67, 1 (1965).

(65) Nuclear Physics Division Progress Report AERE - PR/NP 13 (1968).

* University of Alberta.

\+ On attachment from University of Exeter.

'5.3 MeV' spectra. The full lines represent transitions observed in both runs, the broken lines, transitions observed in the '5.3 MeV' runs only. The energy levels were determined from the measured energies of the gamma rays, and the numbers in parenthesis are intensities relative to the 1266.6 keV gamma-ray. No significant disagreement exists between the present decay scheme and that of Wolff et al.(66) derived from the $^{30}Si(p,\gamma)^{31}P$ reaction. In particular the branching ratio obtained for the decay of the 4593 keV level by Wolff et al(66) is consistent with the relative intensities of the 3326.1 keV and the 4593.4 keV gamma-rays observed here.

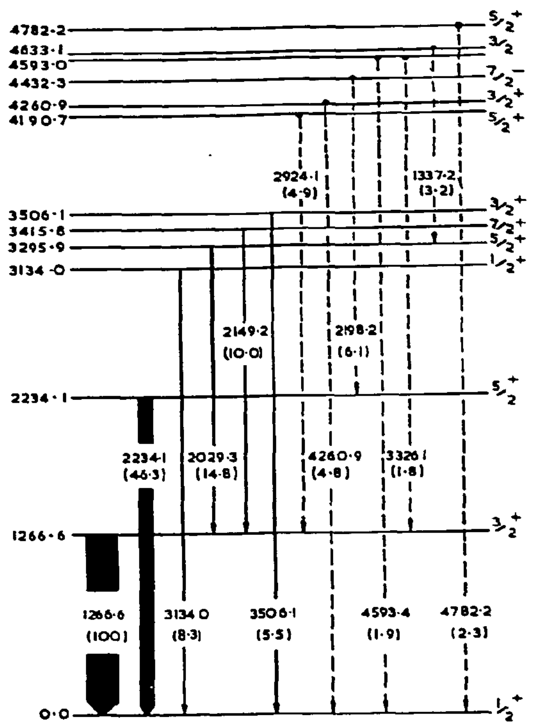

Fig. 12. Energy levels and gamma ray transitions in ^{31}P associated with the $^{31}P(n,n'\gamma)^{31}P$ reaction. The spin assignments are obtained from reference (67).

<u>In-beam spectroscopy using the beta spectrometer - studies of levels in $^{106,108}Cd$ and ^{208}Po (R. Chapman)</u>

The energies, multipolaries and branching ratios of transitions in $^{106,108}Cd$ are being determined from measurements of the prompt internal conversion electron spectra produced in the reactions $^{107,109}Ag(p,2n)^{106,108}Cd$. In-beam γ-ray spectra will also be taken in order to extract absolute conversion coefficients for the transitions.

Preliminary measurements of the prompt internal conversion electron spectrum produced in the reaction $^{209}Bi(p,2n)^{208}Po$ have been made in order to investigate the nuclear level scheme of ^{208}Po. Since these measurements were started, some similar work has been published(68), and further measurements with the beta-spectrometer await evaluation of the published data.

Measurements of monopole matrix elements for $0^{+'} \rightarrow 0^{+}$ transitions in a number of nuclei exhibiting vibrational type energy spectra are being undertaken. The $0^{+'}$ two-phonon vibrational states are being excited by nuclear reactions and the branching ratio of the 0^{+} states measured using the beta spectrometer.

<u>Studies of levels in ^{227}Ac (R. Chapman and F. J. G. Rogers (Chemistry Division))</u>

The energies, multipolarities and branching ratios of transitions in ^{227}Ac are being measured by a study of the internal conversion and γ-ray spectra from a 98.9% pure source of ^{231}Pa (which decays by alpha-emission to ^{227}Ac).

---

(66) Wolff A. C., Mayer M. A. and Endt P. M. Nuclear Physics A107, 332 (1968).

(67) Endt P. M. and C. Van der Leun, Nuclear Physics A105, 1 (1967).

(68) Treytl W. J., Hyde E. K. and Yamazaki T. Nuc. Phys. A117, 481 (1968).

G. Nuclear Structure Information from the Study of Isomeric States

I Isomeric States in the region Z = 63-83 (T. W. Conlon)

This region continues to be of considerable interest because of the variety of nuclear phenomena which can lead to the existence of isomers. These isomers include the shell model isomers expected in the closed shell regions Z = 82, N = 126, where states of high and low spins are expected to have similar energies, isomers the decay of which violates selection rules on the quantum number K and asymptotic quantum numbers, N, n_Z and Ω of the Unifield Model, and finally isomers associated with equilibrium nuclear shapes markedly different from those for lower lying levels. The last group are discussed further in the next section.

In the hope of studying all three types of transition a survey of this region over the time range 10^{-5} to 10^{-1} seconds is continuing. The A.E.R.E. Variable Energy Cyclotron can provide for this work pulsed proton beams with energies up to 50 MeV.

This survey has revealed many new isomers produced by the irradiation of natural targets. Table VI presents a partial summary of the information obtained to date. Only the target and the measured half-life are quoted, because the gamma-ray spectra from each isomeric state have not yet been considered in detail. Fig. 13 (see page 26) shows examples of gamma-ray spectra observed at the stated times after pulsed beam irradiation of selected targets. On the right of Fig. 13 the intensity of particular gamma-rays is shown as a function of time after irradiation.

TABLE VI

Measured lifetimes of isomeric activities observed in current observations

Z	Target	Half life in Seconds ± 20%
64	Gd	6×10^{-5}, 1.8×10^{-4}
65	Tb	4×10^{-4}
66	Dy	8×10^{-5}
67	Ho	5×10^{-4}, 1.2×10^{-3}
68	Er	5×10^{-5}
70	Yb	1.4×10^{-3}
74	W	2×10^{-3}
76	Os	8×10^{-3}
77	Ir	10×10^{-5}
82	Pb	1.1×10^{-3}

Experiments are now underway to identify - and to investigate in detail - the decay scheme of the isomeric nuclei. These experiments involve irradiation of separated isotopes of the targets of Table VI, and careful measurements of the energy of the K_α X-ray produced by internal conversion in the isomeric nucleus, of the relative intensities of the gamma-rays emitted, and in some cases, of the excitation functions for the states of interest.

II Shape Isomers (T. W. Conlon and A. J. Elwyn)

Shape hindered gamma-ray transitions or shape isomers were predicted(69) to occur in those isotopes of samarium and neighbouring elements with 88 to 90 neutrons. Such transitions have not yet been

(69) Sheline R. K., Kenefick R. A., Nealy C. L. and Udagawa T. Phys. Lett. 18 330 (1965).

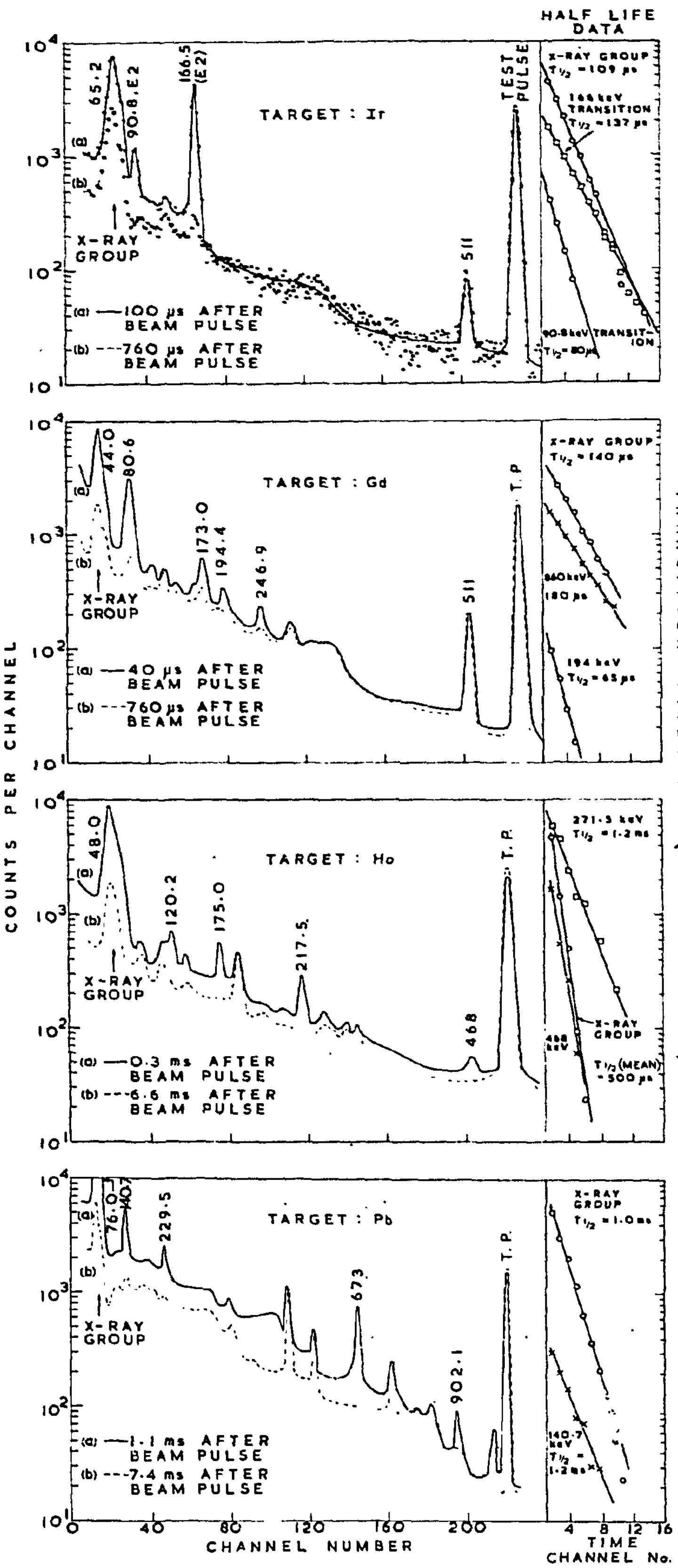

Fig. 13. Gamma ray spectra from isomeric activities induced by irradiation of Ir, Cd, Ho and Pb with 35 MeV protons.

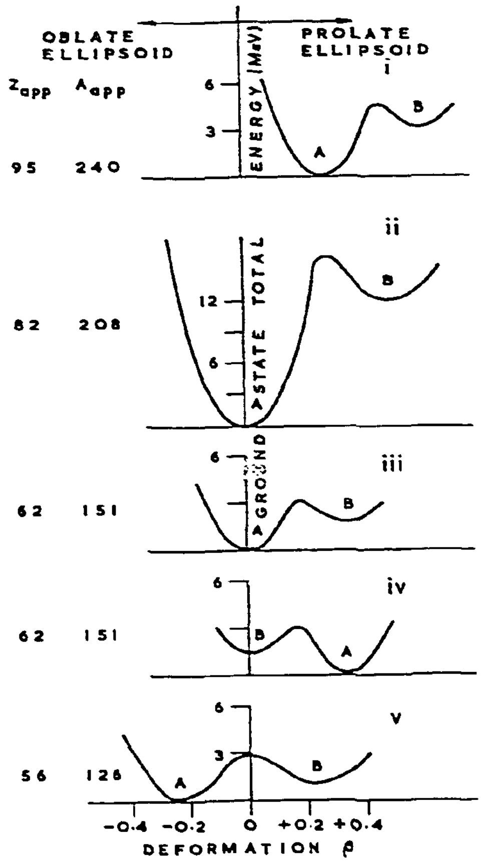

Fig. 14. Characteristic variation of nuclear binding energy with deformation β for particular combinations of N and Z.

confirmed experimentally although one possible example has been discussed(70). Meanwhile further calculations predict that shape isomers should occur in other regions of the periodic table. The current situation is summarised schematically in Fig. 14 where the nuclear energy is plotted as a function of the deformation parameter β. The common feature in this diagram is that more than one minimum occurs in the energy profile. Shape isomerism will occur whenever a transition occurs from a state of nuclear shape depicted by B in Fig. 14 to a state of shape A.

Evidence for the energy profile shown in (i) of Figure 14 is found in the observation of fissioning isomers(71,72,73) while evidence for the profiles shown in (iii) and (iv) has been discussed by Sheline et al(69). Recent calculations by Strutinsky(73) suggest for the Pb region the profile (ii), and finally calculations of Arseniev et al.(74) predict that the profile (v) will occur in the newly discovered region of deformation in the neighbourhood of ^{126}Ba(75). A survey of the type already underway (Section I) is well suited to study transitions in all the cases outlined above provided the half-lives involved are greater than about 10^{-6} seconds. The calculations of Wakai et al.(76) for the case of a nucleus represented by Fig. 14 (i) yield a gamma-ray inhibition of order 10^6 to 10^8 for a change in β from 0.5 (B) to 0.25 (A). This means that all but the fastest El and Ml transitions would have half-lives amenable to study by the techniques of Section I. We are extending the survey to search for the gamma-ray decay branch of the fissioning isomers. We also hope to investigate nuclei in the barium region (Fig. 14(v)) by heavy ion reactions such as $^{A}Sn\,(^{12}C,Xn)^{A+6-X}Ba$.

A programme to develope pulsed beams of ^{12}C ions of the required energy at the Variable Energy Cyclotron has been started.

III Relative Efficiency Calibration of Ge(Li) Dectector between 30 and 500 keV (T. W. Conlon)

The relative efficiency calibration of Ge(Li) detectors below about 500 keV is difficult because of the lack of standard sources with pairs of photons of precisely known relative intensity. The analysis of the data discussed in Section 1 requires a knowledge of the efficiency of the Ge(Li) detector over the

(70) Conlon T. W. Nucl. Phys. A100 No. 3 545 (1967).

(71) Bjornholm M. G., Borgreen J., Westgaard L. and Karnaukov V. A. Nucl. Phys. A97, 444 (1967).

(72) Lynn J. E. Nucl. Phys. (to be published).

(73) Strutinsky, V. M. Nucl. Phys. A95, 420 (1967).

(74) Arseniev D. A., Malov L. A., Sohiczenski V. and Soloviev V. G. Dubna Conf. Report, p. 93 (1968).

(75) Chanda R. N. UCRL Report No. 10798.

(76) Wakai M., Harada K. and Ohnishi N. Dubna Conf. Report, p. 91 (1968).

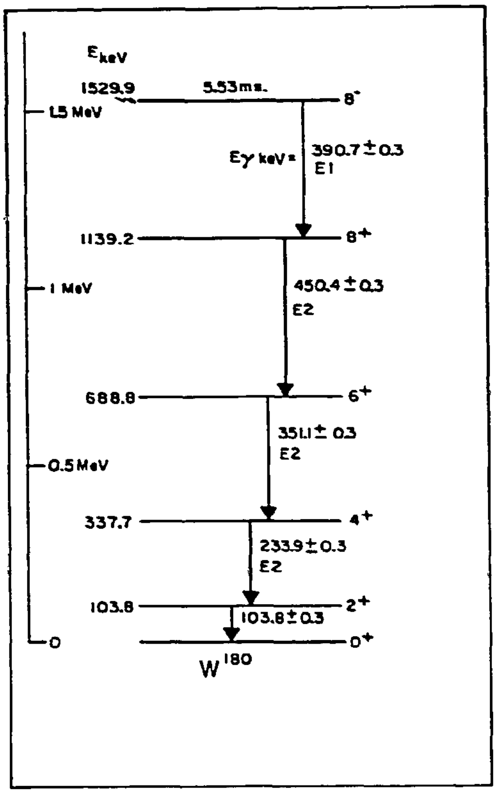

Fig. 15. Decay of 5.5 ms isomeric state of ^{180}W.

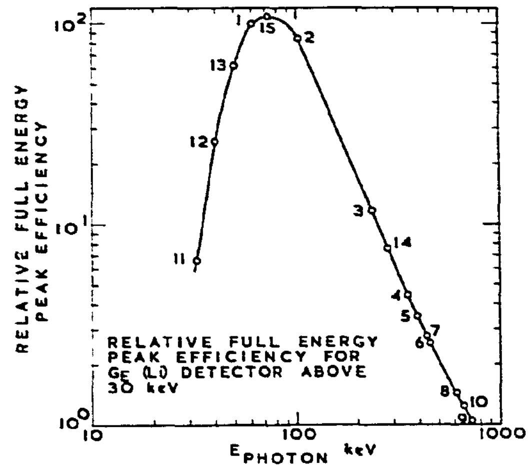

Fig. 16. Relative full energy peak efficiency for Ge(Li) dector above 30 keV.

range 30-500 keV, and we have devised a method for calibration(77) based on the isomeric decay of 5.5 ms $^{180}W^m$, which is shown in Fig. 15. In addition we use ^{137}Cs and ^{203}Hg sources, each of which provides a single gamma-ray and an X-ray of known relative intensity, and the source $^{108}Ag^m$ to extend the calibration(78) to energies greater than 500 keV. The calibration procedure is outlined below.

1. $^{180}W^m$ provides five gamma-rays in direct cascade, with no cross-over transitions of relative intensity greater than 10^{-4} per isomeric decay, and also provides an X-ray group of average energy 61 keV. The intensities of these six transitions after applying corrections for internal conversion provide points 1 to 6 on Fig. 16.

2. $^{108}Ag^m$ provides points 7,8,9 at 432, 618 and 727 keV respectively. The first of these is used to normalise to the ^{180}W points.

3. ^{137}Cs provides calibration point 10 at 662 keV which is used to normalise to the existing points and at 33 keV, point 11.

4. The rapid decrease in relative efficiency below 60 keV shown in Fig. 16 is due to photon attenuation in the non-intrinsic material on the detector surface. From the ratio of relative efficiencies at 33 and 61 keV and the known linear absorbtion coefficients for Ge(78), the effective dead layer thickness was calculated as 0.52 mms. Points 12 and 13 were then calculated using this value.

5. We estimate the uncertainty in those points above 104 keV to be less than ±2%. Other points depend a great deal on calculated and measured conversion coefficients and are assigned limits of error of about ±5%.

---

(77) Conlon T. W., Naumann R. A. and McCarthy A. L. Nucl. Phys. A104, 213 (1967).

(78) Thwaites T. T., Nuc. Phys. Div. Progress Report PR/NP 14, p. 36 (1968).

6. Points 14 and 15 at 74 and 279 keV are provided by a ^{203}Hg source. Point 15 is certainly consistent with neighbouring points to within our assigned ±5% accuracy. It is well worth noting that the relative efficiency calibration below 60 keV provides a method of checking the window thickness of Ge(Li) devices - a quantity not easily measured directly.

E. Prompt γ-rays in photonuclear reactions on ^{12}C (H. A. Medicus (RPI), E. M. Bowey, D. B. Gayther and B. H. Patrick)

Additions to the shielding in this experiment have improved the signal to background ratio. Data have now been taken for bremsstrahlung spectra with end point energies of 34, 27 and 22 MeV, and a PDP-4 programme has been written to help in analysing the results. The relative efficiency of the germanium counter for γ-ray energies greater than 2 MeV was assumed to follow the curve determined by Allen et al.[79] for a similar counter, since our measured response function for 4.44 MeV γ-rays and theirs are almost identical in shape. Expected response functions at gamma ray energies of 2.75 MeV (based on a measurement of the ^{24}Na γ-ray), 4.44 MeV, 6.84 and 9.17 MeV (the last two taken from the results of Allen et al.) were constructed, taking into account the fact that the motion of the recoiling ^{11}C or ^{11}B nuclei causes the γ-ray lines to be broadened. The computer programme can now calculate the response function for any energy between 2.75 MeV and 9.17 MeV by interpolation, and allows the addition of such response functions in varying amounts. With this technique we hope to reproduce the observed experimental data and thus to deduce the intensities of the various γ-ray lines observed.

E. The photonuclear reactions (γ,n) and (γ,2n) in ^{46}Ti (D. B. Gayther, H. A. Medicus (RPI) and J. W. McMillan (Analytical Sciences Division)

Nuclear photodisintegration at excitation energies in the region of the giant resonance is known to arise both from statistical processes and from direct interactions. However the detailed nature of photonuclear absorption in the high energy tail region is not well understood. Measurements in this region have recently been made on a number of medium and heavy nuclei[80]. The results show that at excitations of 25 MeV photoneutron production can be accounted for entirely by statistical processes whereas at 30 MeV a significant fraction of the neutrons appear to come from direct interactions. The type of direct interaction which occurs at this energy is not apparent. Photon absorption by a single nucleon can account for direct interactions in the giant resonance, but the calculated cross-sections in the tail region fall off rapidly with increasing excitation. On the other hand the quasi-deuteron model[81] successfully explains photonuclear absorption at excitations well above 100 MeV but is not usually thought to apply to the 30 MeV region. Recently, however, Levinger[82] has modified this model for the region below 100 MeV and measurements with 55-85 MeV photons are in good agreement with his predictions[83]. It is therefore possible that the quasi-deuteron effect gives rise to the greater part of the direct interactions at even lower energies. We have measured the relative yields of (γ,np) and (γ,2n) reactions produced in a medium weight nucleus, ^{46}Ti, at excitations in the 30-40 MeV region in order to look for this effect. The relative yields from the two reactions due to statistical processes can be calculated with reasonable accuracy and an observed relative yield of (γ,np) grossly in excess of the calculated value should indicate the existence of a quasi-deuteron type of process.

Six samples of natural titanium have been irradiated with bremsstrahlung of 31, 35 and 39 MeV. The electrons were magnetically analysed to produce a beam of accurately known mean energy with a 6% energy spread. The tantalum converter was backed with 5.7 cm of carbon to reduce the energy of transmitted electrons to below the thresholds of the reactions being studied. The yield of the ^{46}Ti(γ,np)^{44}Sc

(79) Allen B. J., Bird J. R. and Engstrom S. Report AAEC/TM 380.

(80) Patrick B. H. and Bowey E. M. Nuc. Phys. Div. Progress Report AERE - PR/NP 12, p. 32 (1967).

(81) Levinger J. S. Phys. Rev. 84, 43 (1951).

(82) Levinger J. S. Proc. International Conference on Low and Intermediate Energy Electromagnetic Interactions, Vol. 3, p. 411 (Academy of Sciences of U.S.S.R., Moscow, 1967).

(83) Kaushal N. N., Winhold E. J., Yergin P. F., Medicus H. A. and Augustson R. H. to be published in Phys. Rev.

reaction was determined by monitoring the 1.156 MeV line from the 4 hr ^{44}Sc with a Ge(Li) diode following 1 hr irradiations of Ti targets, while the yield of the $^{46}Ti(\gamma,2n)^{44}Ti$ reaction, which was produced in 24 hr irradiations, was determined by monitoring the 1.156 MeV ^{44}Sc line from 47 yr ^{44}Ti after chemically separating the highly active ^{46}Sc and ^{47}Sc obtained from isotopic impurities in the samples. The ^{44}Ti yield was measured several days after the irradiation to ensure that the 1.156 MeV line due to the $^{46}Ti(\gamma,np)^{44}Sc$ reaction had completely died away. The various reaction yields were normalised to the same bremsstrahlung flux by determining the photoactivities induced in thin cobalt foils irradiated together with the titanium samples.

Activation analysis of the (γ,np) reactions is now complete and the analysis of the (γ,2n) reactions is in progress. The yield ratios to be expected from statistical processes will be calculated with the help of an existing computer programme.

Analysis of (t,p) reactions (R. Chapman)

The scanning and analysis of the exposures listed in the last progress report[84] are continuing. Proton angular distributions are being constructed and spin and parity assignments made from the characteristic shapes of these distributions.

F. Nuclear structure of the tin isotopes (P. E. Cavanagh, C. F. Coleman, A. G. Hardacre and J. F. Turner)

1 Level structure of the odd tin isotopes

The technical aspects and detailed experimental results of this work (see Progress Reports PR/NP 9 onwards) are described in the report AERE - R 5863, and will be submitted for publication in Nuclear Physics. The report lists the excitations of the observed levels, the peak excitation cross-sections, and gives detailed angular distributions for excitation by the (p,d) reaction. J values for levels belonging to the $l = 2$ spin orbit doublet are assigned on the basis of observed differences[85] in the forward angle peaks of the corresponding angular distributions. The characteristic transition from particle-like to hole-like behaviour of the mass dependence of the quasiparticle energies, reflected in the Q-value plot for the excitations of the major single particle levels[85], is made much more obvious by using as the reference energy for excitations in any particular odd nucleus the mean of the binding energies of its even neighbours. Finally, the existence of systematically occurring sets of collective levels is pointed out, emphasized by the otherwise unexpected appearance of $l = 1$ angular distributions to levels at excitations ranging from 2.4 MeV in ^{111}Sn to 3.0 MeV in ^{121}Sn.

Data analysis (C. F. Coleman)

The analysis of the (p,d) measurements on targets of the even tin isotopes has been completed, and the results are included in the report mentioned above. The (p,p') and (p,t) measurements on $^{117,119}Sn$ are now being analysed, and a report discussing the level structure of the odd tin isotopes is in preparation.

D.W.B.A. analysis of (p,d) measurements on the even tin isotopes (P. E. Cavanagh)

This work is now complete, and is presented in reports AERE - R 5801 and 5901. The former deals with the angular distributions for the 'd' levels, and provides a tentative explantation of 'J' dependence,[85] the latter is concerned with D.W.B.A. calculations for the other configurations in the active shell ($g_{7/2}$, $s_{1/2}$, $h_{11/2}$), with symmetry effects in the nuclear potentials, and with nucleon density distributions within the tin isotopes.

---

(84) Nuclear Physics Division Progress Report AERE - PR/NP 14, p. (1968).

(85) Cavanagh P. E. and Coleman C. F. Nuclear Physics Division Progress Report AERE PR/NP 11 (1967).

II Level structure in the even tin isotopes - data analysis (C. F. Coleman and Mrs. L. A. Winsborrow (Kings College, London))

The analysis of these measurements (PR/NP 12 onwards) is continuing. The angular distributions for excitation by the (p,t) reaction of the even ground states were shown in PR/NP 14, and Fig. 17 shows the distributions for excitation of the 2+ first excited states. The peak cross-sections for excitation of

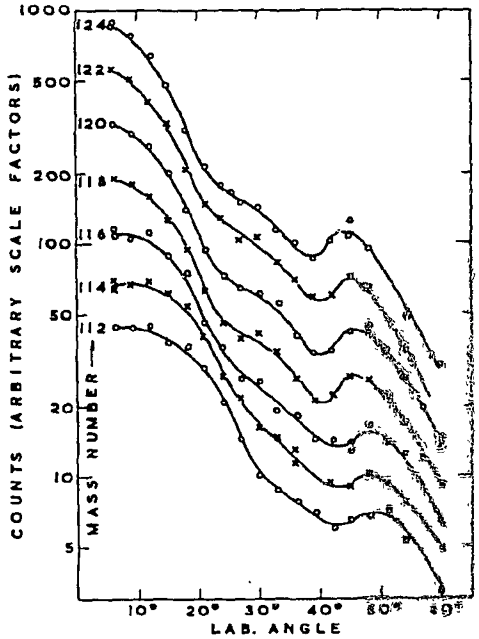

Fig. 17. Angular distributions for (p,t) transitions to the 2^+ first excited states of the even tin isotopes (relative intensities arbitrary).

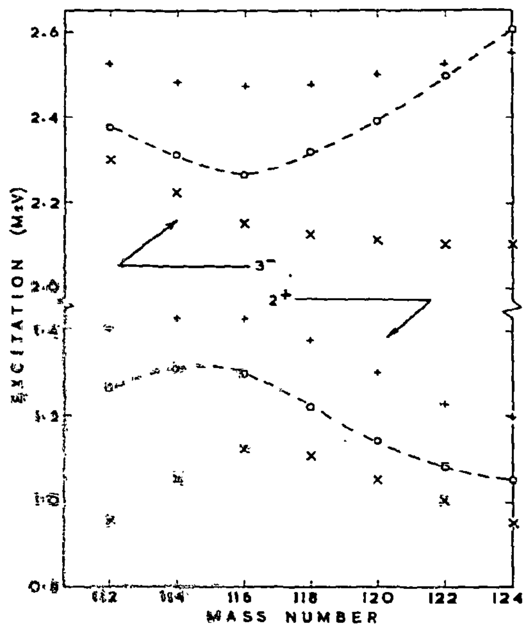

Fig. 18. Comparison of experimental positions (-o-) of the one phonon 2^+ and 3^- states of the even tin isotopes with the first (-+-) and second (-x-) order calculations of Clement and Baranger[86].

the ground states fall slowly by ~25% as the mass number rises from 110 to 122, but those for excitations of the 2+ first excited states increase almost threefold over the same range, presumably because $V_{s_{1/2}}^2$ increases steadily over this range, and the $(d_{3/2}, d_{5/2})_{2+}$ and $(d_{3/2}, g_{7/2})_{2+}$ couplings are important components of the wave functions for the quadrupole phonon states. The excitations of the 2^+ and 3^- one phonon states in $^{112 \rightarrow 124}$Sn derived from our (p,p') measurements are plotted in Fig. 18, along with values calculated by Clement and Baranger[86], using ($2p_{3/2}$, $1f_{5/2}$, $2p_{1/2}$, $1g_{9/2}$, $2d_{5/2}$, $1g_{7/2}$, $3s_{1/2}$, $2d_{3/2}$, $1h_{11/2}$, $2f_{7/2}$, $1h_{9/2}$, $1i_{13/2}$) neutron single particle configurations and similar proton configurations. The '+' and 'x' symbols represent first and second order calculations respectively. Unfortunately the second order corrections move the masses at which the extremal excitations appear away from the experimental values. The maximum in the 2^+ excitations at A = 114 is due to the fact that if it were not for the presence of the low statistical weight $s_{1/2}$ configuration near the Fermi surface there would be a sub shell closure at A = 114. However, the excitations of the 3^- levels show no evidence for this incipient closure, but merely the expected minimum in the mid-shell region. This discrepancy arises from the odd parity of the octupole levels, which entails that the two quasiparticle expansion of the wave functions should contain large contributions from components with one quasiparticle outside the active shell. In addition, the contributions from components involving the $S_{1/2}$ configuration are comparatively small.

(86) Clement D. R. and Baranger E. U. Nuc. Phys. 120, 25 (1968).

F. Optical Model Programme - Elastic scattering of 50 MeV protons (A. G. Hardacre and J. F. Turner)

Observations of the elastic scattering of 50 MeV protons from a range of nuclei, designed to extend our knowledge of the energy dependence of the Optical Model, were reported earlier[(87)].

Extraction of cross-sections from the experimental data has been resumed, and for Ni^{58} and Ni^{60} is now virtually complete. The results for these isotopes are plotted relative to Rutherford scattering in Fig. 19. The relative uncertainty in the data arising from statistical errors varies from $\sim\pm1\%$ at forward scattering angles to $\sim\pm3\%$ at backward angles, where counting rates became a limiting factor, and is overridden in regions of rapid angular variation of the cross-section by the effects of uncertainties in the beam position. At worst these effects are equivalent to an uncertainty of the cross-section of $\sim\pm4\%$.

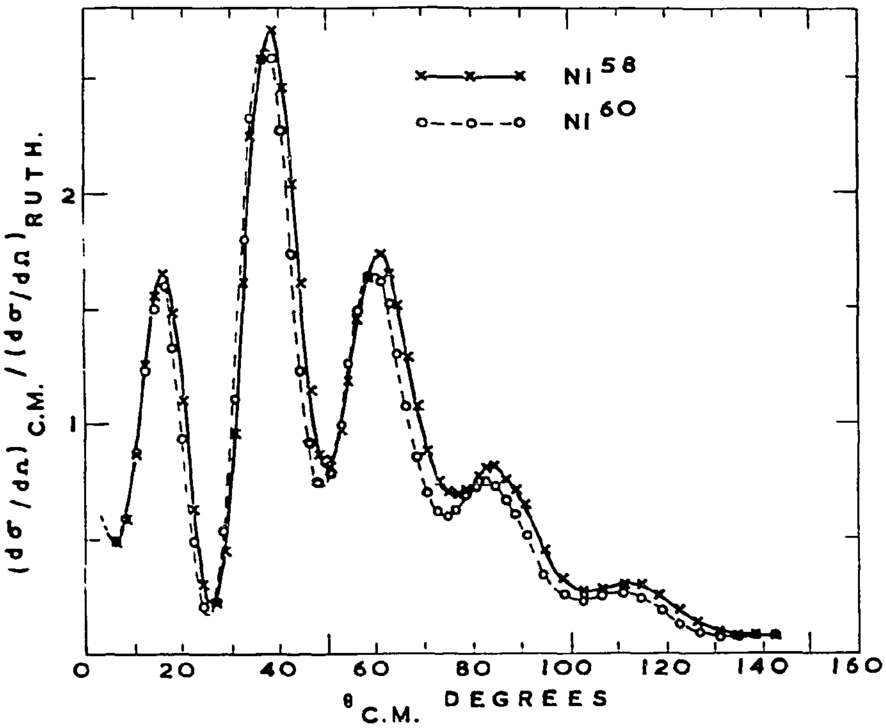

Fig. 19. Elastic scattering of 50 MeV protons from $^{58,60}Ni$, taken relative to the Rutherford cross-section.

The overall normalisation factors are based on an early assessment of target thickness and for this reason are still subject to an error of $\sim\pm10\%$. It is hoped that this error will be reduced following a more precise target survey.

(87) Nuclear Physics Division Progress Report PR/NP 11, p. 27 (1967).

H. Neutron time-of-flight experiments

I Asymmetry in charge particle production for 100 MeV polarized neutrons (A. Langsford and G. C. M. Sharman (Oxford))

Data from this experiment[88] (carried out in collaboration with Southampton University and the Rutherford High Energy Laboratory) are now being analysed. Progress has hitherto been hampered by the problems of reading the data from the 7-track magnetic tape on which it was recorded.

II High precision n-p total cross-section (A. Langsford and P. J. Clements (Oxford))

All our data from this experiment have now been subjected to a preliminary analysis, which, however, did not include corrections for correlations in the neutron time spectra arising from dead time effects and from after-pulsing[89] in the detectors. These correlations led to discrepancies $\sim \pm 0.5\%$ in the cross-section values calculated for different transmission sample combinations in the region 1-5 MeV, where the data have highest statistical accuracy. First calculations indicate that the application of suitable corrections will significantly reduce this discrepancy. Bearing in mind the effect of these corrections, our results so far support the measurements of Engelke et al[90] rather than the somewhat smaller cross-section values measured in earlier experiments.

III (p-n) reactions in light nuclei (A. Langsford and R. A. Bell (Oxford))

An experiment to study (p,n) reactions in light nuclei at 100 MeV is in active preparation. This experiment will repeat the earlier work in the same field[91] with greater statistical accuracy and with improved energy resolution, since with the availability of the 100 m flight path, a resolution of ± 0.3 MeV at 100 MeV is expected. DWBA calculations are being made and experimental conditions simulated in computer programs in an attempt to anticipate the results we are likely to obtain. In this way the understanding of the experiment will be increased while it is still in progress and will permit an increased amount of "on-line" analysis to be made.

II. A study of Σ^- beta decay (I. M. Blair and A. E. Taylor, in collaboration with the Rutherford Laboratory and Queen Mary College, London).

The objective of this experiment is to measure the electron momentum - Σ^- spin correlation coefficient in the decay process

$$\Sigma^- \rightarrow n + e^- + \nu$$

in order to check the current theory of weak interactions. A detailed description has been given in previous progress reports. The data have been taken, and analysis is in progress. We have taken, besides, the beta decay events, some 20,000 pionic decay events, with the purpose of checking the system and of studying instrumental asymmetries. It now looks likely that from these events we shall also obtain a value for the Σ^- lifetime of accuracy comparable with that of the current world average.

---

(88) Nuclear Physics Division Progress Report AERE PR/NP 13, p. 32 (1968).

(89) Nuclear Physics Division Progress Report AERE PR/NP 12, p. 37 (1967).

(90) Engelke C. E., et al. Phys. Rev., 122, 324 (1963).

(91) Nuclear Physics Division Progress Report AERE PR/NP 9, p. 37 (1966).

H. n-p Bremsstrahlung (I. M. Blair, F. P. Brady and E. Wood, in collaboration with the Rutherford Laboratory and Queen Mary College, London).

We are preparing an experiment to study the reaction $n + p \rightarrow n + p + \gamma$, using the 140 MeV neutron beam from the synchrocyclotron. There is considerable theoretical interest[92,93] in this reaction, as it enables one to study the nucleon-nucleon interaction off the mass-shell. The elastic nucleon-nucleon scattering data can be equally well fitted by a number of different phenomenological potentials, which would however be expected to give quite different results for processes which depend on the off-mass-shell behaviour. Thus a study of radiative nucleon-nucleon scattering should enable one to distinguish between these potentials. Proton-proton bremsstrahlung in this energy region has been investigated fairly thoroughly by the Rochester Group[94]. In this process however, since the centre of charge is at rest in the centre of mass frame, the leading (dipole) term is absent and one is therefore studying second-order effects only. This argument does not apply to neutron-proton bremsstrahlung which should therefore provide a more critical test. Attempts have been made to extract neutron-proton bremsstrahlung information from data on proton-deuteron bremsstrahlung[95,96]. The fact that the two most recent results disagree by an order of magnitude illustrates the difficulties of this approach, and leads to the belief that only the free-nucleon reaction will yield reliable results. Hitherto neutron beams of well-defined energy sufficiently intense to allow one to study such a relatively rare process have not been available, but after completion of the improvement programme on the synchrocyclotron this will no longer be the case.

The experimental technique depends on the fact that at 140 MeV the opening (conjugate) angle for the final state neutron and proton in elastic scattering is about 88.5°, and is very insensitive to incident energy. Thus, detection of a neutron and proton in coincidence at a non-conjugate angle is sufficient signature for a bremsstrahlung event, as no other inelastic process is possible at this energy.

The neutron beam will be produced internally off a lithium deuteride target, which will be cooled using the "heat-pipe" technique[97]. The estimated flux at our apparatus is about 10^7 neutrons per second over an area of 5 cm^2 with an energy spread of about 10 MeV (FWHM). The design of the target is nearing completion and the lithium deuteride is on order; preliminary tests have been carried out on the heat-pipe.

The liquid hydrogen target has been designed around a commercially available cryogenerator. This has the advantage of containing only a small quantity of hydrogen compared with currently used designs, thus minimising the problems of hydrogen safety. The task of designing an accurately rectangular parallel-sided hydrogen target in the form of an appendage has been essentially achieved. Delivery of the cryogenerator is imminent; the ancilliary equipment has been designed and the components ordered.

Arms for the neutron and proton detectors will be placed on either side of the beam in the horizontal plane, covering a range of laboratory angles from 14° to 50°. The arrangement is shown in Table VII, (see page 35). They incorporate flight paths of about 1½ metres so that the particle energies can be estimated by time-of-flight. The proton arms each carry a small scintillator 6 cm high by 1 cm wide and 0.076 cm thick placed close to the hydrogen target, a second scintillator of the same thickness and 8.9 cm square placed 1½ metres downstream from the first, and immediately behind the second a thick scintillator 12.7 cm in diameter and 15.2 cm long in which the protons are stopped. From the heights of the pulses obtained from the small scintillators and the thick scintillator we will be able to estimate dE/dx and total energy respectively, in order to check the time-of-flight measurement. Tests on prototypes of these counters using the 50 MeV beam from the PLA indicate that the resolution is adequate for this purpose. The solid angle subtended by each proton arm, together with the beam profile, defines an interaction volume within the liquid hydrogen target, which is chosen to minimise the effect of the target walls. The

(92) Sobel M. I. and Cromer A. H. Phys. Rev. 132, 2698 (1963).

(93) Duck I. and Pearce W. A. Phys. Letters 21, 669 (1966).

(94) Rothe K. W., Köhler P. F. M. and Thorndike E. H. PRL 16, 1118 (1966)

(95) Edgington J. A. and Rose B. Phys. Letters 20, 552 (1966).

(96) Köhler P. F. M., Rothe K. W. and Thorndike E. H. PRL 18, 933 (1967).

(97) Grover G. M., Cotter T. P. and Erickson G. F. J. Appl. Phys. 35, 1990 (1964).

TABLE VII

Arrangement of neutron and proton arms.

Lab. Angle	Left	Right
14^{o}	N	N*
20^{o}	P	N*
26^{o}	N	P
32^{o}	P	N*
38^{o}	P	P
44^{o}	N	N
50^{o}	N	N

Arms marked (*) can move up to 20^{o} out of the horizontal plane to study "out of plane" events.

Angular resolution (horizontal and vertical) is $\pm 2\frac{1}{2}^{o}$.

neutron arms consist of a thick scintillator 12.5 cm in diameter and 15 cm long, preceded by a veto counter 15 cm square. The arms and their associated hardware have been designed; many of the components have been delivered and the remainder will be arriving shortly.

The electronic logic will be handled by R.H.E.L. integrated circuit modules, for which an order has been placed. Data will be fed on-line to the synchrocyclotron group computer (DDP-516) for checking and preliminary analysis. The necessary computer software is being written.

Our current estimate is that we will detect about 40 event per hour, and we would aim to collect about 10,000 events. We plan to be ready to set up the experiment when the synchrocyclotron recommences operation at the end of this year, and to be taking data in the spring of next year.

MISCELLANEOUS STUDIES IN PHYSICS

Mössbauer Studies

I Mössbauer studies of ^{119}Sn in nickel-based alloys (T. E. Cranshaw)

Mössbauer spectra have been obtained for ^{119}Sn dispersed in alloys of nickel containing 5, 10 and 20% Cu, or 2, 5 and 10% Ge. They can be understood on the assumption that in the nickel the Cu or Ge atoms produce two distinct kinds of disturbance, one of sufficiently long range that it can be considered as uniform throughout the specimen, and one confined to nearest neighbours. The long range disturbance causes the field at ^{119}Sn nuclei remote from alloying nuclei to fall by 1 kOe/per cent Cu and 2.3 kOe/per cent Ge from the value 21 kOe for pure nickel.

A reduction of the field at ^{119}Sn nuclei of (6 - 42c)kOe and (11 - 190c)kOe, where c is the concentration, is caused when a neighbour Ni of the tin atom is replaced by Cu or Ge respectively. Thus at infinite dilution the replacement of a neighbour Ni atom by an atom of either impurity causes the field to become smaller, while at concentrations above 14% for Cu and 6% for Ge, it causes the field to increase.

II Study of Inorganic iron complexes (C. E. Johnson, R. Rickards (Materials Physics Division))

The Fe^{57} Mössbauer spectrum of nitrosyliron bis (NN-diethyldithiocarbamate) has been measured at temperatures between 300°K and 1.3°K in the presence of external magnetic fields. In zero field the spectrum at all temperatures consists of a quadrupole split pair of lines of unequal intensity. The intensity of the absorption increases markedly on cooling from 300°K to 77°K. The isomer shift (0.34 mm sec^{-1} at 77°K, relative to iron) is higher than expected for a low-spin Fe(I) complex and implies that the metal s-electrons are screened from the nucleus by electron donation from the ligands. The quadrupole splitting shows little dependence on temperature and the application of an external magnetic field shows that the sign of the major component of the efg tensor is positive. Magnetic hyperfine interactions are observed at low temperatures in large external magnetic fields. The variation with H/T of the effective hyperfine field at the nucleus follows the Brillouin function for $S = ½$, and the value of the saturation hyperfine field was found to be 110 ± 5 kg. The orbital ground state of the iron atom cannot be deduced from the sign of the quadrupole splitting owing to the large contributions from the bonding electrons. From the magnetic hyperfine splitting it is deduced to be $d_z{}^2$.

III Study of Au Fe alloys (M. S. Ridout)

Iron dissolved in gold has a large positive isomer shift at room temperature relative to face centred iron precipitated in copper. Assuming that the electronic state is unchanged and that the shift is due to the change in atomic volume, the concentration dependence of the isomer shift of iron in gold can be calculated from the concentration dependence of the lattice parameter obtained from X-ray measurements. The experimental value is -0.00256 mm sec^{-1}/per cent compared with the expected value of -0.003 mm sec^{-1}/per cent. Experiments are in hand to confirm these assumptions by varying the lattice parameter of gold-iron alloys by the addition of copper. It is likely that the observed concentration dependence of the hyperfine field can be accounted for by this effect.

In the magnetically ordered range, the quadrupole splitting averaged over all iron sites tends to zero as the temperature is reduced indicating that the angle between the spin direction and the electric field gradient has a mean value close to $\cos^{-1}(1/\sqrt{3})$. The application of a magnetic field of 30 kOe increases the magnitude of the average quadrupole splitting by an amount consistent with a rotation of the spins by approximately 5°.

An account of this work has been submitted for publication.

IV Study of Biological Molecules

Cytochrome c Peroxidase (G. Lang and T. Yonetani (Johnson Foundation))

The Mössbauer spectra of a number of compounds of meso- and proto- cytochrome c peroxidase have been observed. The changes in spectra observed suggest that modification of the porphyrin has only a small effect upon crystal fields. Spectra of the complex ES (produced by adding ethyl peroxide to the enzyme) indicate that the integral spin which is suggested by susceptibiltiy measurements is located in a covalent bond involving the iron. No evidence of the known half integral spin is seen in the Mössbauer spectra. A model has been found which accounts for Mössbauer and susceptibility data.

Myoglobin (G. Lang and T. Yonetani (Johnson Foundation))

A number of compounds of meso- and proto- myoglobin have been examined. Modification of the porphyrin has only a small effect upon the Mössbauer spectrum. All myoglobin compounds appear to be very similar to the corresponding haemoglobin compounds so far as Mössbauer measurements are concerned.

Haemoglobin (G. Lang, M. Winter and R. J. P. Williams (Oxford University))

Recent measurements on ferric haemoglobin at high pH indicate a large high spin component. Spin equilibrium in this material appears to be much more complicated than was first assumed.

Conalbumin (G Lang, R. Woodworth and R. J. P. Williams (Oxford University))

Initial measurements of this material suggest that it is high spin with crystal field splitting factor (D) of the order of a few inverse centimeters.

Dilute Paramagnets (W. T. Oosterhuis and G. Lang)

Mössbauer spectra of dilute reduced protonated nitroprusside, $Fe(CN)_5NOH^{-2}$, indicate that the unpaired electron spin lies in a sigma bond between iron and NO. The effects of transferred hyperfine interaction with the nitrosyl nitrogen are considerable in the zero field spectra. Coupling constants to N and to Fe are in agreement with those found by ESR. Haemoglobin nitric oxide spectra are very similar to this, and this is taken to indicate that the electronic situation there is similar. A paper concerning this work is in final draft stage.

V Study of PdAuFe alloys (G. Longworth)

The long range magnetic interaction in PdFe alloys is thought to be propagated via an exchange polarization of the palladium 4d band. It is known that the addition of a noble metal to palladium has the effect of filling the palladium 4d band and hence should modify the long range magnetic interaction.

A study of the effect of substituting gold for palladium atoms in the PdAuFe system is in progress, using the ^{57}Fe resonance. We find that the mean hyperfine field at the iron nuclei decreases from 320 ± 5 kOe for $Pd_{98}Fe_{02}$ to 230 ± 5 kOe for $Au_{98}Fe_{02}$ but remains approximately constant at a value 276 kOe over the range $0.47 < Au/Pd < 0.61$. The palladium 4d band is believed to be completely filled at Au/Pd 0.55. The isomer shift at the iron nuclei is found to increase approximately linearly from $Pd_{98}Fe_{02}$ to $Au_{98}Fe_{02}$ indicating that there is no appreciable transfer of S electrons from iron to palladium. Measurements are now in progress to determine the ordering temperatures as a function of the Au/Pd ratio in these alloys.

Radio Pulses from Extensive Air Showers (W. N. Charman, J. H. Fruin and J. V. Jelley)

Analysis of the radio observations of EAS arriving from near the zenith suggests that emmission from showers of energy up to $\sim 3.10^{17}$ eV was detected at 200 MHz but not at 3000 MHz. The observed 200 MHz pulse-height spectrum appears to favour an incoherent emission mechanism, although it can also be interpreted in terms of coherent emission from exceptionally thin shower discs caused by extreme fluctuations in shower development. If the observed radiation is indeed incoherent, some new mechanism, other than those[98] involving high-energy shower particles, must be invoked to explain the observed yields.

At high zenith angles the correlation of the observed broadband radio pulses[99] with EAS remains unproven; these observations are continuing.

Searches for high-energy γ-rays from pulsars (W. N. Charman, J. H. Fruin, J. V. Jelley with R. W. P. Drever (Glasgow University))

The observations carried out last winter have now been fully analysed, and a brief report has been published[100]. Following up this work the searchlight installation and associated analysing system have been modified and improved. In particular the timing electronics has been developed by introducing a new varactor-tuned crystal and a Vernier dividing circuit developed at Harvard, which enables the cycling period to be set to an accuracy of 1 in 10^8. In addition, direct monitoring of the cycling period from the MSF time signals radiated from Rugby has now been achieved.

---

(98) Jelley J. V., Charman W. N., Fruin J. H., Smith F. G., Porter R. A., Weekes T. C. and McBreen B. Nuovo Cimento 46, 649 (1966).

(99) Charman W. N., Fruin J. H. and Jelley J. V. Can. J. Phys. S226 (1968).

(100) Charman W. N., Jelley J. V., Orman P. R., Drever R. W. P. and McBreen B. AERE - R 5912 (19).

A considerable proportion of the effort this summer has been devoted to re-furnishing the searchlight installation on loan to University College, Dublin (under EMR contract No. 1561). This installation has now been sent out to R.A.F. Qrendi in Malta where it is hoped the better climate and lower latitude will enhance the efficiency of this work. Evidence obtained[101] with this installation when it was sited in Ireland last winter suggests that γ-rays are emitted from the source CP1133.

Studies of air fluorescence (W. N. Charman, J. V. Jelley, with G. G. Fazio (Smithsonian Astrophysical Observatory, Cambridge, Mass).

Strong fluorescence[102] in the upper atmosphere has been detected and is attributed to the X-ray flash from atomic bombs in space, and a search for similar X-ray flashes from supernova in distant galaxies has been purposed[103].

We have therefore considered the feasibility of developing this same technique to search for X-rays and low-energy γ-rays from pulsars. We have shown that it should be possible to attain a sensitivity by this method which is at least as high as that obtainable with current rocket flights with on-board X-ray telescopes. The advantages of the technique are the wide energy bandwidth (100 eV - 1 MeV), long integrating times (~6 hours), simplicity and low cost, and, above all, the feature that data recorded on a single night can be analysed for any or all of the pulsars above the horizon at the time.

Preliminary experiments have been conducted and the electronic and tape-recording techniques are being developed. This work has had to be carried out at a very dark site free from background light with a 50 Hz component. For this reason the equipment has been transferred to R.A.F. Sparsholt Firs.

Image intensifier and other work

Experimental and theoretical studies have been made of the contribution to tube dark current made by Cherenkov light emitted by cosmic-ray muons in the tube entrance window[104]. The cosmic-ray contribution equals that due to pure photocathode dark current in cooled tubes with quartz windows and 'super' S-11, S-20, CsTe and Bi-alkali cathodes.

For an experiment stimulated by the recent discovery of pulsars[105] we have developed a simple technique[106] for detecting a periodicity of unknown value in the signal from an astronomical source. The temporally-varying signal from the source is recorded as a spatially varying density distribution on a uniformly-moving photographic plate. Coherent illumination of the plate produces a diffraction pattern which is the spatial analogue of the temporal Fourier spectrum of the signal from the source. A prototype system has been constructed and will be used by the Royal Greenwich Observatory, Herstmonceux to seek for periodicity in the optical signals from white-dwarf stars.

Electronic Conduction through Oxide Layers (G. Dearnaley, A. M. Stoneham (Theor. Phys.) and D. Vernon Morgan)

The consequences of the filamentary model of electronic conduction in SiO have been explored more quantitatively. By choosing a simple distribution of filament resistances with a triangular form between limits ρ_1 and ρ_2 it has been shown possible to explain the D.C. and A.C. current-voltage characteristics

---

(101) O'Mongain E. P., Porter N. A., White J., Fegan D. J., Jennings D. M. and Lawless B. G. Nature 219, 1348 (1968).

(102) Westervelt D. R. and Hoerlin H. Proc. I.E.E.E. 53, 2067 (1965).

(103) Colgate S. A. Canadian J. Phys. 46, S476 (1968).

(104) Charman W. N. Progress in Electronics and Electron Physics, to be published.

(105) Hewish A., Bell S. J., Pikington J. D. H., Scott P. F. and Collins R. A. Nature 217, 209, 1968.

(106) Charman W. N. Applied Optics, to be published.

and memory properties of formed SiO films. The results of such a fit, normalized to the peak of the observed current, is shown in Fig. 20 for the D.C. case. In this case the experimental current is the difference between the current before and after forming, i.e., is that part associated with filamentary conduction.

SiO films have been successfully formed on silicon substrates, under evaporated gold electrodes. Two formed states were observed, one of which showed negative resistance, and the second exhibited more ohmic conduction. The latter state appeared to be associated with the appearance, under the microscope, of numerous tiny blisters, presumably due to localized release of oxygen which is trapped under the gold film. These blisters are superficially similar to those observed in the electrical breakdown of anodic SiO_2 layers on silicon, under an aluminium electrode, by Ilahi at E.R.A. It is interesting to speculate that conduction in both cases may be localized in filaments and so lead to intense heating.

Scanning electron microscope observations of silicon oxide films have been begun, with the cooperation of Dr. J. H. Stephen (E. & A.P.).

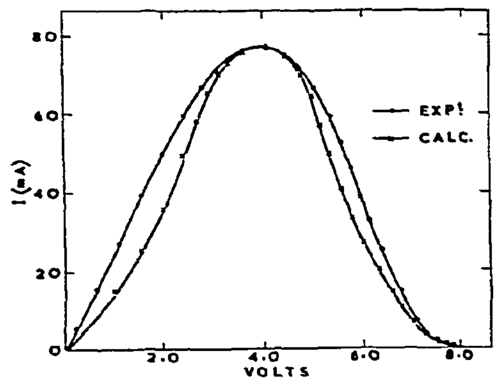

Fig. 20. Calculated current voltage characteristic of a thin metal-SiO-metal device, based upon a filamentary conduction model, compared with experimental results.

C. The Z_1-dependence of atomic stopping (J. M. Poate, I. M. Cheshire (Theor. Phys.) and G. Dearnaley)

The work presented in the last progress report has been published in Physics Letters[107]. Our basic premise is that the Z_1 dependence is due to the size of the incident ion. In order to obtain quantitative results the Firsov theory, which gives good average results, has been modified by replacing the Thomas-Fermi atoms with simple Hartree-Fock wave functions.

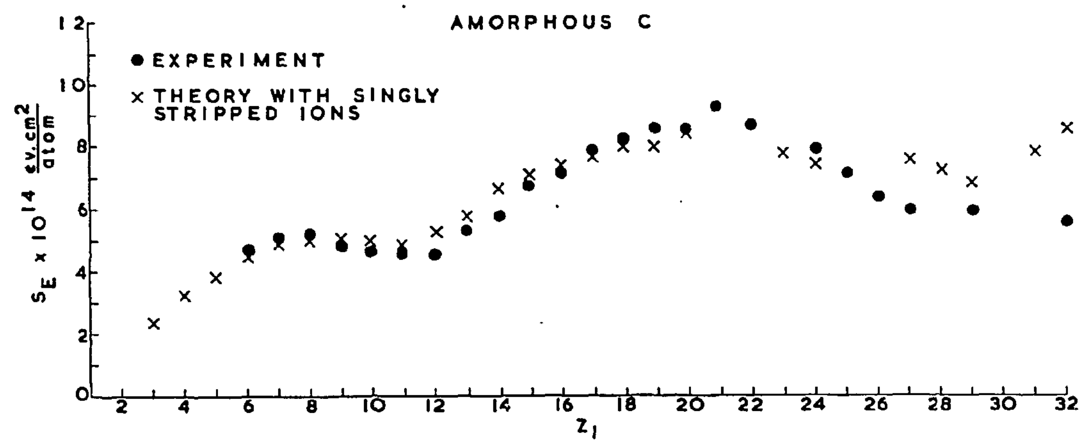

Fig. 21. Electronic stopping cross section, S_e, for various ions transmitted at 10^8 cm/sec through amorphous carbon, plotted as a function of the atomic number of the ion.

This theory explains the channelling data quite well. As a further check on the theory an attempt was made to explain the amorphous carbon stopping cross-section of Hvelplund and Fastrup[108]. Calculations

(107) Cheshire I. M., Dearnaley G. and Poate J. M. Physics Letters 27A, 304, (1968).

(108) Hvelplund P. and Fastrup B. Phys. Rev. 165, 408, (1968).

were carried out integrating over all impact parameters greater than those which would produce an angular deflection of less than the half-angle of acceptance of the in-line analyser. The results are shown in Fig. 21 (see page 39). The fit, whilst surprisingly good for the lower Z_1 values, is not as satisfactory for the higher values. These calculations and discussion will be published in Proc. Roy. Soc. — "Conference on Ion Implantation and Hyperfine Interactions".

The problem of these oscillations in low-energy electronic stopping has attracted some interest of late. El-Hoshy and Gibbons(109) have adopted a somewhat ad hoc approach in the modifications of Firsov's formula. Bhalla and Bradford(110) obtain the oscillations by suitable modifications of Lindhard's electron gas formula with Hartree-Fock atoms. Two more recent treatments by Winterbon(111) and Harrison(112) support the contention that the oscillations are due to a size effect of the incident ion.

It is hoped to carry out further calculations in future to explain other channelling and amorphous stopping data.

The channelling of protons through thin crystals (J. M. Poate, G. Dearnaley)

The original three-axis goniometer with the added facility for holding crystal temperatures between 77°K and 800°K has now been installed on the Cockcroft-Walton accelerator. Transmission experiments will be carried out to determine the effects of lattice vibrations on channelled particles.

H. Further luminescence studies on the synchrocyclotron (I. M. Blair and J. A. Edgington (Queen Mary College, London))

Following on from our recent work(113) on the luminescent and thermoluminescent properties of rocks and meteorites under proton bombardment, the following lines of research are being pursued:-

(i) Study of samples from the lunar surface

This has a direct bearing on the luminescence hypothesis of transient lunar events studied in our previous work, and is a natural next step. A request has been submitted through the appropriate channels for suitable samples.

(ii) Study of the "flash-like" thermoluminescence of silicone grease

During our previous experiment we noted a sharp thermoluminescent peak due to irradiation of the silicone grease upon which our samples were mounted. We have analysed the relevant data in more detail, and find that the peak is centered at -116°C and has an apparent width of 5½°C at a heating rate of 12°C per minute. Such phenomena are extremely rare, there being only one other instance reported in the literature(114), and their origin is unknown. Not all the greases we used showed this phenomena. We intend to study the constituent chemicals of the grease to determine which one is responsible.

(iii) Measurement of short (0-50 nanosecond) luminescent lifetimes

We are developing a technique to measure the exponential luminescent decay rate from trapping levels. This rate is related to the depth of the level. The technique will make use of the pulsed operation of the synchrocyclotron. In collaboration with Dr. D. Pooley of Solid State Division the 400 keV electron accelerator is being used to carry out preliminary tests on alkali halides.

(109) El-Hoshy A. A. and Gibbons J. F. Phys. Rev. 173, 454, (1968).

(110) Bhalla C. P. and Bradford J. N. Physics Letters 27A, 318 (1968).

(111) Winterbon K. B. (to be published).

(112) Harrison D. E. (to be published).

(113) Blair I. M. and Edgington J. A. Nature 217, 157 (1968).

(114) Tanimizu S. and Otomo Y. Phys. Letters 25A, 744 (1967).

Ion Implantation in Semiconductors (G. Deamaley, P. D. Goode and M. A. Wilkins)

Further concentration profiles have been measured for Na^{24} and P^{33} ions implanted into silicon crystals. It has been shown that the deep penetration of Na^{24} ions is strongly dependent on the crystal orientation (see Fig. 22) and on the ion energy. This suggests strongly, though not conclusively, that it results from a true ion channelling mechanism and not by enhanced diffusion of interstitial sodium.

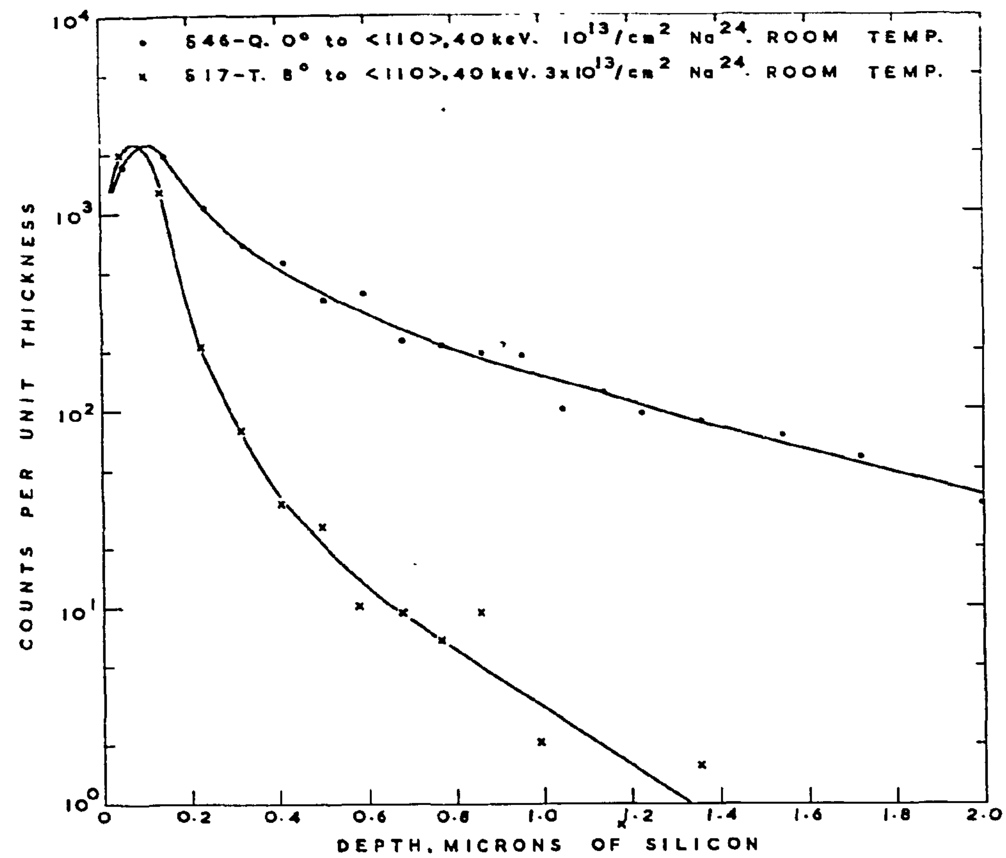

Fig. 22. The effect of crystal orientation on the concentration profile of ^{24}Na ions implanted into silicon.

Further P^{32} ion implantations into silicon have shown that the resulting concentration profile is influenced by the crystalline perfection. Batches of silicon have been ordered from other suppliers to ascertain which material offers the optimum characteristics for channelled implants.

For range determination in amorphous silicon, using the anodic stripping technique, it is necessary to know the anodization rate of amorphous as opposed to crystalline silicon. This has now been determined by a weighing technique, and is 16% higher than in the latter case.

The location of implanted ions by the channelling technique (J. M. Poate, G. Dearnaley and R. Alexander (Oxford))

The scattering chamber and goniometer which were designed for this study are now in use. The equipment has been tested, and proven satisfactory, by channelling 2 MeV protons through thin Si crystals and examining the transmission patterns.

The Preparation of Lithium-drifted Germanium detectors for gamma-rays (G. Dearnaley, G. Proctor, J. V. Dutt and B. D. Rogers)

Work has continued on the evaluation of 7.5 cm diameter Ge crystals produced by A.S.M. Ltd., Wembley, under contract EMR/AE 1943. Over this time the material has shown a considerable improvement and can be reliably drifted to depths approaching 1 cm. It has become clear that the dislocation density can often be important in determining the rate of lithium precipitation, and thus the number of lithium re-diffusions necessary in fabricating a detector. The production of low dislocation density crystals has therefore been initiated. Improved care in processing the material prior to crystal-pulling has resulted in an encouraging increase in carrier lifetime, and the relative merits of different methods of measuring this parameter are now better assessed.

The problem of achieving a low diode reverse current is now being approached by carrying out the final 'clean-up' drift within the cryostat so that there is no subsequent exposure to the atmosphere. The effect of atmospheric exposure even at the earlier stage of ion drift has been shown to be significant, and is now arranged to be minimised.

A very large volume (90 cm^3) detector is undergoing drift by the A.C. technique between two lithium diffused layers. It is approaching the stage at which one layer is to be ground off and replaced by an ion-implanted contact. This combination of techniques has already proved successful in the smaller devices prepared for proton detection.

The Preparation of Lithium-drifted Germanium Particle Detectors (G. Dearnaley, A. G. Hardacre and B. D. Rogers)

The A.C. drift technique has been applied to achieve a 9.5 mm total depletion depth in a planar diode in which the p-type contact has been produced by Ga^+ ion implantation (channelled). The Co^{60} spectrum shows no multiple peaks or other irregularities which would result from an inadequately compensated zone at the centre. The energy resolution (10 keV FWHM) was limited in this preliminary measurement since the leakage current had not been reduced below 5.10^{-9} A. Tests with 5 MeV alpha-particles show only a small window thickness (0.5 - 1μ), adequately low for proton detection.

In other material of the highest drift mobility a 9 mm drift has been obtained by conventional D.C. drifting, following Ga^+ ion implantation.

There are therefore two techniques available for the production of germanium proton detectors suitable for use up to the maximum VEC energies ($\sim$60 MeV). It is planned to compare the performance of detectors prepared in these two ways.

Industrial applications of the Mössbauer effect

I Ferrous-ferric ratios in partially sintered ores (T. E. Cranshaw, C. E. Johnson and The Steel Company of Wales)

Several specimens of partially sintered ores from the Steel Company of Wales have been examined at room temperature and at 77°K. In general, the specimens show a spinel-like behaviour, but the appearance of a non-magnetic, probably ferrous component could be observed in specimens to which large ($\sim$10%) quantities of CaO had been added. The method seems promising for the determination of ferrous-ferric ratios.

II Fluidised Beds (T. E. Cranshaw and M. S. Ridout)

The Mössbauer absorption spectra of Sn in a fluidised bed of $Al_2O_3 + SnO_2$ are being examined in an attempt to deduce the particle velocity distribution. Preliminary results with particles 105 → 125 microns indicate that the velocity range in a bed approximately 5 mm thick perpendicular to the gas flow is less than 0.4 mm sec^{-1}.

III Cation Distribution and Magnetic Properties of Manganese-Zinc Ferrites from Mössbauer Effect Measurements (C. E. Johnson (Materials Physics Division) and J. S. Carlow (Hirst Research Centre, GEC, Wembley, Middlesex)).

The Mossbauer spectra of Fe^{57} in the manganese-zinc ferrite $Mn_{0.5}Zn_{0.5}Fe_2O_4$ have been measured at temperatures between 450 and 4.2°K, and the 4.2°K measurement was repeated in a magnetic field of 30kG. The material studied (ferroxcube III) has a Curie temperature T_c of 430°K, and is technically important because of its high saturation moment of about $7\mu_B$ per formula unit at 0°K.

Above T_c the spectrum showed a small quadrupole splitting $E_Q = e^2Qq/2 = 0.4$ mm/sec and a chemical isomer shift characteristic of ferric iron. At room temperature magnetic hyperfine splitting was observed, but the lines were very broad, indicating a non-uniform value of the local magnetization owing to the different environments of the iron atoms. The lines became less broad as the temperature was lowered, revealing considerable detail in their structure. At 4.2°K there were six lines with widths not much larger than the natural width. There was a small quadrupole splitting, and a mean hyperfine field of 550 kG. It has been shown(115,116) that the application of an external magnetic field may be used to distinguish the Mössbauer spectra of iron atoms in octahedral and tetrahedral sites. When 30 kG was applied at 4.2°K the spectrum contracted showing that all the iron is in octahedral sites; no sign of tetrahedral iron was detected in the spectra.

The small line broadening observed in the spectrum at 4.2°K presumably arises from the random distribution of Mn^{2+} and Zn^{2+} ions in the neighbouring tetrahedral sites. Each possible environment has a slightly different chemical isomer shift, quadrupole splitting and hyperfine field and the resulting spectrum of the whole crystal, therefore, has lines of differing breadths.

The magnetic behaviour is well described by the formula $Mn_{0.5}Zn_{0.5}Fe^{3+}{}_2O_4$ which would predict a saturation moment of $7.5\mu_B$. The difference between this and the observed value may be accounted for by incomplete saturation in the neighbourhood of the diamagnetic zinc ions.

A Proton Microprobe (J. A. Cookson, F. D. Pilling)

An important technique for analysing the surfaces of materials consists of scanning them with a well defined beam of electrons or protons and observing the characteristic X-rays, and also for a proton beam, the nuclear γ-rays. Mainly because of the absence of the Bremstrahlung continuum generated by an electron beam, the use of protons has potentially much the greater sensitivity for detection of elements present in low concentration. However the technique is at present limited by the poor spatial resolution of proton beams and by the background from any collimating apertures close to the target. The present project aims to make available on the IBIS accelerator a beam of 3 MeV protons of diameter not greater than 10μm and containing at least 10 nA of current.

In the system under development the IBIS beam is collimated by an aperture of diameter 65μm and then focused with a system of magnetic quadrupoles. Using protons of 1.5 MeV an image of 15μm diameter with about 10 nA of current has been achieved. Developments aimed at reducing the beam size below 10μm and using 3 MeV protons are in train.

---

(115) Armstrong R. J., Morish A. H. and Sawatsky G. A. Phys. Lett. 23, 414 (1966).

(116) Sawatsky G. A., van der Woude F. and Morish A. H., Phys. Lett. 25A, 147 (1967).

Electron Scattering (D. W. Colvin)

A review of the theoretical and experimental literature on electron scattering provided the basis for calculations of the multiple scattering parameter of electrons of energy 0.1 to 5 MeV in gases. It is intended that these be compared with some recent measurements carried out by D. L. Allan.

Chemical analysis using a Po-Be neutron source (D. L. Allan and B. H. Armitage)

As part of a collaborative study with Analytical Sciences Division of the use of neutrons for chemical analysis some preliminary experiments have been carried out to explore the possibility of making a determination of certain chemical constituents in rather massive samples (several kg) of materials using a small Po-Be neutron source. The method is to set up a 3 in. x 3 in. NaI detector and the neutron source in close proximity to the sample and to detect the γ-rays following neutron inelastic scattering. The method appears to be most promising in the case of nuclides whose γ-ray spectrum excited in the $(n,n'\gamma)$ process contains a single dominant γ-ray line.

Pronounced γ-ray peaks have been detected in the $(n,n'\gamma)$ spectra of Si, Fe, S, Mg and Al samples (in that order of intensity). The data do not yet permit a proper estimate of ultimate sensitivity to be made but it seems that a 1% silicon constituent could be detected after 15 minutes of counting time using the neutron source at present available (intensity $\sim 10^6$ neutrons per second).

These investigations were prompted by the suggestion[117] that the technique might be of use in determining the amount of quartz present in ball clay. However, it has been found that the method is unsuitable for moist samples (like ball clay) because of the energy moderation of the fast neutrons that occurs when a large quantity of water is present.

Position sensing detector array for the Buechner spectrograph (D. L. Allan, G. V. Ansell and R. K. Jolly)

An eight element array of position sensing detectors has been mounted in the focal plane of the Harwell broad range charged particle magnetic spectrograph Fig. 23 and used successfully to measure the deuteron spectrum from the reaction $^{56}(d,d')$ at $E_d = 11.5$ MeV (Fig. 24 see page 45).

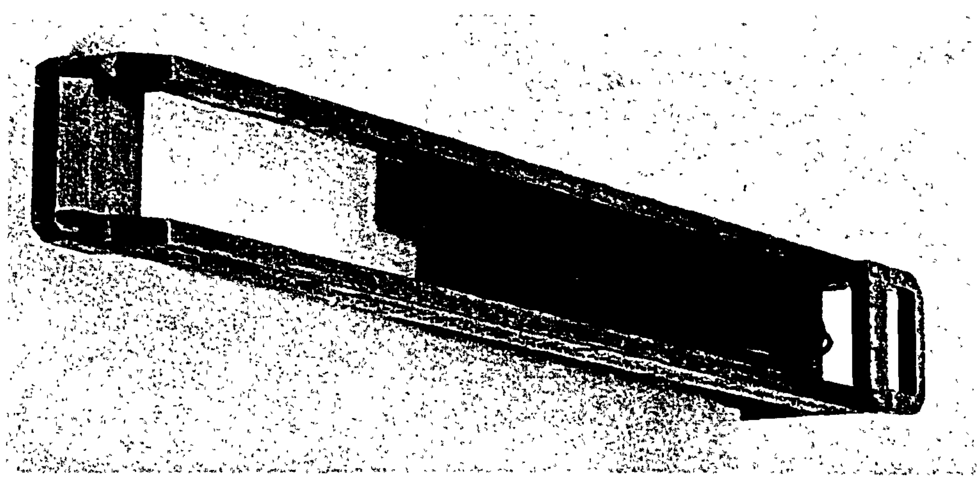

Fig. 23. Eight element array of position sensitive detectors mounted in holder.

---

(117) Ferguson A. T. G. Private communication.

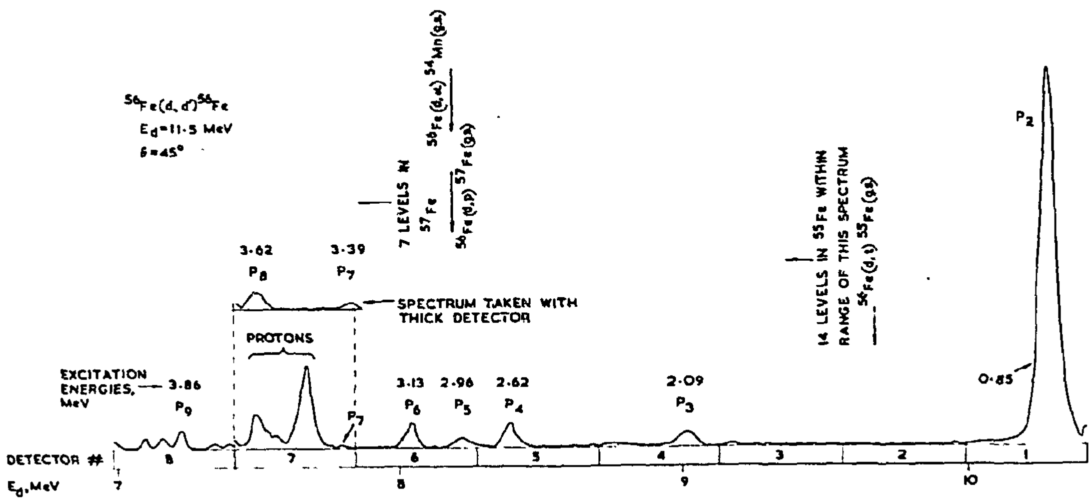

Fig. 24. Sample spectrum for $^{56}Fe(d,d')$.

The energy pulse ($\propto$ E) and the position pulse ($\propto$ E.x) from each detector are fed to a divider circuit which generates an output pulse whose amplitude is proportional to the position coordinate x. This pulse is digitized and stored in the memory of a PDP-8 data processer. The E-pulse is also used to generate a routing pulse which directs the x-pulse to the appropriate block of 256 channels in the set of 2048 channels available for data storage. The 'x' pulses are routed to the eight blocks of 256 channels in such a way that the stored data from the PDP-8 can be displayed as a continuous spectrum on a CRT screen.

A system has been incorporated to allow particles of a single kind to be selected from amongst the many protons, deuterons, alphas etc. that may result from irradiation of the target under investigation. For this purpose the E-pulses are passed through eight selector units, whose windows are separately adjusted to admit only pulses whose amplitudes are appropriate to the chosen particle type. The outputs of the eight selectors are mixed and used to command the divider circuit, so that only the selected pulses can cause an x-pulse to be delivered to the ADC.

Procedures have been devised that allow the electronic equipment to be set up quickly before the experiment. A number of careful measurements have been made to check the uniformity of efficiency of the detectors.

Further details can be found in an A.E.R.E. report[118].

Installation of multigap spectrograph (D. L. Allan and P. Humphries)

The AWRE multigap spectrograph has now been installed in Room G03 of the tandem experimental area and officially handed over to the Nuclear Physics Division. Vacuum tests have been carried out on the spectrograph shell and the magnet coils have been run at full current. The work of installing the beam flight tube and beam optics equipment will begin shortly.

The new dark-rooms are now ready for use and the automatic photographic plate processing machine has been operated satisfactorily.

(118) A.E.R.E. Report R 5897, 1968.

The six gap (orange type) beta-ray spectrometer (R. Chapman)

The performance of the spectrometer has now been fully investigated using radioactive sources of ^{137}Cs and ^{198}Au. The cooperation of the six gaps has been appreciably improved by field trimming. This is illustrated in Fig. 25. It is hoped that a further improvement in resolution will shortly be achieved

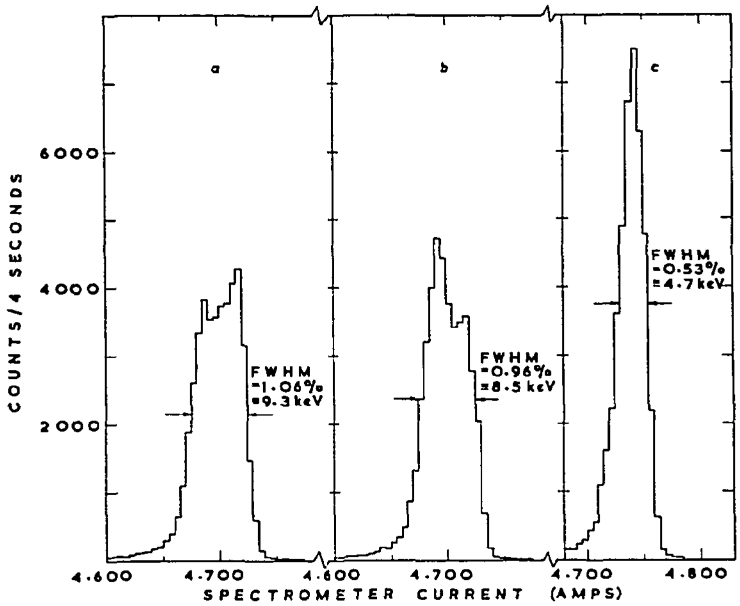

Fig. 25. The K-662 keV internal conversion line from a ^{137}Cs source. Each spectrum was recorded with a detector slit width of 0.5 mm and with all six gaps in operation.

(a) The K-662 keV electron line with no compensation for earth's magnetic field and no field trimming.

(b) The K-662 keV electron line with compensation for earth's field in operation.

(c) The K-662 keV electron line with both compensation for earth's field and field trimming in operation.

by using a detector slit contoured to accommodate the slightly different positions of the images on the focal cylinder.

An accurate energy calibration of the magnet is now under way. It has been found that when a demagnetisation cycle is followed by a premagnetisation step, as recommended by Gregers Hansen et al.[119] the peak position for the K-412 keV internal conversion line from ^{198}Hg is reproducible to better than 2 parts in 3,000 of the electron momentum.

Computer control of beta spectrometer (R. Chapman, R. I. Macdonald, J. L. Rose)

The automatic control of the spectrometer by the PDP-8 computer is now functioning satisfactorily. The system has proved to be very reliable over many weeks of use.

(119) Gregers Hansen P., Loft Nielsen H. and Wilsky K. Ris. Report No. 68.

Electron Conversion Coefficients (J. A. Cookson and R. Chapman)

Conversion electron spectra measured with the β-spectrometer often yield K/L ratios from which the multipolarities of the transitions can be deduced. However in some cases the results are ambiguous, either because there is too little variation of the K/L ratios with multipolarity, or because of failure to resolve complex spectra. It is likely that in some of these cases observation of the γ-ray spectrum with resolution of a few keV will make it possible to extract conversion coefficients and hence multipolarities. For experiments using an accelerator beam it may be necessary to take measurements at a number of angles.

Work so far has been confined to measurements of the ratio of K-electron intensity to γ-ray intensity for transitions with known conversion coefficients. A number of sources are being obtained which will make it possible to provide a calibration curve over a wide range of transition energies as a preliminary to measurements of reactions induced by the tandem beam.

ACCELERATOR OPERATION, MAINTENANCE AND DEVELOPMENT

MODIFICATION PROGRAMME FOR 500 keV COCKCROFT-WALTON GENERATOR (G. Dearnaley and P. D. Goode)

Ion beams were obtained from the machine during early June and ion implantation began in July, after optimization of the focusing. On target beams of A^+ (120 μA), Cu^+ (35 μA), H_2^+ (60 μA), Fe^+ (8 μA), P^+ (20 μA), Zn^+ (20 μA) and B^+ (2.5 μA) have so far been obtained. Some time has been spent in finding the best method of introducing material into the ion source, e.g. as a gas, or by sputtering, or by a novel technique to be described later. The results of these implantations, as reported by users, appear to be highly satisfactory.

The new general-purpose ion implantation chamber supplied by Vacuum Generators Ltd. has been installed and pumps down to 2×10^{-7} torr. Beam scanning and magnetic focusing operate satisfactorily, but it is clear that the improved machine stabilization system which has been designed is required as soon as possible. At present the system is that which existed before the modification.

The machine has performed very reliably, apart from one or two of the units supplying power to the ion source. The emission stabilizer in particular has given repeated trouble and has now been by-passed, without any noticeable loss in performance.

3 MV PULSED VAN DE GRAAFF GENERATOR I.B.I.S. (A. T. G. Ferguson, D. R. Porter, F. D. Pilling and E. A. Gove)

Analysis of machine running		Hours	Hours	%
Total Scheduled time		2081		100.0
Installation work				
Scheduled maintenance & conditioning			275	13.2
Setting up ion source & beam aligning			110	5.3
Scheduled experimental time			1696	81.5
		1696		100.0
Time lost through breakdowns			270	15.9
Available experimental time			1426	84.1
		1426		100.0
Experimental Usage				
(1)	Nuclear Physics Division		559	39.2
(2)	Analytical Science Division		233	
(3)	Metallurgy Division		55	
(4)	Research Reactors Division		46	
(5)	Electronics and Applied Physics		8	
(6)	Solid State Physics		8	
	Sub-Total other A.E.R.E. Divisions		350	24.5
(7)	Glasgow University		232	
(8)	Oxford University		114	
	Sub-Total University Users		346	24.3
(9)	A.E.E. Winfrith		105	7.4
	Machine development		66	4.6

A new accelerating tube had to be fitted during August. In the top terminal a certain amount of trouble has been experienced with the source focus transformers and with the gas feed to the ion source, particularly the palladium leak. Otherwise the machine has run very well, giving conventional beams of up to 100 microamps on target, and a beam of several nanoamps focused onto a spot a few microns in diameter.

Facilities for reducing the pulse repetition frequency from 1 MHz in steps to 100 kHz have been installed to permit the calibration of neutron detectors with rather slow time response.

5 MV VAN DE GRAAFF GENERATOR (A. T. G. Ferguson, K. C. Knox, F. D. Pilling and S. Waring)

All the installation work has been carried out and the machine is now in limited service. Tests of the accelerator without the tube indicated that while it would hold in excess of 7 MV without major breakdown, at this voltage many small breakdowns occurred across the insulators. These breakdowns would give rise to serious instability in an accelerated beam. Investigations raised suspicions that many of the insulators had not been made to specification. As an interim measure the whole set was modified, and satisfactory operation up to 4.5 MV was then achieved with the accelerator tube installed. The electron suppressed accelerator tube has been technically very satisfactory, with X-ray levels very low and no signs of steering evident. A mechanical failure of the top glass insulator was experienced. This has now been replaced and modifications have been made to reduce stresses. The beam optics and general handling of the accelerator have been excellent.

A new set of insultators will be installed in December 1968 and it is hoped that by careful operation higher voltages will be achieved with adequate stability.

13 MeV TANDEM GENERATOR (P. Humphries)

Analysis of Machine Running (1st May 1968 - 31st October 1968)

	Hours	Hours	%
Total scheduled time	1612		100
Scheduled Maintenance		400	24.8
Setting up ion-source and beam		108	6.7
Not Required		44	2.7
Scheduled Experimental time	1060	1060	65.8
			100
Time lost through breakdowns		4	0.4
Available Experimental time	1056	1056	99.6
			100
Experimental Usage			
(1) High Voltage Laboratory		594	56.3
(2) H.V.L. Manchester, Birmingham (Collab)		218	20.6
(3) Oxford University		41	3.9
(4) Bradford University		78	7.4
(5) Analytical Sciences Division		12	1.2
(6) Medical Research Council		43	4.0
Machine Tests		70	6.6
		1056	100

Machine Performance

The machine ran quite steadily until the end of August, when instabilities at the higher voltages became apparent. These were eventually attributed to excessive movement of the charge belt and several changes of belt were made before normal machine stability was regained.

Recent experimental runs have included the use of analysed proton beams of 9μA at 12.5 MeV with beam spot sizes of 1 mm x 3 mm. With these conditions the beam transfer through the machine was 80% and around the analyser magnet 75%.

Mercury Pool Source

The Mercury Pool Source continued to function satisfactorily, and further machine running has confirmed the initial indications regarding the high degree of reliability and greatly increased beam outputs.

Machine Facilities

The beta-spectrometer is now being used for experimental work. The floor supports for the angular correlation table have been strengthened and assembly work will continue during the next few months.

The multi gap spectrograph has been installed and handedover to Nuclear Physics Division but there are still a number of outstanding items of work to be completed before calibration experiments can begin.

In July and August of this year A.W.R.E. tested a pair of A.E.R.E. Spiral Inclined Field Accelerator Tubes. Although conditioning time was considerably reduced, beam transfer and X-ray loading were disappointing.

Helium Negative Ion Source - Development (R. H. V. M. Dawton and N. Allen)

The lithium evaporator for charge exchange vapour has been tested at an operating temperature of 630°C. The optimum exchange energy was 17 keV as compared with 12½ keV for the potassium vapour and the beam output was somewhat less, say 10%, but one cannot attribute this with certainty to the lithium. The lithium consumption was 40 mgm per hour, measured over some 80 hours of operation.

The relative ease with which the lithium evaporator can be serviced warranted some little effort to increase the beam output. An examination of the positive beam showed that, for optimum transmission through the evaporator, the beam was focussed somewhat before the centre of the 6" long tube. This resulted in the beam being clipped. As the source and boiler could not be moved closer together, the narrower part of the beam passage was increased from ¼" to $^5/_{16}$" diameter. As a result the total beam increased by 50%, giving 4¼μA through a ¼" receiver aperture. The lithium consumption with this larger diameter has not been measured but it would be surprising if it exceeded 70 mgm per hour.

Cleaning procedures necessary during a recharge of the evaporator have been established.

The analysing magnet has been manufactured, calibrated and found to be satisfactory.

Helium Negative Ion-Source-Installation (P. Humphries)

The complete Helium Ion-Source is being assembled in Hanger 10 and it is hoped to have this operational during the next few weeks. The ion source will stay in Hanger 10 until all necessary experimental, modification and operational work is completed. It is anticipated that the ion-source should be installed in the Tandem during March/April 1969.

Preparatory work for the installation is currently being carried out in Building 477.

45 MeV ELECTRON LINEAR ACCELERATOR (P. P. Thomas)

Analysis of machine running

	Hours	Hours	%
Total scheduled time	4320		100.00
Scheduled machine tests		192	4.34
Scheduled maintenance and installation work		444	10.46
Scheduled experimental time		3684	85.20
	3684		100.00
Time lost through breakdown		395	10.74
Machine off at users' request		23	0.64
Available experimental time		3266	88.62
	3266		100.00

Experimental usage

			Hours	%
(1)	Experimental Runs – Cell I		2709	83.00
	Mr. N. J. Pattenden	N.P.		
	Dr. C. A. Uttley	"		
	Dr. G. D. James	"		
	Dr. M. G. Sowerby	"		
	Mr. M. G. Schomberg	"		
	Mr. M. C. Moxon	"		
	Dr. B. H. Patrick	"		
	Dr. J. Murray	"		
	Miss E. M. Bowey	"		
	Dr. H. Postma	F.O.M. Netherlands		
	Dr. A. Asami	J.A.E.R.I., Japan		
	Dr. P. Axmann	Austrian A.E.		
	Dr. S. Malmskog	Swedish A.E.		
(2)	Experimental Runs – Cell II			
	Dr. D. B. Gayther	N.P.	101	3.08
	Dr. W. G. Burns	Chem.	6	0.18
(3)	Experimental Runs – Cell IV (Sole use of machine)		440	13.44
	Dr. B. H. Patrick	N.P.		
	Dr. D. B. Gayther	"		
	Dr. H. A. Medicus	R.P.I., Troy, N.Y., U.S.A.		
	Dr. J. Winhold	"		
	Miss E. M. Bowey	N.P.		
(4)	Irradiations for Analytical Sciences Division		10	0.30
	Dr. J Hislop	A.S.		

		Hours	Hours	%
(5)	Experimental Runs — Cells III and IV (simultaneous with Cell I running)	1706		100.00
(5A)	Dr. R. N. Sinclair A.P. Mr. D. Day "		946	55.44
(5B)	Dr. B. H. Patrick N.P. Dr. D. B. Gayther " Miss E. M. Bowey " Dr. H. A. Medicus R.P.I., Troy, N.Y., U.S.A. Dr. J. Winhold "		166	9.75
(5C)	Dr. M. S. Coates N.P. Mr. B. P. Clear "		217	12.74
(5D)	Mr. J. Williams Imperial College (EMR) Dr. H. Lichtblau Univ. of Birmingham (EMR)		197	11.44
(5E)	Dr. G. D. James N.P. Dr. B. H. Patrick "		168	9.86
(5F)	Dr. D. B. Gayther N.P.		12	0.77

Machine development

Energy Measurements (M. S. Coates, P. P. Thomas and B. P. Clear)

Electron energy measurements under different beam conditions have been made using a two slit system and the Cell II bending magnet as a spectrometer. The magnet was calibrated using the floating wire technique. With the geometry shown in Fig. 26 the current in the fixed plate was recorded automatically as the magnet excitation current was changed. Some results are shown in Fig. 27 (see page 53). The large energy spreads for pulse lengths comparable with the filling time ($\sim 0.25\mu$sec) are due chiefly to the beam loading effects but the spreads for the long pulse lengths should be smaller than observed. Investigations of various factors with a view to reducing this spread will be reported later. So far only increasing the water flow to cool the bunching section has produced a significant improvement, and this was quite small.

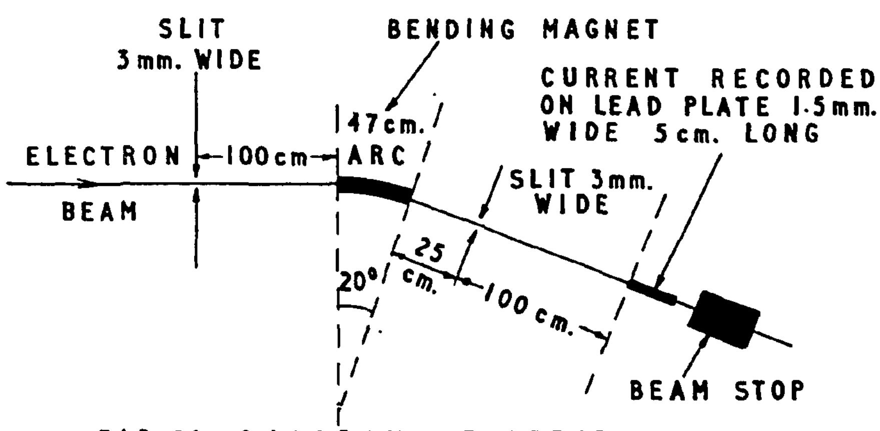

FIG.26. DIAGRAM OF SPECTROMETER

Fig. 26. Spectrometer layout for measurements of beam energy spread.

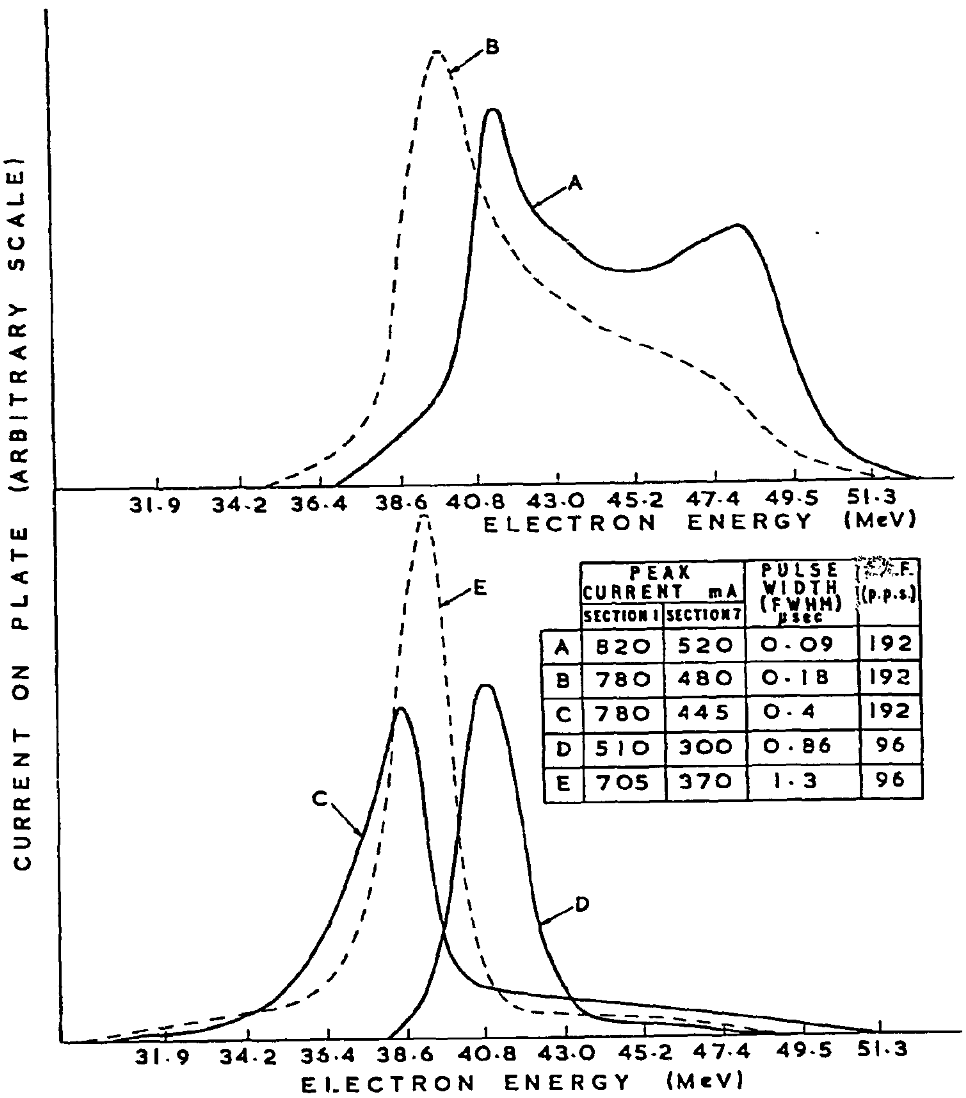

	PEAK CURRENT mA		PULSE WIDTH (FWHM) µsec	[illegible].F. (p.p.s.)
	SECTION 1	SECTION 7		
A	820	520	0·09	192
B	780	480	0·18	192
C	780	445	0·4	192
D	510	300	0·86	96
E	705	370	1·3	96

Fig. 27. Measurements of energy distribution in electron beam.

New Beam Bending System (M. S. Coates and B. P. Clear)

The present 90° bending magnet system for Cell III cannot transmit electrons with an energy spread exceeding ±4%. The energy spread with present machine conditions is considerably higher than this (cf Fig. 27) and although it is reasonable to expect some improvement for long pulses, for short pulses an improvement could only be achieved at considerable expense. Consequently an improved 90° bending system has been designed incorporating the present pulsed magnet, three quadrupoles and another bending magnet. This system should transmit electrons with an energy spread of at least ±8%. The quadrupoles are available and it will be possible to carry out experimental tests in Cell II shortly.

Secondary Emission Beam Position Monitor (M. S. Coates and B. P. Clear)

A beam positioning device has been constructed and tested which detects the secondary electron emission from a thin foil placed in the path of the primary electrom beam. In principle the arrangement shown in Fig. 28 is similar to secondary electron monitors previously reported[120], except that the emitting electrode is divided into four quadrants, each having a separate output. These outputs suitably displayed can be used to monitor the poisition of the primary electrom beam so that it can be made to fall symmetrically on the quadrants. The device will be used to maintain the position of the electron beam falling on a neutron producing target used in neutron spectrum measurements.

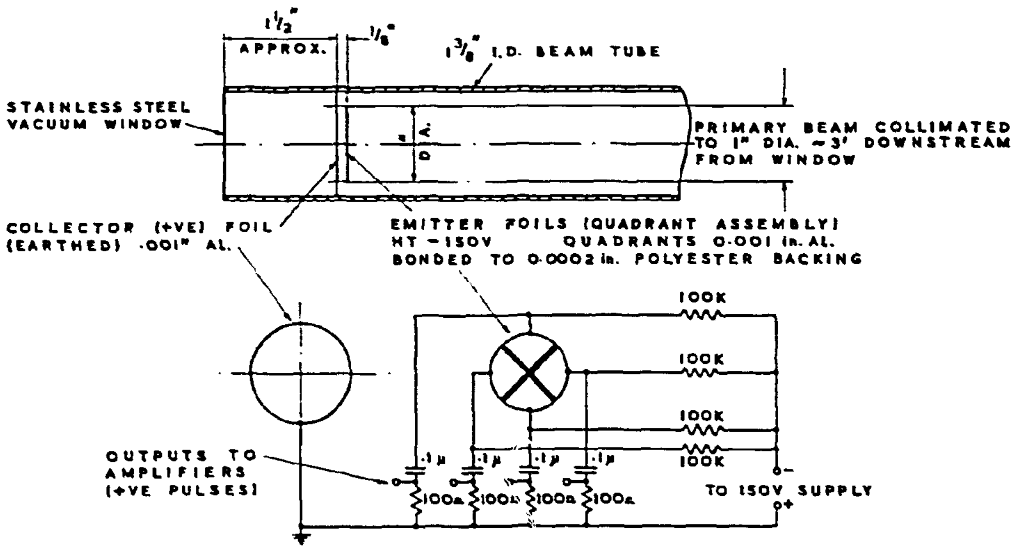

Fig. 28. Schematic diagram of beam position monitor.

Beam Tube Windows (M. S. Coates and P. P. Thomas)

The mercury cooled neutron booster target is isolated from the accelerator vacuum system by a thin stainless steel window which is liable to early failure when subjected to long pulses of electrons.

The window is thus a weak link in plans to increase the booster output and investigations into alternative designs and methods of manufacture are in hand.

New High Power Neutron Target (P. P. Thomas)

A 5 kW water cooled natural uranium target has been designed and is being manufactured. Installation in Cell II is planned for early 1969. When completed, this target will provide a source for neutron inelastic scattering experiments with an intensity some 5 times greater than that of the target at present in use.

(120) Tautfest G. W. and Fechter H. R. Rev. Sci. Inst. 26, 229 (1954).

E PDP-4 data processors (E. M. Bowey, G. B. Dean and J. B. Brisland)

During the period of this report the main computer system was in use for 2077 hours. Electro-mechanical faults of the peripheral equipment were predominant, but did not interfere seriously with the scheduled program.

Some software has been commissioned for the Dectape system, and all programs in general use are now available on a Dectape systems tape. Considerable difficulties have been experienced using FORTRAN programming with Dectape, and these are still being resolved by Digital Equipment Corporation.

The second PDP-4 was commissioned in April. Additional wiring has been carried out to permit the attachment of specialised peripheral equipment now being designed and constructed for use with the on-line multiparameter experiments.

SYNCHROCYCLOTRON IMPROVEMENT PROGRAMME

Magnetic field survey and the extraction system (G. C. Cox, E. A. C. Crouch, A. Langsford and D. West)

Magnetic measurements play an essential part at all stages of the design and installation of the regenerative extractor. The results obtained with the automatic survey equipment (G. C. Cox and A. Langsford) have been analysed using orbit computer programs in a continuous process of correcting the extractor.

In the initial design a radial survey of the magnetic field in the cyclotron at a single azimuth (Scanlon and Spencer 1962) was used and cylindrical symmetry was assumed. To check this assumption and other things the bare magnet was surveyed at radii from 37" to 56" and at intervals in azimuth of 2°.

The required regenerator strength versus radius computed from this survey was about 7% lower than that derived previously. In addition, the measurements gave the behaviour of the magnet under ideal conditions, as a standard for comparison purposes. The amplitude of the first harmonic component of the magnetic field (which alone influences the orbits of charged particles to any appreciable extent) is given in Table VIII column [2] .

TABLE VIII

First harmonic component of magnetic field as a function of radius.

Radius (inches) [1]	Amplitude of First Harmonic (Gauss)		
	Bare Magnet [2]	With Headers only [3]	With Headers and Shimmed Regenerator [4]
32		1.1	
36		1.3	
40	2.0	1.7	4.0
44	2.3	2.0	2.1
48	2.7	0.6	7.1
52	6.5	10.3	293.2
56	8.4	44.0	

At 48" radius the orbit centre for a charged particle would be displaced 3 mm by a field with this asymmetry.

Steel equipment, which might influence the field configuration, was next put in place. It consisted of the R.F. vacuum tank and the vacuum pump header. The R.F. tank produced a field bump of some 50 gauss at 48" radius, extending over a considerable region. Pole face shims to counteract this have been made and will be tested in the later stages of the work. The headers alone (see Table VIII, column $\boxed{3}$) produced only a small effect in the most critical region (below 48" radius) where the beam is still being accelerated. For comparison purposes we have included in Table VIII column $\boxed{4}$ the measured first harmonic components of field with the latest version of shimmed regenerator in place (see below). The condition with headers is now used as a reference from which the effects of regenerator and channel are measured. Field survey work on the regenerator was next carried out. Manual surveying described in the last progress report had established both an approximately correct cross-sectional shape for the regenerator and its angular extent.

It was intended to make further fine adjustments by varying the angular extent. Accordingly two regenerators of angular extent 23° and 20° were surveyed. To establish, in addition, the radial position of the regenerator the 20° regenerator was displaced 1 cm in radius and re-surveyed. It became clear that the 20° regenerator was close to the required length, and, although a problem arose at this stage concerned with the finite extent of the real regenerator as opposed to the calculated one, the 20° regenerator was rather arbitrarily adopted at this stage. It gave an overshoot of 100 gauss just inside the radius at which extraction should set in. Calculations by I. M. Blair were used to arrive at suitable shims to reduce this effect. The adopted shims reduced the overshoot to 37 gauss. This shimmed regenerator was now surveyed in two radioal positions 1 cm apart and by then it was possible to check that the starting condition for extraction was satisfied (this condition concerns the slope of the regenerator strength versus radius at the starting radius for extraction). Calculations carried out with the computer programs indicated that in the outer position of the 20° regenerator protons of 160.8 MeV should be extracted, at the inner position, protons of 157.7 MeV. In the meantime channel shimming was in progress. The track of the channel depends on the regenerator, the undisturbed field, and the field depression in each section of channel, which in turn depends on the shimming. In the first instance we set up the channel (12 sections, each 6" long) in a position based on the estimated fields produced by the unshimmed regenerator and measurements of field depression in single channel sections, taken before the channel was designed. Calculations of the shimming required to give acceptably low perturbation fields were made by I. M. Blair. The measured field near the channel sections, however, were found to differ appreciably from those assumed for the calculations. Accordingly we decided to measure the field effects to be shimmed out as a first step in channel shimming. A second generation of shims has been designed and is about to be tested. The field discrepancies we observed outside the channel sections persuaded us to prepare to measure the field depression inside the channel before attempting to put a floating wire through it.

Shimming calculations (I. M. Blair)

The regenerator and channel of the extraction system, designed by D. West, operate by perturbing the magnetic field of the synchrocyclotron over prescribed regions. The perturbations naturally spread out beyond these regions, and it is necessary to eliminate their effect in the field regions through which the particles travel prior to extraction. Consequently calculations are being performed to decide on the size, shape and position of static iron shims to achieve this purpose.

A saturation technique is used, and the effect of magnetic images in the magnet poles is taken into account. Though simple in concept, the calculations agree quite well with the measured perturbation distribution from iron test blocks. The saturation intensity of magnetisation for the type of iron to be used for the shims can be deduced from this comparison.

With the aid of these calculations, adequate shims for the regenerator have been designed, built and tested. They have also proved useful in the design of the channel itself, in particular for the focussing elements. Work is in progress on the design of shims for the channel, and satisfactory shimming of the first section has now been achieved.

Pulsed deflection system for neutron beams (P. H. Bowen and A. Langsford)

The pulse forming system[121] has undergone intensive tests, and works reliably with voltages of up to 70 kV on the anode of the CX 1168 thyratron. This valve delivers to the deflection system a 35 kV pulse with a 15-20 ns rise time which is adequate for present requirements. However attempts to run the system at the maximum voltage recommended by the manufacturer, 80 kV, result in the thyratron failing to extinguish. This problem has been discussed with the manufacturer and modifications have been tried, but no improvement has been observed.

A fully engineered deflection electrode assembly is being manufactured and will be available on 1st December. Some modifications to the thyratron control circuits and to the high voltage supply have been made to facilitate control and to allow remote operation of the beam deflection system. A complete investigation of the performance of the system awaits the availability of internal beams in the synchrocyclotron.

New R.F. system (P. E. Dolley and G. B. Huxtable, with members of Engineering Division)

Following the successful conclusion of a prolonged high-voltage test run lasting one month, the new R.F. system was installed in the cyclotron pit in July. It has since been operated in its normal working environment of cyclotron-tank vacuum and magnetic field (but with no ion-source at the machine centre). The testing program is being phased in with other activities in the cyclotron tank.

There are small differences between the shapes of the cyclotron tank and the tank in which the preliminary tests were carried out. As a result some small changes in the geometry of the resonator are required in order to achieve the correct frequency-sweep, and these are being made.

The erosion of the rotor bearings by R.F. currents, which has caused a lot of trouble, has now been greatly reduced by means of a 'guard-ring' technique. Oil contamination in areas of high voltage gradient has continued to cause sparking from time to time; modifications to the oil sealing system have improved the situation but the trouble is not yet completely cured.

We expect that most of the design aims of the R.F. system will be realised. However, the maximum pulse repetition rate will be 1200 Hz, not 1600, to conform with a more realistic assessment of the changes of synchronous phase angle of the particles over the acceleration cycle, and this will ease some of the mechanical problems of the rotating capacitor. In the early stages of operation, the peak dee voltage when accelerating He^3 ions will be limited to 25 kV, not 30 kV, to reduce sparking.

Some electronic equipment for control and fault protection has been produced, and a routine procedure for the operation of the R.F. system is being developed. Changing the frequency range from one particle to another (protons, He^3's, or deuterons and alphas) should take no more than 5 minutes.

Engineering support (P. G. Davies, R. Bint, W. H. Holland and J. Stevens)

General support has been given during the installation and subsequent testing of the R.F. system, ion source and extractor studies.

The main vacuum system was rebuilt with new headers and tank end-plates remade in time for the high power R.F. testing. Difficulties with the special corner seals needed to seal the North plates to the supporting pillars were overcome after development and testing.

All new shielding walls are complete, with the exception of an access hole in the North wall. Work is in hand to provide smooth, uniform collimating slots in the South and East walls.

Work on equipping the beam tunnels is well advanced. This includes the provision of vacuum pumps for the 32" lines, interlocking, safety gases and the laying of cables to the main neutron counting room.

(121) Nuclear Physics Division Progress Report AERE PR/NP 11, p. 47 (1967).

Electrical installation in the pit is complete, including the re-siting of safety boxes made necessary by the revised layout. Interlocks and remote controls are being provided in the Control Room, the layout of which is being modified to suit the needs of the improved machine.

All the beam handling supplies have been concentrated in the old Rectifier House. Installation of generators and the new time-of-flight pulser system is well advanced.

Ion-source development (E. Wood and J. P. Scanlon)

Ion-Source Positioning Mechanism

This has now been installed in the cyclotron. The ion-source feed tube (5.6 cm diameter and about 4 m long) enters the magnet pole gap axially through an 20 cm diameter vertical hole in the upper magnet yoke, via a vacuum lock. To locate the ion-source and to provide magnetic shimming the low portion of the hole contains a system of rotatable steel plugs, and the feed tube contains a further shimming plug. The locating hole in the plug system and the top end of the feed tube are moved in consort by a motor driven epicyclic gear train, mounted above the magnet yoke. This provides horizontal movement of the source both radially and azimuthally with respect to the machine centre. The source may also be rotated about the axis of the feed tube by a separate drive.

To prevent collisions between source and dee structure, the geometry of these objects is reproduced by a model mounted at the top of the feed tube; contact between the moving and stationary parts of the model operates interlocks in the driving control circuit. Remote indication of the source position is provided by an X-Y plotter.

The system has been checked out mechanically and electrically, showing that the model geometry can be aligned with that of the machine centre to sufficient accuracy and that the anti-collision protection works under all circumstances.

A magnetic survey of the central region has shown that residual field disturbances in the vicinity of the plugs should shift the orbit centre co-ordinates of accelerated particles by less than 2.5 mm.

Ion-Sources

The first source, a hot-cathode calutron of conventional design with an "R.F." puller electrode (connected to the live dee), is ready for testing in the cyclotron. Although such sources have been used successfully elsewhere, a typical filament life is only 40-50 hours. Work at the Rutherford Laboratory, however, has shown that pulsed cold-cathode calutron sources with long electrode life can be made to give adequate emission for use in synchrocyclotrons. These sources have the additional advantages of cooler running and absence of high-current filament leads. A design study is being made for such a source to replace the hot-cathode type.

For some experiments it is essential that as much of the circulating beam as possible should have small phase oscillation amplitudes. Calculations made here (and verified by independent work at C.E.R.N.) show that a calutron source with an R.F. puller is far from ideal in this respect. A short term solution which is being adopted is to provide an "open" ion-source for such applications. The more satisfactory long term solution lies in the provision of a calutron source with D.C. extraction voltages.

Particle dynamics in the cyclotron (J. P. Scanlon)

A further series of calculations made with the computer code 'MOCWAC'(122) showed that given a suitably shaped dee with an area 50% greater than the present design, generation of radial betatron oscillations could be reduced by a factor of up to three. This could result in a considerable improvement in extraction efficiency for charged particle beams, but it remains to be seen whether such a dee could be designed with sufficiently small capacity to ground for use with the present R.F. system.

(122) Nuclear Physics Division Progress Report, AERE PR/NP 14, p. 71 (1968).

An attempt has been made to analyse the slow extraction problem in which acceleration of particles is transferred from the dee to an auxiliary "Cee" electrode with a controlled voltage and frequency programme. Qualitative results have been obtained which indicate that transfer of stable orbits from dee to cee in the modified cyclotron may be somewhat less efficient than previously. The basic reason is that although the 'Q' of the R.F. system remains almost unchanged, the repetition rate of the machine has been increased by a factor of five and therefore the switch-off time for the dee is five times larger relative to the acceleration period. Thus the energy spread of the internal beam is increased appreciably as the dee is switched off, and a smaller fraction of the particles are picked up into stable orbits by the cee.

The present cee R.F. system only operates in the proton frequency band, and consequently will not pick up deuterons, α particles or $^3He^{++}$'s.

To remedy this situation, two possibilities exist:

(a) To provide two more frequency bands;

(b) To accelerate in the cee on higher harmonics, i.e., 2nd for protons, 3rd for $^3He^{++}$ and 4th for deuterons and α-particles using a 60^{o} cee.

For (b) the R.F. frequency would have to be tunable over the range 42 ± 2 MHz, because of the different relativistic mass increases in the three cases. Our calculations indicate that the dee-cee transfer efficiencies would not be very different for the two methods.

Solid hydrogen target assembly (E. Wood)

Preliminary tests at low temperature have shown the difficulties of determining the level of liquid He in the reservoir and the temperatures at the extrusion nozzle and in the cylinder in which the hydrogen will be solidified prior to extrusion. A combination of carbon resistor level-temperature sensors and Cu/Au-Co thermocouples is being fitted in an attempt to overcome these problems.

Magnetic median plane device (E. Wood)

Pressure of other work has prevented much progress with this device. Nevertheless laboratory tests have shown that changes of 10" of arc can easily be detected and this sensitivity would enable the magnetic median plane in the synchrocyclotron to be determined to about 1 mm.

Measurement of magnetic centres of quadrupoles (E. Wood)

The use of colloidal magnetic fluid for determining the magnetic centres of quadrupole magnets has been further developed. An accuracy of ±0.1 mm was recently observed in tests carried out in collaboration with Dr. Coulson.

REPORTS, PUBLICATIONS AND CONFERENCE PAPERS

REPORTS

AERE - R 5732	A non-destructive measurement of the fluctuations in area density of a graphite block using a 147 MeV proton beam. R. A. Bell, P. J. Clements and A. Langsford.
AERE - R 5801	J-dependence and spectroscopic factors in the 2d-shell for the tin isotopes. P. E. Cavanagh.
AERE - R 5863	A study of the nuclear structure of the odd tin isotopes by means of the (p,d) reaction. P. E. Cavanagh, C. F. Coleman, A. G. Hardacre, G. A. Gard and J. F. Turner.
AERE - R 5875	Anodic oxidation of silicon. M. A. Wilkins.
AERE - R 5891	Structure in sub-threshold fission modes. J. E. Lynn.
AERE - R 5897	A position sensing detector array for a charged particle magnetic spectrograph. D. L. Allan, G. V. Ansell and R. K. Jolly.
AERE - R 5901	Spectroscopic factors, symmetry effects and nuclear density distributions for the tin isotopes. P. E. Cavanagh.
AERE - R 5912	A search for high energy gamma-rays from the pulsating radio source CP1133. W. N. Charman, J. V. Jelley, P. R. Orman, R. W. P. Drever and B. McBreen.
AERE - R 5924	Fission components in ^{242}Pu resonances. G. D. James.
AERE - R 5945	The neutron resonance parameters of ^{240}Pu. M. Asghar, M. C. Moxon and N. J. Pattenden (to be published).
AERE - NP/GEN 54	The energy levels of ^{19}F and ^{19}Ne. K. Gul, B. H. Armitage and B. W. Hooton.

MEMORANDA

AERE - M 2065	Evaluation of the ^{239}Pu fission cross section in the energy range 1 keV to 100 keV. G. D. James and B. H. Patrick.
AERE - M 2082	Fission components in ^{234}U resonances. G. D. James and E. R. Rae.

PUBLICATIONS

ADAMS J. M., ADAMS A. and CALVERT J. M. Mass determination of the nuclei ^{12}N, ^{16}F, ^{22}Mg and ^{26}Si using the (^{3}He,n) reaction. J. Phys. A (Proc. Phys. Soc.), (Ser. 2) 1, 549 (1968).

ALLAN D. L. An experimental study of the configurational connexions between the states of an odd and even nucleus. Nuc. Phys. A114, 211 (1968).

ALLAN D. L., BRITT H. C. and RICKEY F. A. Jr. Analogue states and the nuclear structure of ^{181}Hf. Phys. Letters, 27B, 11 (1968).

ARMITAGE B. H. and HOOTON B. W. Energy loss of oxygen and sulphur ions in matter. Nuc. Instrum. and Methods, 58, 29 (1968).

ASGHAR M., CHAFFEY C. M. and MOXON M. C. The neutron resonance parameter and average capture cross section of ^{165}Ho. Nuc. Phys. A108, 535 (1968).

BJERREGAARD J. H., HANSEN O., NATHAN O., VISTISEN L., CHAPMAN R. and HINDS S. The reactions ^{207,208}Pb(t,p)^{209,210}Pb and the two particle, one hole states of ^{209}Pb. Nuc. Phys. A113, 484 (1968).

CHARMAN W. N., FRUIN J. H., JELLEY J. V., PORTER R. A. and SMITH F. G. Evidence for radio pulses from extensive air showers at large zenith angles. Sov. Phys. (JETP) 26, 59 (1968).

CHESHIRE I. M., DEARNALEY G. and POATE J. M. The Z_1-dependence of electronic stopping. Phys. Letters, 27A, 304, (1968).

COATES M. S., GAYTHER D. B., GOODE P. D. and TRIPP D. J. Time of flight measurements of the neutron spectrum in a sub-critical fast reactor assembly. J. Nucl. Energy 22, 547 (1968).

COOKSON J. A. The ^{13}C(d,n)^{14}N reaction. Phys. Letters, 27B, 619 (1968).

FREEMAN J. M., JENKIN J. G., ROBINSON D. C., MURRAY G. and BURCHAM W. E. The beta end-point energy for the superallowed Fermi decay ^{14}O(β^+)^{14}N*. Phys. Letters, 27B, 156 (1968).

HANSEN O., NATHAN O., VISTISEN L. and CHAPMAN R. Proton quasi-particle states in ^{143}Pm. Nuc. Phys. A113, 75 (1968).

JAMES G. D. and RAE E. R. Fission components in ^{234}U resonances. Nuc. Phys. A118, 313 (1968).

JELLEY J. V. and WILLSTROP R. V. Search for optical flashes from the radio source CP1919. Nature 218, 753 (1968).

LANGSFORD A., BOWEN P. H., COX G. C. and SALTMARSH M. J. M. Isobaric analogue states in (p,n) reactions at 94 MeV. Nuc. Phys. A113, 433 (1968).

LYNN J. E. The theory of neutron resonance reactions (Clarendon Press, Oxford, 1968).

SANTO R., STOCK R., BJERREGAARD J. H., HANSEN O., NATHAN O., CHAPMAN R. and HINDS S. Proton pick-up from the even calcium isotopes. Nuc. Phys. A118, 409 (1968).

IN COURSE OF PUBLICATION

CHAPMAN R., HINDS S. and MACGREGOR A. E. A study of ^{52,54,56}Cr by the (t,p) reaction. Nuc. Phys.

CHARMAN W. N. Properties of photomultipliers with caesium telluride photocathodes. J. Sci. Instrum. (J. Phys. E.)

CHARMAN W. N. A simple technique for detecting a periodicity of unknown value in the signal from an astronomical source. Applied Optics.

COATES M. S., GAYTHER D. B., JAMES G. D. and LANGSFORD A. The fission cross-section of ^{235}U in the energy range 0.1 to 10 MeV. AERE Report.

DAWTON R. H. V. M. Heavy negative ion beams. Nuc. Instr. & Methods.

DEARNALEY G. A theory of the oxide-coated cathode. Thin Solid Films.

DEARNALEY G., FARMERY B. W., MITCHELL I. V., NELSON R. S. and THOMPSON M. W. Proton channelling through thin crystals. Phil. Mag.

FREEMAN J. M., JENKIN J. G. and MURRAY G. The position decay of ^{10}C and the ft value of the superallowed Fermi transition $^{10}C(\beta+)^{10}B^{**}$. Nuc. Phys.

GAYTHER D. B., MEDICUS H. A. and McMILLAN J. W. The photonuclear reactions (γ,2n) and (γ,np) in ^{46}Ti. Nuc. Phys.

GUL K., ARMITAGE B. H. and HOOTON B. W. The energy levels of ^{19}F and ^{19}Ne. Nuc. Phys.

HANSEN O., NATHAN O., CHAPMAN R. and HINDS S. Vibrational states of ^{207}Tl. Nuc. Phys.

JAMES G. D. Fission components in ^{242}Pu resonances. Nuc. Phys.

JAMES G. D. and PATRICK B. H. A correlation analysis of the slow neutron fission cross-section of ^{239}Pu. Phys. Letters.

JOLLY R. K., GOLDBERG M. D., SEN GUPTA A. K., DARCEY W., CHAPMAN R. and HINDS S. DWBA and the 3.12 MeV state in ^{60}Ni. Phys. Letters.

MEDICUS H. A., BOWEY E. M., GAYTHER D. B. and PATRICK B. H. Photodisintegration of ^{12}C into excited states of ^{11}C and ^{11}B. Phys. Letters.

ROBINSON D. C. An evaluation of least square methods of analysing decay data. AERE - R 5911.

CONFERENCE PAPERS

Invited Papers

DEARNALEY G. The Range and Energy Loss of Implanted Ions. Symposium on Ion Implantation and Hyperfine Interactions. Royal Society, London, 2-3 May, 1968.

DEARNALEY G. Ion Implantation in the U.K. Gordon Conference on Particle-Solid Interactions, Meriden N.H. July 15-19, 1968.

LYNN J. E. Structure Effects in Nuclear Fission. International Symposium on Nuclear Structure, Dubna, USSR, July 1968.

MEDICUS H. A., BOWEY E. M., GAYTHER D. B. and PATRICK B. H. Photodisintegration of ^{12}C into excited states of ^{11}C and ^{11}B. American Physical Society Meeting, Miami Beach, U.S.A., November 1968

Contributed Papers

UK/USSR Seminar on Nuclear Constants, Dubna, USSR, 11-14 June, 1968

ASAMI A. and MOXON M.C. Low Energy Neutron Scattering Cross-section of ^{10}B. UK/19.

ASAMI A., MOXON M. C. and STEIN W. E. A new Technique for the Partial Wave Assignment of a Slow Neutron Resonance. UK/18.

ASGHAR M., MOXON M. C. and PATTENDEN N. J. The Neutron Resonance Parameters of ^{240}Pu. UK/20.

JAMES G. D. and PATRICK B. H. Evaluation of the ^{239}Pu Fission Cross-section in the Energy Range 1 keV to 100 keV. UK/14.

JAMES G. D. and RAE E. R. Fission Components in ^{234}U Resonances. UK/15.

JAMES G. D. Multilevel Analysis of ^{239}Pu Fission Cross-section near 83 eV. UK/16.

MOXON M. C. The Average Level Spacing from Neutron Cross-section Data. UK/17.

MOXON M. C., RAE E. R., RIEHS P., STEIN W. E. and THOMAS B. W. Gamma-ray Spectra from Neutron Resonance Capture. UK/22.

PATRICK B. H., SCHOMBERG M. G., SOWERBY M. G. and JOLLY J. E. Measurements of Eta, Alpha and the Neutron Cross-sections of ^{239}Pu. UK/24.

RAE E. R. Some Notes on the Accuracy of Neutron Cross-section Measurements. UK/21.

SCHOMBERG M. G., SOWERBY M. G., BOYCE D. A. and EVANS F. W. The Direct Measurement of $\alpha(E)$ for ^{239}Pu. UK/23.

SOWERBY M. G. and PATRICK B. H. The Ratio of the $^{6}Li(n,\alpha)$ to $^{10}B(n,\alpha)$ cross-section in the Energy Range 10 eV to 70 keV. UK/25.

Proceedings of the First International Colloquia on Nucleon-Nucleon and Pion-Nucleon Interactions, Dubna, 11-15 June, 1968

LANGSFORD A. N-p Interactions at 20-150 MeV. p.27.

10th International Conference on Cosmic Rays, Calgary, June 19-30, 1968

CHARMAN W. N. and JELLEY J. V. The Atmospheric Electric Field as a Source of R.F. Emissions from EAS, and Some Notes on Bremsstrahlung. Can. J. Phys. 46, S216 (1968).

CHARMAN W. N., FRUIN J. H. and JELLEY J. V. The Harwell-Grove Radio Installation for Detecting EAS at low elevation. Can. J. Phys. 46, S220 (1968).

JELLEY J. V. Antennas, receivers and problems of the Radio Detection of Large Air Showers. Can. J. Phys. 46, S225 (1968).

SMITH F. G., BRAY A. D., PORTER R. A., TORBITT W. S. and JELLEY J. V. Experimental Tests of the Mechanism of Radio Emission from Showers. Can. J. Phys. 46, S230, (1968).

FRUIN J. H. and JELLEY J. V. Servo Systems for Cherenkov Light Receivers. Can. J. Phys. 46, S1118 (1968).

International Colloquium on Nuclear Electronics, Versailles, 10-13 September, 1968

DEARNALEY G., HARDACRE A., G. and ROGERS B. D. Ion-implanted Germanium Particle Detectors.

4th Symposium on Photoelectronic Image Devices, London, 16-20 September, 1968

CHARMAN W. N. Cosmic Rays and Image Intensifier Dark Current.

Meeting on Amorphous Materials, Edinburgh, 24th September, 1968

DEARNALEY G. Electronic Conduction in Oxide Layer Structures.

Meeting on Techniques and Materials for Semiconductor Detectors, Ispra, 1-2 October, 1968

DEARNALEY G., HARDACRE A. G. and ROGERS B. D. Germanium Proton Detectors by Ion-implantation.

Theses

Some problems in neutron physics — An investigation of the p-wave neutron strength function in the mass 100 region. Thesis for the degree of Doctor of Philosophy submitted by C. M. Newstead to the University of Oxford, October 1967. Degree conferred December 1967.

The measurement of average neutron capture cross-sections in the mass region above 100. Thesis for the degree of M.Sc. submitted by M. C. Moxon to the University of London, June 1968. Pass result obtained October 1968.

DIVISIONAL STAFF

Division Head: Dr. B. Rose

Group Leaders: Mr. D. L. Allan
Dr. P. E. Cavanagh
Dr. T. E. Cranshaw
Dr. G. Dearnaley
Dr. A. T. G. Ferguson
Dr. J. M. Freeman
Dr. J. V. Jelley
Dr. E. R. Rae
Dr. A. E. Taylor

J. M. Adams
B. H. Armitage
Dr. I. M. Blair
P. H. Bowen
Dr. W. N. Charman
B. P. Clear
Dr. C. F. Coleman
Dr. J. A. Cookson
Dr. W. M. Currie
K. M. Diment
Dr. L. G. Earwaker
P. D. Goode
Dr. O. N. Jarvis
J. E. Lynn
R. I. MacDonald
N. J. Pattenden
D. R. Porter
M. S. Ridout
Dr. J. P. Scanlon
A. C. Sherwood
W. Spencer
B. W. Thomas
J. F. Turner
S. Waring
Dr. C. Whitehead

E. Wood
G. V. Ansell
D. A. Boyce
Miss E. M. Bowey
Dr. M. S. Coates
D. W. Colvin
G. C. Cox
G. B. Dean
P. E. Dolley
J. H. Fruin
Dr. D. B. Gayther
A. G. Hardacre
G. Huxtable
Dr. G. D. James
Dr. A. Langsford
M. C. Moxon
Dr. B. H. Patrick
F. D. Pilling
B. D. Rogers
M. G. Schomberg
Dr. M. G. Sowerby
Dr. C. A. Uttley
D. West
M. A. Wilkins

Fellows, Temporary Research Associates and Attached Staff in Nuclear Physics Division

Dr. A. Asami	T.R.A.	
R. A. Bell	Attached	Oxford University
Dr. H. C. Benöhr	Attached	University of Surrey
Dr. R. Chapman	Fellow	
Dr. T. W. Conlon	Fellow	
Dr. J. C. Dutt	Attached	Pakistan Atomic Energy Commission
Dr. A. J. Elwyn	Attached	Argonne National Laboratory
M. Khalequzzaman	Attached	Bedford College, London University
Dr. R. K. Jolly	Fellow	
Dr. L. G. Lang	T.R.A.	
Dr. H. A. Medicus	T.R.A.	
Dr. H. Marshak	Attached	National Bureau of Standards, Washington
Dr. J. Martin	S.F.T.A.	
Dr. C. D. McKenzie	Attached	University of Melbourne
Dr. J. Murray	Fellow	
Dr. W. T. Oosterhuis	Attached	Carnegie Institute of Technology, Pittsburgh
Dr. J. Poate	Fellow	
W. D. N. Pritchard	Attached	Exeter University
Dr. D. C. Robinson	Fellow	
M. B. Shah	Attached	University of Surrey
Dr. T. T. Thwaites	Attached	Pennsylvania State University
Dr. G. L. Wick	Fellow	
Mrs. L. A. Winsborrow	Attached	Kings College, London University